UNIVERSITÀ
DEGLI STUDI
DI PADOVA

SEDE AMMINISTRATIVA: UNIVERSITA' DEGLI STUDI DI PADOVA
DIPARTIMENTO DI BIOLOGIA

SCUOLA DI DOTTORATO IN: BIOSCENZE
INDIRIZZO: GENETICA E BIOLOGIA MOLECOLARE DELLO SVILUPPO
CICLO XXIII

SNARE complexes associate in a rosette-like structure at the *Drosophila* neuromuscular junction

Direttore della Scuola: Ch.mo Prof. GIUSEPPE ZANOTTI

Coordinatore d'indirizzo: Ch.mo Prof PAOLO BONALDO

Supervisore: Prof. MAURO ZORDAN

Dottorando: DAMIANO ZANINI

“Twenty years from now you will be more disappointed by the things that you didn't do than by the ones you did do. So throw off the bowlines. Sail away from the safe harbor. Catch the trade winds in your sails. Explore. Dream. Discover.”

Mark Twain

Index

Abstract

Secretion in all eukaryotic cells involves a family of proteins known as SNAREs (soluble N-ethylmaleimide-sensitive factor attachment protein receptors). In the nervous system, these proteins are the main molecular constituents of the synaptic vesicle fusion machinery. The release of molecules contained inside exocytic granules and synaptic vesicles is mediated by the assembly of a four helix bundle complex: the SNARE complex. It is formed by the coil-coiling of three proteins: the v-SNARE VAMP/Synaptobrevin and the t-SNAREs, Syntaxin and SNAP-25 (synaptosome-associated protein of 25 kDa). A cooperative interaction between SNARE complexes has been suggested to be necessary for the fusion of a synaptic vesicle with the presynaptic membrane to occur. Previous experiments, made with botulinum neurotoxins type A and E on mouse neuromuscular junction, led to predict a central role of the SNAP-25 C-terminus in protein-protein contacts between SNARE complexes. Previously conducted sequence comparisons and molecular dynamics simulations, led to the finding that this central role in such interactions could be played by a key Arginine residue at the SNAP-25 C-terminus. In particular, the SNAP-25 Arg206 residue possibly forms an ionic bond with a negative charge amino acid of Syntaxin from an adjacent SNARE complex. A computational model, based on such interactions, proposes that the formation of the vesicle/presynaptic membrane fusion pore is catalyzed by a SNARE supercomplex consisting in a "ten petal" rosette. This prediction was tested in *Drosophila melanogaster* by altering the putative key amino acids, thought to be involved in rosette formation, by site-directed mutagenesis. Two transgenic lines (harboring the mutation bearing constructs in a SNAP-25 *wild-type* background) were thus generated: *UAS-SNAP-25*^{WT} (control) and *UAS-SNAP-25*^{R206A}. Using the UAS/GAL4 system the expression of these constructs was directed specifically in the nervous system. The mRNA expression profiles, the locomotor behaviour and the morphology of the neuromuscular junction of these mutants were characterized in third instar larvae. Electrophysiological recordings performed at the larval neuromuscular junction showed that the *ElavALl4/UAS-SNAP-25*^{R206A} mutants present a decrease in the probability of vesicle fusion as compared to *ElavGAL4/UAS-SNAP-25*^{WT}, our control, in both spontaneous and evoked exocytosis. These findings highlight the key role of Arg206 and support the model entailing the involvement of a rosette of SNARE complexes in the process of neuroexocytosis.

Riassunto

L'esocitosi regolata è un processo essenziale in tutte le cellule eucariotiche. A livello della sinapsi, il rilascio di molecule contenute all'interno delle vescicole è mediato dalla formazione del complesso SNARE, costituito dall'interazione di tre proteine: sintassina, SNAP-25 e VAMP/sinaptobrevina. Numerose evidenze sperimentali suggeriscono che la cooperazione tra complessi SNARE adiacenti sia necessaria affinché una vescicola sinaptica si fonda con la membrane plasmatica. Da un'analisi della sequenza amminoacidica dell'isoforma neuronale di questa proteina è emerso che, nella porzione C-terminale, un residuo aminoacidico è altamente conservato anche se non è situate nella regione di interazione tra SNAP-25 e le altre componenti molecolari del complesso. In mammifero, tale residuo è l'arginina in posizione 198. Esperimenti condotti incubando la giunzione neuromuscolare di topo in presenza della tossina botulinica di tipo A hanno evidenziato il ruolo chiave della porzione C-terminale della proteina SNAP-25 nel processo di fusion vescicolare e, in particolare, dell'Arg198, poiché la tossina taglia esattamente la proteina a monte di questo residuo, determinando il blocco dell'esocitosi. Inoltre, simulazione di modeling effettuate al computer hanno suggerito che tale arginine interagisce con un amminoacido carico negativamente posizionato sulla sintassina del complesso SNARE adiacente, formando di un legame ionico. Questa ipotesi è stata verificata *in vivo* usando *Drosophila melanogaster* come organismo modello. Poiché nel moscerino della frutta la sequenza di SNAP-25 è più lunga di quella in mammifero, l'arginina conservata risulta essere in posizione 206. Tale Arg206 è stata sostituita con un'alanina mediante mutagenesi sito-specifica. Quindi, sono state generate due linee transgeniche in cui i costrutti pUAST-SNAP-25^{WT} e pUAST-SNAP-25^{R206A} sono stati inseriti in background SNAP-25 *wild-type*. Sfruttando il sistema GAL4/UAS, i transgeni sono stati espressi nel sistema nervoso utilizzando il driver pan-neuronale ElavGAL4. In entrambe le linee *ElavGAL4/UAS-SNAP-*25^{WT} (controllo) (controllo) e *ELAV-GAL4/UAS-SNAP-*25^{R206A} (mutante) sono stati quantificati i profili di espressione dell'mRNA dei trascritti mutante e *wild-type*; inoltre, è stata caratterizzata la giunzione neuromuscolare a livello larvale, musurandone la morfologia e la morfometria. L'analisi elettrofisiologica del rilascio spontaneo ed evocato ha mostrato una significativa riduzione della probabilità di fusione tra vescicola e membrana plasmatica. Questo risultato conferma il ruolo chiave ricoperto dall'Arg206 durante il processo di esocitosi a livello del terminale sinaptico e supporta l'ipotesi secondo cui i complessi SNARE cooperano tra loro, formando un supercomplesso necessario alla formazione del poro di fusione.

Abbreviations

ADHD: attention-deficit/hyperactivity disorder

BoNT: botulinum neurotoxin

CNS: central nervous system

DA: dopamine

ECP: exo/endo cycling pool

EJP: evoked junction potential

ELAV: embryonic lethal abnormal vision

HRP: horseradish peroxidase

IRP: immediately releasable vesicles

ISN: intersegmental nerve branch

MEPC: miniature end plate current

MEPP: miniature end plate potential

NMJ: neuromuscular junction

NSF: N-ethylmaleimide sensitive fusion ATPase

RP: reserve pool

RRP: readily releasable pool

SDT: short-term synaptic depression

SN: segmental nerve

SNAP-25: synaptosome-associated protein 25 kDa

SNARE: soluble N-ethyl maleimide sensitive factor attachment protein receptors

SYX: syntaxin

SV: synaptic vesicle

SYT: synaptotagmin

VAMP: vesicle-associated membrane protein

TN: transverse nerve

1. INTRODUCTION

1.1. Preface

Everyone's favorite research fruit fly is *Drosophila melanogaster* (Greek for dark-bellied dew lover), a species of Diptera, of the Drosophilidae family.

Within a few years of the rediscovery of Mendel's rules in 1900, *Drosophila* became a favorite model organism for genetics research. Starting from Charles William Woodworth (credited with first breeding *Drosophila* in quantity, while he was at Harvard University) and Thomas Hunt Morgan (awarded the Nobel Prize in Physiology or Medicine in 1933), the fruit fly has become one of the most valuable of organisms in biological research, particularly in genetics and developmental biology.

Its importance for human health was recognized by the award of the Nobel Prize in medicine/physiology to Edward Bok Lewis, Christiane Nusslein-Volhard and Eric Wieschaus in 1995.

1.2. The fruit fly as model organism

Drosophila was among the first organisms used for genetic analysis, and today it is one of the most widely used and genetically best-known of all eukaryotic organisms. The reasons for its popularity are several: they go from the ease of maintenance due to its high fecundity and short life cycle, to the large availability of genetic transformation techniques that allow the manipulation of the completely sequenced genome (Adams *et al.*, 2000), passing from the easy identification of different phenotypes and the possibility of keeping stocks carrying lethal by alleles using recessive lethal and multiple inversion-bearing "balancer chromosomes" which act as suppressors of recombination with their non-inverted homologs.

Furthermore the *Drosophila* larval body wall muscles, and in particular the neuromuscular junction (NMJ), constitutes a versatile model system to address most of the basic questions concerning synaptic function such as ion channels function, mechanisms of fast

neurotransmitter release, synapse physiology, functional and structural synaptic plasticity, and synapse development and formation. Due to its relative simplicity, easy accessibility, and the presence of large muscles with a well-defined synapse, the larval body wall preparation has contributed importantly to our understanding of the genetic mechanisms of synaptic vesicle release and vesicle recycling (Budnik and Ruiz-Cañada, 2006).

In the mid to late 1970s Yuh Nung Jan and Lily Yeh Jan were the pioneer investigators the third instar larva body wall and NMJ (Jan and Jan, 1976a, b). They described the pharmacological and physiological properties of this model system and they also performed the first genetic analysis of synaptic transmission and short-term synaptic plasticity (Jan and Jan, 1978).

In the 1980s Chun-Fang Wu and Barry Ganetzky used the body wall preparation to study properties of ion channels involved in synaptic transmission (Ganetzky and Wu, 1982a, 1983). Few years later studies by the Keshishian lab highlighted the accessibility of the larval synapse, making developmental analysis simple (Anderson *et al.*, 1988).

In the 1990s Vivian Budnik demonstrated that the larval NMJ is involved in regulatory mechanisms which allow synaptic plasticity in neuronal networks (Budnik *et al.*, 1990). Soon after the NMJ became the subject of studies by the Goodman lab when they focused on the identification of genes involved in the formation of a functional synapse, to be more precise on the mechanism of axonal pathfinding (Nose *et al.*, 1992).

Thus, for all the above reasons, as well as the well-characterized genetics, nowadays the fly NMJ constitute an excellent model system for investigating features of synaptic transmission such as synapse physiology, development and plasticity, since many of the molecules involved in vesicle fusion at the synapse terminal are highly conserved between humans and *Drosophila* (Zhang, 2010), making the studies on larval body wall muscles and the NMJ highly relevant for the scientific community.

Even if the *Drosophila* genome size is less than 1/20 of the human one, about 50% of fly protein sequences have mammalian homologs and almost 75% of known human disease genes have a recognizable match in the genetic code of fruit flies (Reiter *et al.*, 2001). The fruit fly is also being used as a genetic model for several human diseases including neurodegenerative disorders such as Down syndrome as well as Parkinson, Huntington, and Alzheimer diseases. Furthermore, *Drosophila* has been used in neuropharmacological research, including studies on the effects of cocaine (Andretic *et al.*, 1999) and alcohol (Heberlein, 2000) on the nervous system and behavior.

1.3. Anatomy of larval body wall

As already anticipated, the short life cycle is one reason for the use of *Drosophila* as a model system. In lab conditions, at 25°C, generation time is about 10 days: the egg hatches after 12-15 hours. The resulting larva grows for about 4 days while molting into second instar at about 24 h and third instar approximately 48 h after hatching. Then the larva encapsulates in the puparium and undergoes a four-day-long metamorphosis after which the adult emerges.

The *Drosophila* larval neuromuscular system exhibits bilaterally symmetric and segmentally reiterated organization (Fig. 1.1). Each segment contains a repeated pattern of 30 skeletal muscle fibers which share common physiological and contractile properties (Crossley, 1978). These supercontractile muscles are very large and the identification is unique, based on their size, such as shape, orientation within the muscle fields, relative attachment sizes within the cuticle, as well as the innervations by the central nervous system (CNS). Muscles anchor to specialized cells in the epidermis called tendon cells and may also attach to each other. Due to the dimensions (a longitudinal muscle can reach the size of 40µm wide x 400µm long), a muscle can be impaled with microelectrodes relatively easily, providing for relatively straightforward electrophysiological intracellular records. Each mature muscle consists of a single myofiber, a single multinucleated cell which is anchored to the cuticle by its internal projections; in contrast each muscle in the *Drosophila* adult or vertebrate system consists of several bundles of myofibers (Budnik and Ruiz-Cañada, 2006).

During the development of the embryo, reiterated sets of approximated 80 motorneurons are generated in each segment of the ventral nerve chord. Each motorneuron has its unique cellular identity and is characterized by its axonal trajectory and innervations of a particular target muscle, as well as by its operation and its dendritic harborization within the CNS (Landgraf *et al.*, 2003). From the ventral ganglion of the CNS, 32 motorneurons (Landgraf *et al.*, 1997) arise to extend their axons to innervate each hemisegment of the larval body wall muscles. Those motorneuron axons are grouped into six major nerve branches: ISN (intersegmental nerve branch), SNa (segmental nerve branch a), SNb (segmental nerve branch b), SNc (segmental nerve branch c), SNd (segmental nerve branch d), and TN (transverse nerve) (Hoang and Chiba, 2001).

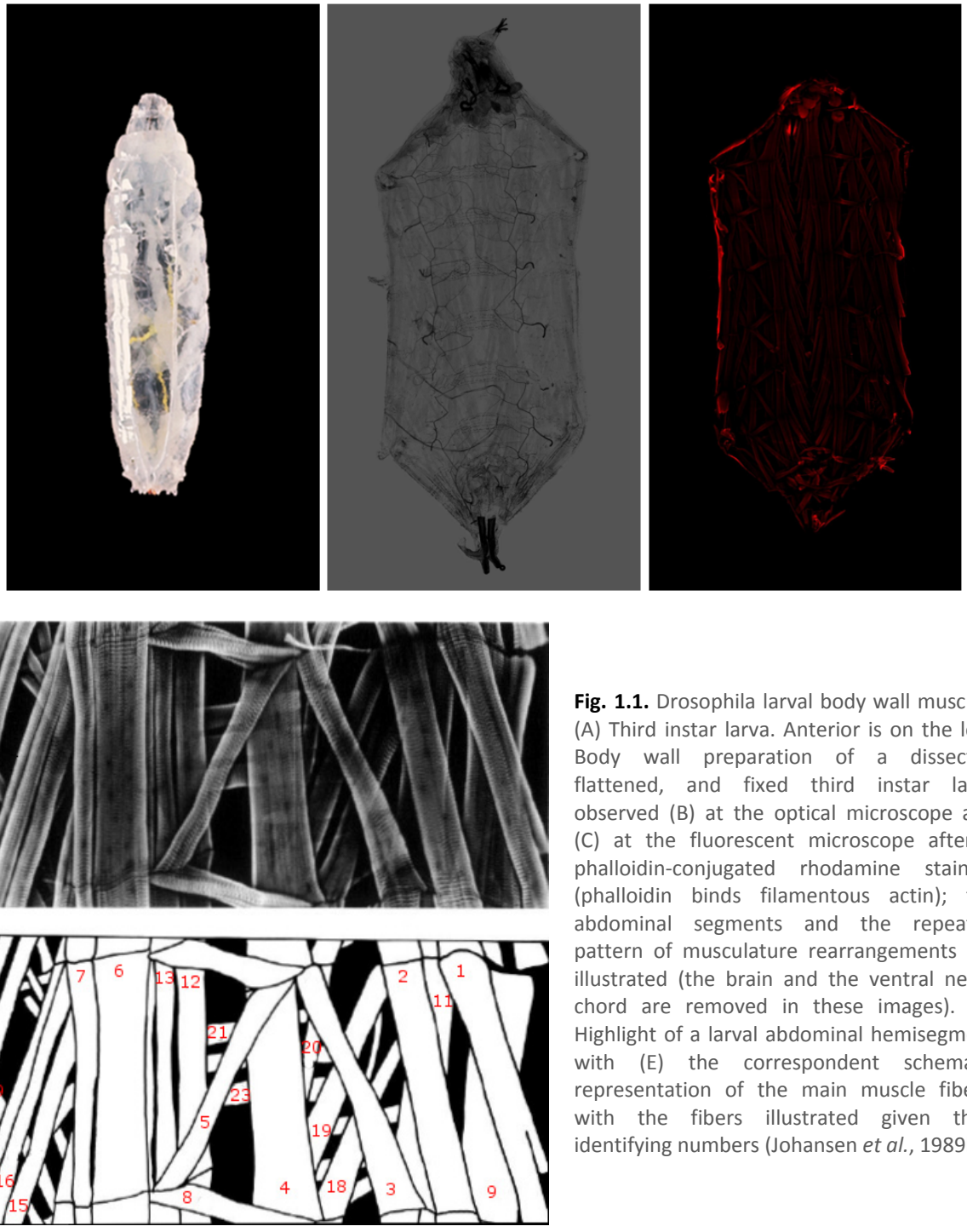

Fig. 1.1. Drosophila larval body wall muscles. (A) Third instar larva. Anterior is on the left. Body wall preparation of a dissected flattened, and fixed third instar larva observed (B) at the optical microscope and (C) at the fluorescent microscope after a phalloidin-conjugated rhodamine staining (phalloidin binds filamentous actin); the abdominal segments and the repeated pattern of musculature rearrangements are illustrated (the brain and the ventral nerve chord are removed in these images). (D) Highlight of a larval abdominal hemisegment with (E) the correspondent schematic representation of the main muscle fibers, with the fibers illustrated given their identifying numbers (Johansen *et al.*, 1989b).

The dorsal (distal) region of the neuromuscular system includes 10 muscles (1, 2, 3, 4, 9, 10, 11, 18, 19, and 20) and a single ISN nerve branch that supplies all motorneuron axons that reach these muscles. The lateral neuromuscular region contains six muscles (5, 8, 21, 22, 23, and 24). A single SNa nerve branch supplies all motorneuron axons innervating these muscles. The motorneurons in the SNb and SNd nerve branches innervate the 10 ventral (proximal) muscles (6, 7, 12, 13, 14, 15, 16, 17, 28, and 30). The SNc and TN motorneurons

innervate four ventral (proximal) muscles (25, 26, 27, and 29) in the superficial (close to the cuticle) layers of the musculature (Hoang and Chiba, 2001).

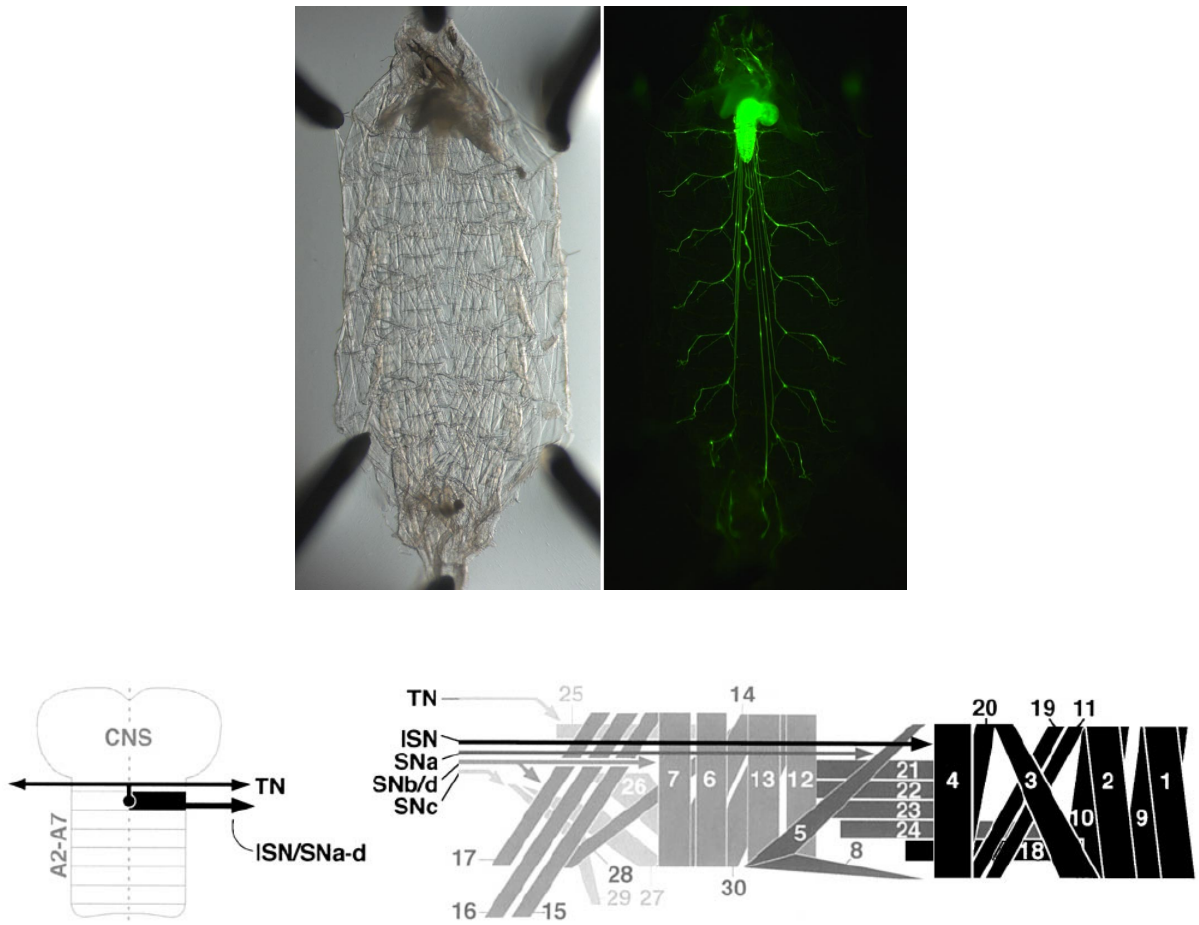

Fig. 1.2. Neuromuscular system of the *Drosophila* larva. Body wall preparation of an *ElavGAL4*/*UAS-EGFP* larva seen (A) at the optical microscope and (B) at the fluorescent microscope; the whole nervous system is labeled in green. The bilaterally symmetrical and segmentally reiterated organization of the CNS (C) and the body wall muscles (D) are illustrated. The schematic shows the dorsal view of a fillet-dissected preparation after a dorsal midline incision. Anterior is at the top. The second abdominal right half-segment (A2) is highlighted. Each CNS segment has a dorsal midline nerve exit, from which the bilaterally symmetric TN nerve branches extend, and a pair of lateral nerves exit on each side, from which the ISN, SNa, SNb, SNc, and SNd nerve branches arise. Thirty muscles (1–30) in each half segment are innervated by the motorneurons through these six nerve branches (Hoang and Chiba, 2001).

1.4. Morphology of the neuromuscular junction

Chemical synaptic transmission is an important means of neuronal communication in the nervous system. When the Ca^{2+} concentration increases due to a depolarization of the axon terminal, synaptic vesicles (SVs) fuse with the plasma membrane and the neurotransmitter is released in the synaptic cleft. Transmitters elicit synaptic response in the postsynaptic cell by

binding to specific receptors and activating them. The exocytosis is followed by the recycling of SVs at the presynaptic terminals.

As already anticipated, the *Drosophila* larval NMJ shares several important features with central excitatory synapses in the vertebrate brain, also in humans: it is glutamatergic (Jan and Jan, 1976a), with homologous ionotropic glutamate receptors, and it is organized into a series of boutons that can be added or eliminated during development. Both the *Drosophila* NMJ and vertebrate central synapses exhibit dynamic functional plasticity (Petersen *et al.*, 1997). In addition, the basic cellular and molecular mechanisms which regulates the cycle of synaptic vesicles are the same in both fly and humans (Zhang, 2010). Because of these properties, the fly NMJ constitutes an excellent model system for dissecting the cellular and the molecular mechanism of synaptic transmission.

In the larva body wall, the abdominal segments from A2 to A7 are almost identically organized (Bate, 1993). All larval motorneurons in these segments have been morphologically described and, during the development of the neuroectoderm, the respective precursor cells have been identified. They have been also linked to their muscle targets (Jia *et al.*, 1993). Almost all the morphological features of these motorneurons have been defined (Hoang and Chiba, 2001).

Except for muscle 4 which is monosynaptic, all the body wall muscles are innervated by two specific motorneuron axons. At the larval stage, motorneurons can be divided into three classes on the base of the dimension of their boutons at the axon terminal (Atwood *et al.*, 1993).

The most abundant class of motorneurons are of type-I. Type-I boutons are restricted in distribution and possess relatively prominent terminal enlargements. Within this class, the axons may be divided into 2 subclasses on the base of the bouton dimensions, big (Ib) and small (Is) (Johansen *et al.*, 1989a): type-Ib boutons are large (about 3-5 mm), the terminals bearing them tend to be short and minimally branching and they contain mainly small and clear vesicles of 30/40nm diameter. Type-Is boutons are, on the average, slightly smaller (about 1-1.5 mm) than type-Ib boutons, the terminals bearing them can often be longer and more elaborate than those with type-Ib boutons and they contain a cocktail of different clear and dense-core vesicles (Jia *et al.*, 1993). Both these two types of motorneurons primarily release glutamate, the main excitatory neurotransmitter at the NMJ (Atwood *et al.*, 1993).

The other two classes (type-II and type-III) have a neuromodulatory function and they release octopamine (Monastirioti *et al.*, 1995) or a variety of peptides (Cantera and Nassel,

1992). Type-II boutons are small (about 1-2 um), more widely distributed and the terminals bearing them are very long and the most elaborate of all axon terminal types. Moreover, type-II boutons are thought to be on most muscles (Johansen *et al.*, 1989). Type-III boutons are of medium size (about 2-3 µm) and the terminals bearing them are of medium length but are thought to occur only on muscle 12. In addition to glutamate, type-III boutons contain insulin, a putative neural cotransmitter (Gorczyca *et al.*, 1993).

The characteristic peristaltic locomotor behavior of a larva is the result of four principal components: the cuticular exoskeleton, which provides frictional contact with the substrate through hooklike protrusions (denticles), the arrays of body wall muscles, the motorneurons located in the ventral chord which innervate these muscles and the input provided by interneurons (predominantly cholinergic). This makes *Drosophila* larva an attractive experimental model to study how the neuronal network that underlies such a simple behavior can regulates the motor system of the animal.

Muscles labeled as 6, 7, 12 and 13 constitute the ventral longitudinal abdominal muscles. Three classes of nerve innervate these muscles: type-Ib, type-Is, and type-II. Whereas muscles 12 and 13 receive both type of innervations, muscles 6 and 7 receive only type-I endings (Fig. 1.3) (Atwood *et al.*, 1993). This difference in innervation pattern allows the two axons to be reliably identified. Consistent with vertebrate studies, there is a correlation between muscle fiber size and terminal size (Lnenicka and Keshishian, 2000).

Neurons use electrical (electrical synapses) and chemical (chemical synapses) signals to receive, process, and communicate informations. The basic currency of signaling by excitable cells (neurons and muscles) is electrical current. Accordingly, electrophysiology is the study of how neurons generate, integrate and transmit electrical signals in neuronal networks, causing all nervous system responses and behaviors. The fly larval body wall muscles do not express voltage gated Na^+ channels (Hong and Ganetzky, 1994; Wu and Haugland, 1985) and thus do not produce rapid action potentials. Neither do they exhibit Ca^{2+}-dependent regenerating potentials in the absence of the tracheal system, which is the open respiratory system composed of spiracles, tracheae, and tracheoles that terrestrial arthropods have to transport metabolic gases to and from tissues (Yamaoka and Ikeda, 1988). Hence, all recordings from the muscle fibres are passive membrane properties or pure synaptic responses (Wu and Haugland, 1985). Moreover, the muscle is isopotential (Jan and Jan, 1976b). Hence the electrode can be inserted anywhere in the muscle to record the synaptic potential. For electrophysiological recordings on the larval NMJ the scientific community has chosen to focus most of their investigations on the muscle 6 and 7 NMJs because of their

large size and their central position in the body wall, that preserve them from any damage during the process of larval dissection.

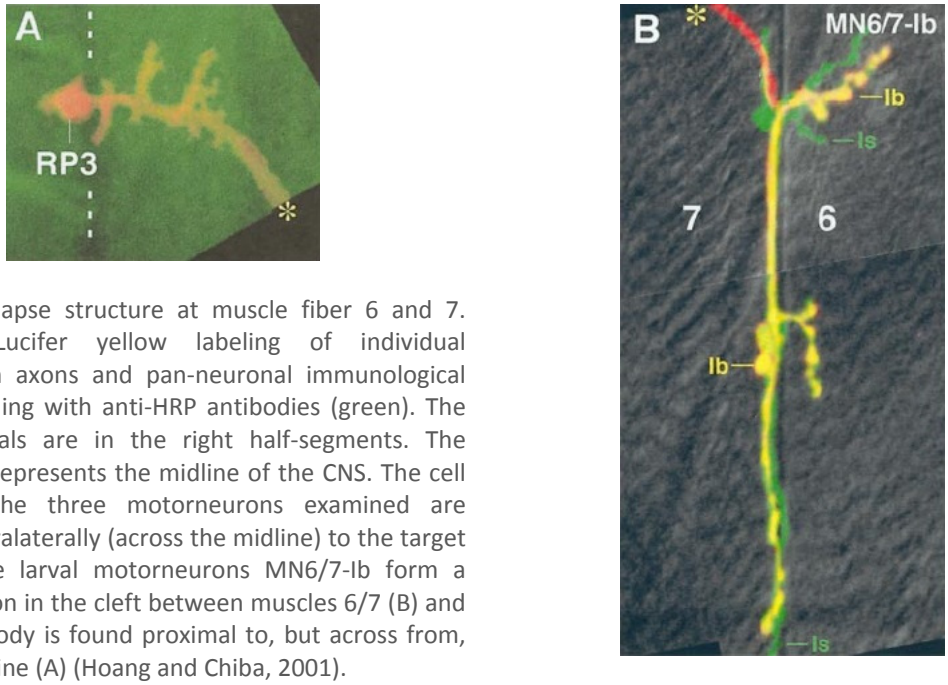

Fig. 1.3. Synapse structure at muscle fiber 6 and 7. Single-cell Lucifer yellow labeling of individual motorneuron axons and pan-neuronal immunological counter-labeling with anti-HRP antibodies (green). The axon terminals are in the right half-segments. The dashed line represents the midline of the CNS. The cell bodies of the three motorneurons examined are located contralaterally (across the midline) to the target muscles. The larval motorneurons MN6/7-Ib form a type Ib bouton in the cleft between muscles 6/7 (B) and whose cell body is found proximal to, but across from, the CNS midline (A) (Hoang and Chiba, 2001).

Two axons with distinctive endings contribute to the innervation of muscles 6 and 7: axon 1 and axon 2. The differences between axon 1 and axon 2 are several. The axon 1 terminal creates numerous synapses containing presynaptic dense bodies, which are the putative active zones for transmitter release; this axon also has more numerous mitochondria, and a profuse subsynaptic reticulum around or under the synaptic boutons (Atwood *et al.*, 1993). The dimension of the boutons at the NMJ is bigger, 30% wider than the axon 2 boutons (Lnenicka and Keshishian, 2000). Axon 2 presents fewer synapses and dense bodies per bouton, fewer intraterminal mitochondria, and a less-developed subsynaptic reticulum. The dimension of axon 2 boutons at the NMJ is smaller. Approximately 800 synapses are provided by axon 1, and approximately 250 synapses are provided by axon 2 (Atwood *et al.*, 1993). Also the electrophysiological profile of these two axons is different. The excitatory postsynaptic potential produced by axon 1 is generally smaller than that produced by axon 2 (Lnenicka and Keshishian, 2000).

The morphological structure of the synapse is also different from that of vertebrate neuromuscular junctions. The *Drosophila* nerve terminal is embedded in the muscle and its perimeter is completely surrounded by subsynaptic muscle membrane, which is extensively folded at synaptic terminals. In contrast to vertebrate NMJs that present a 50-60 nm wide cleft between the nerve and the muscle membranes and contain a basal lamina (Peters *et al.*, 1991), the fly NMJ show a 15-20 nm wide cleft and has no basal lamina; this structure in

Drosophila is comparable to central synapses in humans (Prokop and Meinertzhagen, 2006). Furthermore, the main neurotransmitter at the larval NMJ is glutamate; the same amino acid is used at the great majority (over 90%) of fast excitatory synapses in the brain and spinal cord of vertebrates (Usherwood, 1981).

In *Drosophila*, synapses in type-I terminals are often characterized by the presence of presynaptic electron dense structures referred to as T-bars, due to their T-shaped appearance in electron microscopy cross-section (Fig. 1.4) (Atwood *et al.*, 1993).

In the presynaptic inner membrane, at the periphery of the nerve terminal all along the perimeter of synaptic boutons, vesicles are physically attached to T-bar ribbons, the specific release sites (Kidokoro *et al.*, 2004), closely associated with clusters of Ca^{2+} channels (Prokop, 1999). Such T-bar ribbon conformation facilitates synaptic release (Reiff *et al.*, 2002) inducing local Ca^{2+} concentration increasing in microdomains (Llinas *et al.*, 1992).

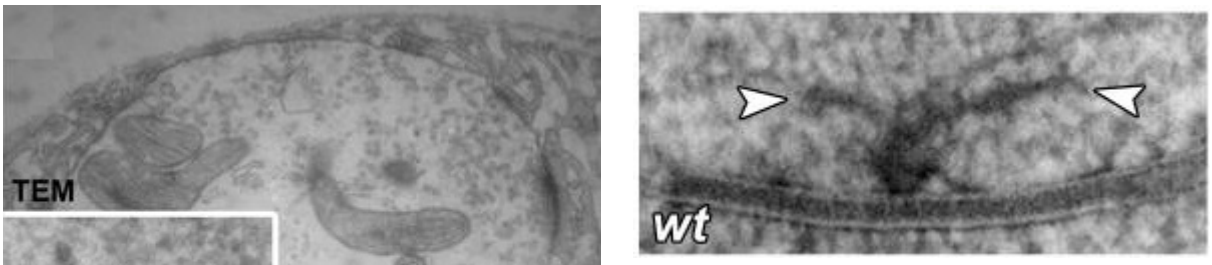

Fig. 1.4. T-bar structure at the *Drosophila* NMJ. (A) Electron microscopy photograph of the synaptic bouton. An electron dense zone corresponding to the area where synaptic vesicles aggregate near the plasma membrane is emphasized. (B) Electron microscopy photograph of T-bars structure (Fouquet *et al.*, 2009).

1.5. Vesicle fusion cycle

Synaptic transmission is the process by which neurons secrete neurotransmitter molecules from the nerve terminal onto target cells. In the 1950s Bernhard Katz and his colleagues recorded the first synaptic response at the frog NMJ using an intracellular microelectrode; the experiments provided several elements for the understanding the synaptic transmission. The process is initiated when an action potential reaches the presynaptic nerve terminal. This action potential induces the opening of Ca^{2+} channels, and the resulting Ca^{2+} transient stimulates synaptic vesicle exocytosis with the consequent neurotransmitter release at the presynaptic active zone of the nerve. Even at rest, synapses have a finite but low probability

of release, causing spontaneous events of exocytosis. In both cases the neurotransmitter is released in defined units, called quantal units. The units appeared to be the same in both spontaneous and evoked release processes (Fatt and Katz, 1951, 1952).

Effective neurotransmission requires the precise spatial regulation of protein-lipid interactions. More than 1000 proteins function in the presynaptic nerve terminal, and hundreds are thought to participate in exocytosis (Sudhof, 2004). Also plasma membrane and vesicle lipids regulate functional aspects of neurotransmission (Davletov and Montecucco, 2010; Rohrbough and Broadie, 2005). In fact neuronal lipid rafts, sphingolipid- and cholesterol-enriched micro domains that are distributed in both surface and organelle membranes, are involved in the targeting, localization and functional modulation of many neuronal ion channels and receptors (Tsui-Pierchala *et al.*, 2002) as well as for synaptic vesicle targeting, docking, priming and fusion at the active zone (Rohrbough and Broadie, 2005). Lipid rafts play a key role in the regulation of membrane fluidity and curvature, parameters directly relevant to membrane restructuring during synaptic vesicle fusion and budding (Chernomordik and Kozlov, 2008; Megighian *et al*., 2007; Rohrbough and Broadie, 2005).

Synaptic vesicles undergo a trafficking cycle in the nerve terminal to support rapid and repeated rounds of release (Fig. 1.5). That cycle can be divided into several sequential steps: the synaptic vesicles are charged with the neurotransmitter that is actively transported into the lumen (Sudhof, 2004); cytoskeletal and tethering proteins interact with vesicles to drive them in proximity of the active zone (Rohrbough and Broadie, 2005). In preparation for neurotransmitter release, synaptic vesicles are converted into a state of competence for Ca^{2+}-triggered fusion-pore opening (Sudhof, 2004). Three soluble N-ethylmaleimide-sensitive factor (NSF)-attachment protein receptors (SNAREs) are involved in these preliminary steps: synaptobrevin, syntaxin and synaptosome-associated protein-25 kDa (SNAP-25). These proteins drive the assembly of the SNARE complex which constitutes the minimal fusion machinery. This complex regulates the neuronal exocytosis process allowing: the establishment of tight membrane contact between vesicle and plasma membrane (docking), the formation of a scaffolding on which to build the fusion machine, and the binding of lipid surfaces (priming) (Sollner *et al*., 1993; Weber *et al*., 1998).

When an action potential invades a nerve terminal, voltage-gated Ca^{2+} channels open, and the resulting wave of intracellular Ca^{2+} triggers fusion-pore opening and neurotransmitter release. The calcium sensor of exocytosis is constitute by synaptotagmin, a protein with two C-terminal C2 domains to which Ca^{2+} bind driving the fusion between vesicle and plasma membranes (Sudhof and Rizo, 1996).

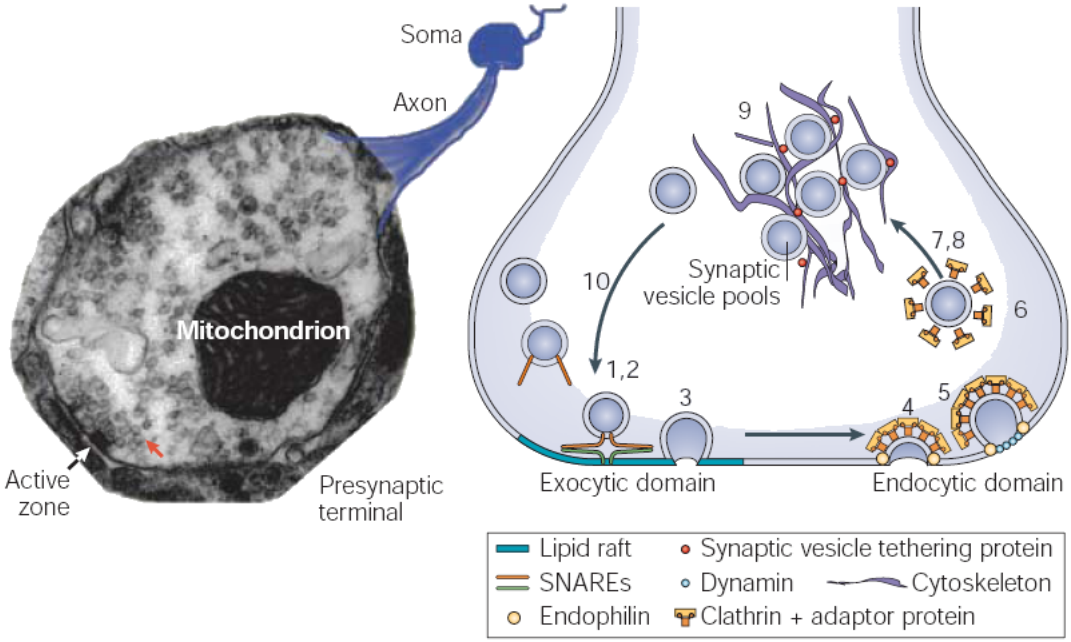

Fig. 1.5. The synaptic vesicle cycle. (A) Electron micrograph of the presynaptic terminal bouton at the *Drosophila* NMJ, containing vesicles (red arrow), presynaptic organelles and an electron-dense active zone, which defines the site of vesicular fusion and neurotransmitter release. (B) Scheme of the presynaptic terminal, highlighting the main stages of the synaptic vesicle cycle. Ten steps can be defined: (1) synaptic vesicle docking to the plasma membrane, (2) vesicle priming for fusion, (3) Ca^{2+}-triggered vesicle fusion, (4) clathrin-mediated budding and synaptic vesicle formation, (5) fission of a new vesicle, (6) clathrin uncoating, (7) neurotransmitter loading, (8) vesicle trafficking, (9) tethering in a reserve pool and (10) mobilization and targeting to the plasma membrane release site. The plasma membrane (turquoise zone) shows where exocytosis occurs in lipid raft domains that localize SNARE proteins. Endocytosis occurs in adjacent specialized regions which might have distinct raft-like features. Endophilin regulates membrane reshaping, facilitating vesicle budding. Cytoskeletal and tethering proteins interact with vesicle lipids to traffic and sequester synaptic vesicles (Rohrbough and Broadie, 2005).

Synaptic vesicles recycling may follow three alternative pathways: (1) vesicles are reacidified and refilled with neurotransmitters without undocking, thus remaining in the readily releasable pool (step 6, called “kiss-and-stay”) (Barker *et al.*, 1972); (2) vesicles undock and recycle locally (called “kiss-and-run”) (Ceccarelli *et al.*, 1973) to reacidify and refill with neurotransmitters; or (3) vesicles endocytose via clathrin-coated pits and reacidify and refill with neurotransmitters either directly or after passing through an endosomal intermediate (Heuser and Reese, 1973).

In *Drosophila* NMJ, two types of endocytosis have been observed: active zone endocytosis that occurs at the presynaptic active zone facing the specialized postsynaptic membrane and non-active zone endocytosis that operates at the area away from the active zone. Once SVs are formed by endocytosis, they are delivered to two SV pools: the exo/endo cycling pool (ECP) the reserve pool (RP) (Kidokoro, 2006). Different pools of synaptic vesicles were defined on the basis of the rates of release under various stimulation conditions. In a temperature-sensitive paralytic mutant of *Drosophila*, *shibire*, two distinct pools have been

identified and characterized (Poodry and Edgar, 1979). The ECP may be electrophysiologically divided into the readily releasable pool (RRP) and the immediately releasable pool (IRP). While the RRP and the IRP are recruited in synaptic transmission during low frequency nerve-stimulation, while the RP participates only during high frequency stimulation (Kidokoro, 2006). Moreover, in the case of high sustained stimulation, endosomes were revealed to be an obligatory component of the vesicle recycling pathway in all synapses (Wucherpfennig *et al.*, 2003). The IRP and the RRP locates in the vicinity of release sites, exactly in the periphery of presynaptic boutons, while the RP spreads toward the center of boutons. These two pools are separately replenished by endocytosis but the vesicles can move from a RP to RRP, and vice versa, leading to changes in synaptic efficacy. The size of the RP is approximately 62,000 vesicles, five to seven times larger than that of the RRP. The IRP is smaller (estimated to be 230 vesicles) and can be exhausted with a few stimuli and probably represents docked vesicles (Kidokoro *et al.*, 2004). Vesicles in the IRP are in dynamic equilibrium with those in the RRP (Li and Schwarz, 1999).

1.6. Core of the fusion machinery: the SNARE complex

Intracellular membrane or vesicle fusion involves a highly conserved family of proteins termed SNAREs. One particular example of vesicular fusion is exocytosis, defined as fusion of an intracellular trafficking vesicle with the plasma membrane. Constitutive exocytosis comprises all fusion processes where vesicles are generated, transported, and undergo exocytosis continuously. In contrast, regulated exocytosis is triggered by second messengers such as Ca^{2+} in response to activation or membrane depolarization (Burgess and Kelly, 1987).

The same molecular mechanism is required in all eukaryotic cells, from the yeast secretion, example of metazoan constitutive exocytosis, to the mammalian synaptic neurotransmitter release, example of regulated exocytosis (Bennett and Scheller, 1994; Sollner and Rothman, 1994).

The release of molecules contained inside exocytic granules and synaptic vesicles is mediated by the assembly of a SNARE complex which constitutes the main molecular constituents of the synaptic vesicle fusion machinery. As in humans and other vertebrates, also the synaptic vesicle fusion at the *Drosophila* NMJ requires the same synaptic proteins. The 'minimal fusion machinery' is composed by two target-SNAREs (t-SNAREs), syntaxin and SNAP-25 on the plasma membrane, and one vesicle-associated SNARE (v-SNARE), neuronal synaptobrevin (also known as VAMP) on synaptic vesicles (Weber and Cyran, 1998). Those

SNAREs create a stable ternary core complex, with 1:1:1 stoichiometry, from helices in their cytoplasmic domains with the formation of a 4-helix bundle with 1 helix donated by syntaxin and by synaptobrevin and 2 helices donated by SNAP-25 (Montecucco *et al*., 2005; Sollner *et al*., 1993).

Neuronal synaptobrevin, also known as VAMP (vesicle-associated membrane protein), is a 13 kDa integral membrane proteins of the vesicle. The protein structure consists of four parts: a N-terminal proline-rich segment; a segment of around 60 aminoacids, which is well conserved among isoforms and contains heptad repeats typical for coiled-coils and a short a-helix that inserts into the interfacial region of the lipid bilayer (de Haro *et al.*, 2004); a single transmembrane segment; and a poorly-conserved intra-lumenal tail (Montecucco *et al.*, 2005).

Drosophila has two characterized members of synaptobrevin gene family. Mutant phenotypes and gene-expression patterns indicate that one isoform is exclusively neuronal (n-syb) and required for only synaptic vesicle secretion, whereas the other synaptobrevin isoform (syb) is ubiquitous and essential for cell viability (Sudhof *et al.*, 1989). The nerve-evoked synaptic currents were absent from the neuromuscular junctions of *n-syb* mutant embryos, while minis were readily detected (Kidokoro, 2003).

Neuronal syntaxin (Cerezo *et al.*, 1995) is a t-SNARE expressed ubiquitously in the plasma membrane, but it acts as the central member of the core complex, mediating synaptic vesicle fusion only at presynaptic active zones (Jahn and Hanson, 1998). The protein is bound to the presynaptic membrane of neurons by a transmembrane segment linked to a short C-terminal domain exposed to the cell surface and a large cytosolic portion that includes two domains with distinct structural features. The N-terminal domain consists of three long α-helices that are likely to be involved in protein-protein interactions, whereas the central portion contains coiled-coil forming heptad repeats required for the assembly and stability of the SNARE complex mediating vesicular fusion at the synapse (Bennett *et al*., 1993). Several syntaxin isoforms coexist within the nervous tissue. Targeted vesicle fusion is regulated by a large number of syntaxin-binding interactions that control its functional conformation (Bajjalieh and Scheller, 1995).

In experiments performed at the *Drosophila* neuromuscular synapse, nether nerve-evoked synaptic currents nor minis were observed in syx^{null} mutant embryos (Kidokoro, 2003). Furthermore the fundamental role in neurotransmission, syntaxin is absolutely required in non-neuronal processes. In *Drosophila*, proper cellularization of the embryo requires this protein that is known to be important for membrane trafficking and biogenesis (Burgess *et*

al., 1997). Syntaxin is also essential for cell viability in the developing eye, it is required for the completion of oogenesis, and it may play a role in membrane stabilization in the nervous system (Schulze and Bellen, 1996).

SNAP-25 (Oyler *et al.*, 1989) is localized on the cytosolic face of the nerve membrane via palmitoylated cysteines located in the middle of the polypeptide chain. Both the N- and C-terminal halves of SNAP-25 contain heptad repeats. SNAP-25 is highly conserved among species with little variation in length. Upon interaction with syntaxin, SNAP-25 forms a three-helix bundle complex, which might function as a Synaptobrevin receptor on the plasma membrane (An and Almers, 2004). Moreover, SNAP-25 stoichiometrically binds to the putative calcium sensor synaptotagmin and this interaction is believed to be important for the calcium-dependent phase of neurotransmitter release (Bai *et al.*, 2004).

Prior to exocytosis, the t- and v-SNAREs are thought to form a trans complex composed of one helix each from syntaxin and synaptobrevin and two helices contributed by SNAP-25 (Fig. 1.6) (Sutton *et al.*, 1998). Starting from the N-termini of the SNAREs, the coil-coiling interactions proceed until the formation of a four-helices bundle with a parallel orientation, which brings the transmembrane segment of VAMP and syntaxin close to each other and close to the C-terminus and to the palmitoylated central loop of SNAP-25 (Lin and Scheller, 1997).

This SNARE complex has a trans configuration with respect to the membrane location of the two TM domains, one of which resides in the synaptic vesicle membrane and the other is embedded in the synaptic plasma membrane. This conformation of the pre-fusion SNARE complex is stabilized by a core complex of 16 hydrophobic interactions layers (Lagow *et al.*, 2007). The surface of the SNARE complex has major grooves and charges enabling the possibility of additional specific protein-protein interactions (Lin and Scheller, 1997).

At this state the vesicle is docked, linked to the plasma membrane. The vesicles then undergo a priming process in which they become fusion competent; at this stage the SNARE complex, which is forming in the N- to C-terminal direction, is in a partly assembled intermediate (Sorensen *et al.*, 2006) and the vesicle is in a hemifused state.

Vesicle fusion can be constitutive or triggered by calcium. In the latter case when the Ca^{2+} concentration increases due to the depolarization of the axon terminal, the fusion pore forms and the neurotransmitter is released (Katz and Miledi, 1967). Exocytosis is triggered within about 0.2 ms of the Ca^{2+} influx (Li *et al.*, 1995) through calcium channels located near the ‘active zones’, which are the preferred sites of neuroexocytosis (Jahn *et al.*, 2003).

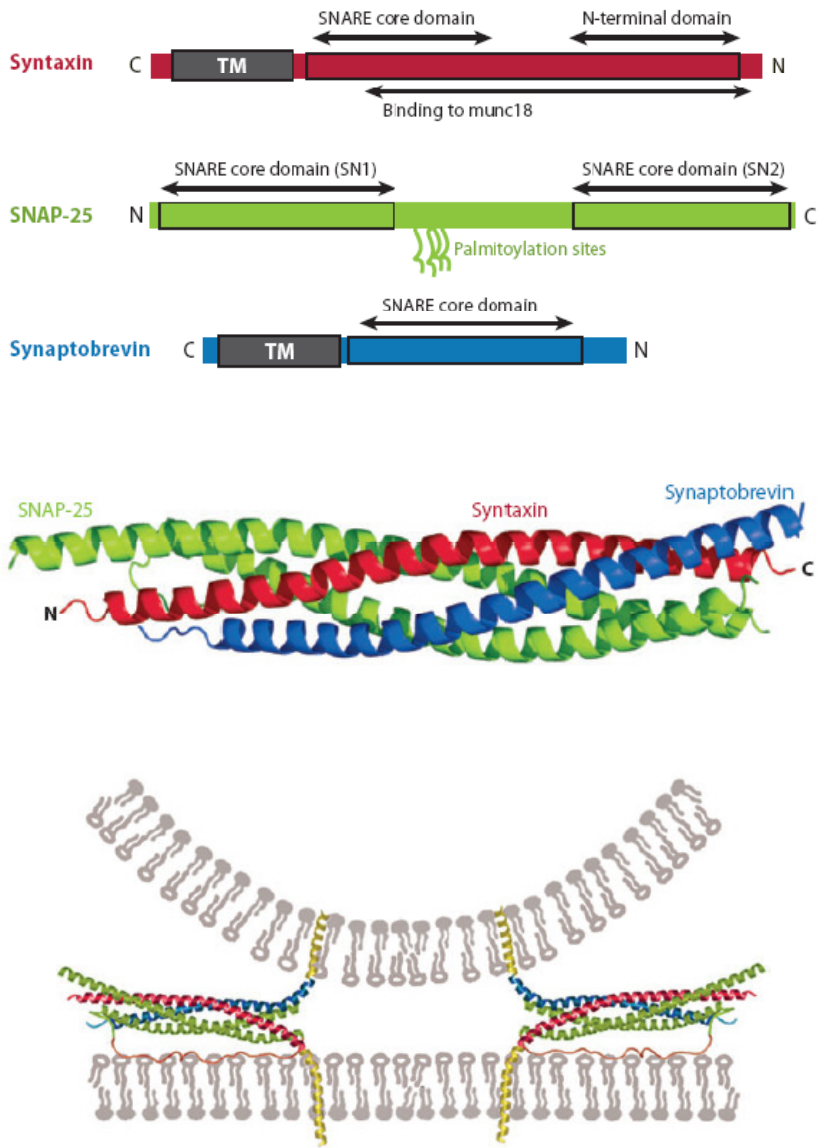

Fig. 1.6. Structure of the synaptic SNARE complex. (A) Cartoon representing the primary domain structure of neuronal SNAREs. Synaptobrevin (blue) and syntaxin (red) present one transmembrane domain (TM) and one conserved domain (corresponding to the α-helix core domains) each. On the other hand, SNAP-25 (green) presents two conserved domains, no TM but four palmitoylation sites (green tails) which anchor the protein to the plasma membrane. (B) Ribbon model of the synaptic trans-SNARE complex helical bundle formed by the coil coiling interactions of synaptobrevin (blue) syntaxin (red) and SNAP-25 (grey). The helical bundle is based upon high resolution crystal data. (C) Model of the *trans* state of two SNARE complexes that dock a liposome to a supported bilayer *in vitro*. This model was obtained by modifying the membrane-proximal end of the crystal structure of the neuronal SNARE complex to allow the transmembrane domains to enter into the juxtaposed membranes. The transmembrane domains were assumed to be helical. The connecting regions between the transmembrane domains and the core complex are likely flexible. Two SNARE complexes are shown (Brunger *et al.*, 2009).

SNAREs are linked directly to Ca^{2+} triggering of exocytosis, most likely in conjunction with a Ca^{2+} sensor (Sorensen *et al.*, 2002). Numerous auxiliary proteins have been found to be essential for Ca^{2+}-dependent neurotransmitter release, such as synaptotagmin, the Ca^{2+}

sensor, (Perin *et al.*, 1990), complexin (McMahon *et al.*, 1995), Munc18 (Bracher *et al.*, 2000), and Munc13 (Varoqueaux *et al.*, 2002).

As vesicles undergo fusion, the SNARE complex rearranges its configuration from trans to cis (Fig. 1.7). After this remodeling, all the SNARE proteins are localized to one membrane (Lin and Scheller, 1997).

After fusion, the SNARE complex assumes a cis configuration (i.e. with the two TM regions within the same membrane). The cis complex is then thought to be rapidly disrupted by the N-ethylmaleimide sensitive fusion ATPase (NSF) (Lin and Scheller, 1997) and additional proteins; the coiled four-helix bundle is unwound, the SNAREs are allowed to be recycled into synaptic vesicles (Sankaranarayanan and Ryan, 2000) and the synaptic vesicles are retrieved by membrane fission (Jahn *et al.*, 2003).

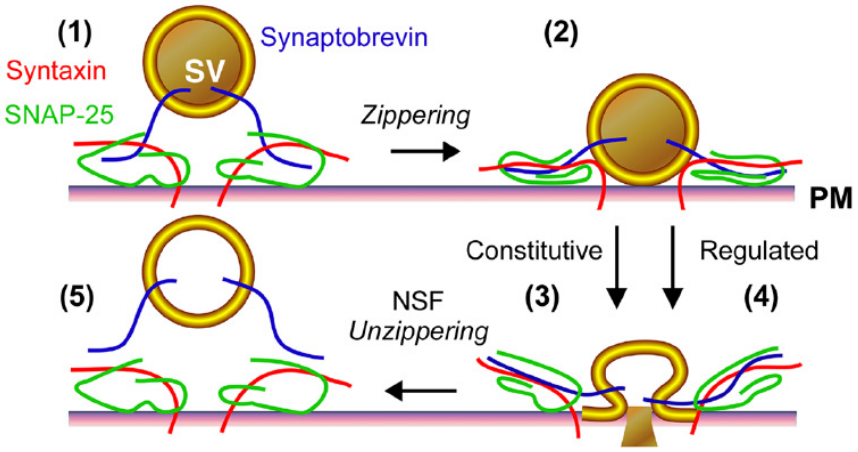

Fig. 1.7. Model of SNARE complex assembly and disassembly in a synaptic vesicle cycle. (1) Synaptobrevin forms a partial trans SNARE complex with syntaxin and SNAP-25. (2) By zippering in an N- to C-termini direction, the SNARE proteins form a trans complex and bring the synaptic vesicle close to the plasma membrane. SNARE-mediated synaptic vesicle exocytosis occurs either spontaneously (3) or evoked by Ca^{2+} (4). (5) cis SNARE complexes are thought to be disassembled by NSF ATPase prior to vesicle recycling. PM, plasma membrane; SV, synaptic vesicle (Lagow *et al.*, 2007).

1.7. SNAP-25: gene and protein

SNAP-25 is a component of the core complex involved in the docking and fusion of synaptic vesicles in nerve terminals. It is located to the plasma membrane (Oyler *et al.*, 1989), anchored by palmitoylated cysteine residues in the central part of the protein (Hess *et al.*, 1992a). SNAP-25 contributes with two a-helices to the formation of the SNARE complex where it assembles with syntaxin and synaptobrevin, which contribute with a single a-helix

each (Sollner *et al.*, 1993). Also the loopy region of the protein, linking the two helices, seems to be intimately involved in fast Ca^{2+} triggering (Nagy *et al.*, 2008).

In mammals, the protein is critical for evoked glutamatergic and cholinergic transmission in central neurons and at neuromuscular junctions (Washbourne *et al.*, 2002). Beyond this specialized functions in regulated secretion pathways in neuronal and neuroendocrine cells, SNAP-25 expression has been detected in granulosa cells (Jo *et al.*, 2004), pancreatic cells (Marshall *et al.*, 2005), chromaffin cells (Lopez *et al.*, 2007; Sorensen *et al.*, 2003), sperm (Hutt *et al.*, 2005), and cumulus cells of ovulating follicles (Shimada *et al.*, 2007). Also in these non neuronal cells, SNAP-25 is required for regulating the release of specific vesicle-contained factors by forming a complex with syntaxin and synaptobrevin.

Like other nerve terminal proteins, SNAP-25 shows strong evolutionary conservation (Catsicas *et al.*, 1991) and sequence homologies to yeast secretion proteins (Bennett and Scheller, 1993). The human SNAP-25 gene is located on chromosome 20; it spans more than 88 kb of genomic DNA and consists of eight different exons (Bark and Wilson, 1994). The protein is located within the presynaptic terminals of hippocampal mossy fibers and the inner molecular layer of the dentate gyrus. The mRNA was found to be enriched within neurons of the neocortex, hippocampus, piriform cortex, anterior thalamic nuclei, pontine nuclei, and granule cells of the cerebellum (Oyler *et al.*, 1989).Furthermore, the human *Snap* locus, like the chicken (Bark, 1993), rat (Jacobsson and Meister, 1996), goldfish and zebrafish (Risinger and Larhammar, 1993), has two alternatively spliced copies of exon 5 (5A and 5B). SNAP-25 is alternatively spliced into two forms, SNAP-25A and SNAP-25B, which results in a difference of nine amino acid residues in the composition of the palmitoylated cysteine-rich domain thought to be responsible for association of the protein with membranes (Bark and Wilson, 1994). This implies that the two isoforms differ in their ability to stabilize vesicles in the primed state (Sorensen *et al.*, 2003) and their capacity or efficiency to be modified by fatty acylation, suggesting divergent abilities to interact with neuronal membranes (Bark, 1993). The B form predominating in the adult nervous tissue. In addition, zebrafish and goldfish have two loci encoding SNAP-25 due to a gene duplication that seems to be unique for Actinopterygian fish (Risinger and Larhammar, 1993) .

In the fly the gene is located on chromosome 3, in an heterochromatic region (Fig. 1.8). *Drosophila Snap-25* contains eight exons distributed over a distance larger than 120 kb and it presents a complex gene organization similar to the human one. In contrast to mammals, chicken, and Actinopterygian fish which have two alternatively used forms of exon 5, only one version of exon 5 has been found in *Drosophila* (Risinger *et al.*, 1997).

Nevertheless the fly *Snap-25* has 3 annotated transcripts and 3 annotated polypeptides: SNAP-25A, SNAP-25C and SNAP-25D. The A isoform corresponds to the neuronal SNAP-25 protein, while the D isoform (shorter due to the alternative spicing of exon 7) has an unknown function. Also the C isoform, which differs from the A one due to an alternative spicing of exon 4, has an unnoted function. Neuronal SNAP-25A mRNA expression and protein are primarily if not exclusively located in the central nervous system (Risinger *et al.*, 1997), as observed in human (Oyler *et al.*, 1989).

While the human protein consists in 206 amino acid residues, in *Drosophila* this sequence is a bit longer, precisely 212 bp (base pairs). This difference affects the N-terminal portion of the protein, where the fly isoform presents one more α-helix turn.

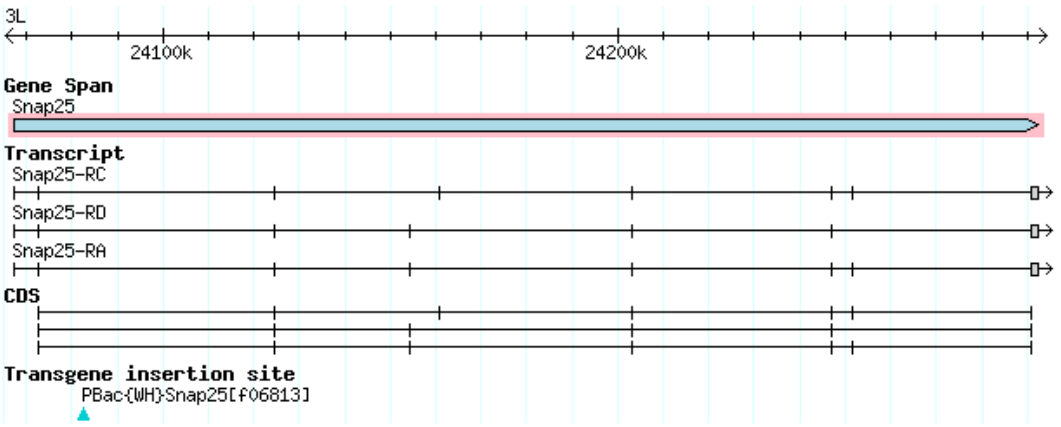

Fig. 1.8. Gene model and products of *Drosophila Snap-25* (http://flybase.org).

1.8. Models of SNAP-25 mutants

SNAP-25 mutants have been generated not only in cell cultures but also in few animal models, such as the fly and the mouse.

Flies carrying null alleles of *Snap-25*, generated by X-ray-induced mutagenesis (Vilinsky *et al.*, 2002), die at the pharate adult stage, and electroretinogram recordings of these animals reveal that synaptic transmission is blocked. Surprisingly, the synaptic physiology at the larval NMJ is normal. This has been explained by the presence of SNAP-24, a closely related *Drosophila* SNAP-25 homologue that can substitute for SNAP-25 in null larvae. Nevertheless, the endogenous levels of SNAP-24 are low in the adult nervous system, so the vicariant role of SNAP-24 is not sufficient to restore a normal phenotype of SNAP-25 null animals (normal synaptic transmission in the optic lobes) (Vilinsky *et al.*, 2002). However, if a *wild-type* or

mutant form of SNAP-25 is present, then SNAP-24 does not appear to take part in neurotransmitter release at the larval NMJ. The apparent redundancy between SNAP-25 and SNAP-24 is due to inappropriate genetic substitution and highly dependent on the genetic and temporal context (Rao *et al.*, 2001).

Looking at the amino acid sequences, SNAP-24 differs from SNAP-25 in the cysteine-rich domain, where it contains three instead of four cysteine residues, which could potentially affect its membrane association dynamics. *In vitro* studies, however, show that SNAP-24 can form core complexes with syntaxin and both synaptic and non-synaptic v-SNAREs (Niemeyer and Schwarz, 2000). *In vivo*, SNAP-24 is expressed throughout development and this protein is found at high levels relative to SNAP-25 at the larval stage (Rao *et al.*, 2001). SNAP-24 is involved in the massive glue secretion in salivary glands (Niemeyer 2000). During metamorphosis into adulthood SNAP-25 expression rises significantly relative to SNAP-24 (Rao *et al.*, 2001). In the adult brain, the protein is found concentrated in the mushroom body neuropil, a region where SNAP-25 levels are very low (Vilinsky *et al.*, 2002). Within neurons, SNAP-25 is concentrated at synapses, while SNAP-24 is predominantly in the cell body (Niemeyer and Schwarz, 2000), suggesting that it is not likely to play a major role in neurotransmitter release in normal larval NMJs. These findings underline that the presence of SNAP-25 is fundamental for viability at the pharate adult stage, underscoring the fact that intracellular vesicular trafficking and membrane fusion are important processes for nervous system development and for the function of neural circuits (Vilinsky *et al.*, 2002). Therefore, the roles of SNAP-24 and SNAP-25 in *Drosophila* may be in some ways analogous to the roles of SNAP-25A and SNAP-25B in mammals (Rao *et al.*, 2001).

SNAP-25^{ts} is a temperature-sensitive paralytic mutant which affects synaptic transmission in 3rd instar larvae (Rao *et al.*, 2001). The point mutation involves an amino acid near the N-terminus, the glycine at the position 50, which is substituted with a glutamine. The *SNAP-25^{ts}* mutant has two effects on neurotransmitter release at the larval NMJ, depending upon temperature: at 22°C, the mutation causes the SNARE complex to be more fusion competent and so evoked release of neurotransmitter is greatly increased; at 37°C, the same mutation leads to fusion incompetence, the single SNARE complex becomes unstable causing the dissociation of the multimer and, as a consequence, the release of neurotransmitter is reduced.

At the non-permissive temperature, the SNAP-25^{ts} isoform acts as a “poison” subunit by impairing the normal activity of the SNARE protein complex and causes loss of function. In SNAP-25^{ts} heterozygotes, the amount of *wild-type* SNAP-25 is sufficient to outcompete the SNAP-25^{ts} poison subunit: hence, the mutation has a recessive phenotype. However, in

SNAP-25^{ts} homozygotes, SNAP-24 levels are insufficient to outcompete SNAP-25^{ts}, resulting in an altered synaptic physiology (Rao *et al.*, 2001). The *SNAP-25^{ts}* larval phenotype appears stronger than the null allele one (Vilinsky *et al.*, 2002). This evidence suggested that missense mutants may therefore have a stronger phenotype and may be ultimately more informative as to the function of the gene than complete null mutants (Rao *et al.*, 2001).

In the mouse a semi-dominant negative allele of *Snap-25* was generated using the chemical mutagen ethylnitrosourea (Nolan *et al.*, 2000). The name of the mutation explains the related phenotype consisting in an altered sensory processing of the animals, which reflects in anxiety behavior exhibited in the light/dark test (blind) and apathetic behavior observed in the playground paradigm test (drunk) (Jeans *et al.*, 2007). The electrophysiological phenotype of the mutants results in a reduction in the frequency of spontaneous mEPSCs, although these were of normal amplitude, and a marked short-term depression of EPSCs at low frequency stimulation. The blind-drunk mutation describes an activity-dependent decrease in neurotransmitter release. This effect is the results of a single amino acid substitution (I67T) in a highly conserved domain of the first SNAP-25 α-helix which is orientated toward the core of the complex. As a consequence, the binding affinity within the core SNARE complex results increased and the synaptic vesicle mobilization and replenishment of the RRP are strongly reduced.

As observed in *Drosophila* null mutants, also in the mouse one the absence of SNAP-25 does not lead to a severe phenotype. In fact vesicle docking persisted, but primed vesicle pools were empty and fast calcium-triggered release abolished. Single vesicular fusion events showed normal characteristics, except for a shorter duration of the fusion pore. *Snap-25^{null}* mice rescued by the ubiquitous over expression of SNAP-23. Over expression of SNAP-23 did not support a standing pool of primed vesicles. This shorter (SNAP-23) isoform can partially vicariate for SNAP-25 (Sorensen *et al.*, 2003).

In vitro experiments have been performed on PC12 cells, a widely employed cell line derived from pheochromocytoma, a neuroendocrine tumor of the medulla of the adrenal glands (Bertherat and Gimenez-Roqueplo, 2005). In mammals, chromaffin cells are neuroendocrine cells found just in the medulla of the adrenal gland (a gland located above the kidneys) and in other ganglia of the sympathetic nervous system. These cells, innervated by the splanchnic nerve, secrete numerous bioactive substances including adrenaline (epinephrine), noradrenaline (norepinephrine), and enkephalin endogenous ligands (endorphins) (Young and Abboud, 2006). Transmitters, hormones neuropeptides, and chromogranins are stored in chromaffin granules, large dense core vesicles (Winkler and Westhead, 1980) from which they are released by regulated exocytosis in a calcium ion-dependent and hormonally

controlled manner (Aunis and Langley, 1999). Due to the similarity between neuroexocytosis and neurosecretion, the chromaffin granule has been a model for membrane fusion. The analysis of the molecular mechanism controlling neuroexocytosis has been greatly helped by studies on chromaffin cells. The priming of docked granules followed by their Ca^{2+}-driven fusion with the plasma membrane and the release of the granule content has been studied in these cells, the role of key factors involved has been highlighted, and the cytosolic and membrane proteins have been linked to priming and fusion processes (Jahn and Sudhof, 1999).

With an elegant work using adrenal chromaffin cells, Sorensen and colleagues (Sorensen *et al.*, 2006) demonstrated that SNAP-25 mutations within the N-terminal portion of the SNARE four helix bundle selectively disrupt vesicle priming by interfering with the stability of the hydrophobic interaction layers holding the complex together. Mutations in the C-terminal end affected fusion triggering. In contrast, similar N-terminal mutations were without effects on exocytosis. Mutations in the middle of the complex selectively interfered only with vesicle priming.

In summary, all the existing mutant SNAP-25 isoforms interfere with the stability of the hydrophobic interaction layers holding the complex together; as a result the mutations provoke the non-assembly or the disassembly of the SNARE complex impairing the vesicle docking or priming/fusion processes.

1.9. SNAP-25 and human pathologies

Recently, several evidences suggest that SNAP-25, in concert with other genes and environmental factors, may be involved in different neuropsychiatric and neurological disorders. Alterations in the *Snap-25* gene structure, expression and/or function may contribute directly to abnormal behavioral phenotypes, including schizophrenia, attention-deficit/hyperactivity disorder (ADHD) and epilepsy (Corradini *et al.*, 2009).

Schizophrenia (MIM - Mendelian Inheritance in Man - 181500) is a common mental disorder with a prevalence of approximately 0.5-1% and significant heritability estimated to be about 85% (Cardno and Gottesman, 2000). The clinical symptoms can be classified into two main categories: psychotic or “positive” symptoms, including hallucinations, altered emotional activity, disorganized behavior; and “negative” symptoms, such as delusions, reduced interest and motivation, and cognitive impairment. Evidence from several immunohistochemical and Western blot studies in postmortem brains showed discrepancies

in altered expression levels of SNAP-25 between different brain regions. These evidences implicate SNAP-25 in the etiology of schizophrenia, explaining the depressed functionality of certain neural circuits, but also the hyperactivity of other pathways that may possibly result from compensatory mechanisms (Thompson *et al.*, 1998).

ADHD (MIM 143465) is one of the most prominent childhood neuropsychiatric disorders. The gene encoding SNAP-25 has been identified as responsible for hyperkinetic behavior based on analysis of the *coloboma* mutant mouse. This mutant mouse is heterozygous for a semi-dominant deletion mutation that encompasses 10-12 genes on chromosome 2, including *Snap-25* (Hess *et al.*, 1996). In *coloboma* mutant mice (*Cm*/+), deletion of the *Snap-25* gene results in 50% lower amounts of the *Snap-25* mRNA and protein expression compared to *wild-type* mice. *Coloboma* mice exhibit normal circadian rhythms and, as in case of children with ADHD, they are hyperactive during their active (nocturnal) phase, with locomotor activity averaging three fold the activity of control littermates (Hess *et al.*, 1992b).

Epilepsy (MIM 604233) is a group of heterogeneous neurologic disorders affecting almost 1% of the population. It is characterized by recurrent, unprovoked seizure episodes, due to abnormal synchronous firing of groups of neurons, arising from periodic neuronal hyper excitability. The *coloboma* mutant mouse, in addition to its hyperkinetic activity, displays frequent spontaneous epileptic seizures, which are thought to arise from abnormalities in calcium transients, caused by a SNAP-25 deficiency, in modulating presynaptic voltage-gated calcium channels (Pozzi *et al.*, 2008).

Besides its well characterized role in regulating exocytosis, there is increasing evidence that SNAP-25 also modulates calcium dynamics in response to depolarization. Effects on SNAP-25 expression could result from altered neural circuits or network function, or from more general perturbations to brain development (Corradini *et al.*, 2009).

1.10. Hypothesis of the SNARE supercomplex

The functional importance of SNARE proteins was demonstrated by observations that it is a target of the eight neurotoxins produced by the anaerobic bacteria of the genus *Clostridium*: one tetanus neurotoxin, TeNT, and seven botulinum neurotoxins, BoNT/A-G (Fig. 1.9).

BoNTs (around 150 kDa) are comprised of three independent domains that mediate neuron intoxication: the heavy chain domain mediates the entry into the neuron by binding to neuronal membrane receptor(s), and the consequent uptake into an endosome-like

compartment; the amino-terminal segment of the heavy chain domain allows the penetration of the light chain into the endosome membrane via a pH-dependent translocation process; the light chain, once within the synaptic cytoplasm, mediates the proteolytic cleavage of specific sites on the neuronal SNAREs (Keller *et al.*, 2004) causing the neuromuscular blockade.

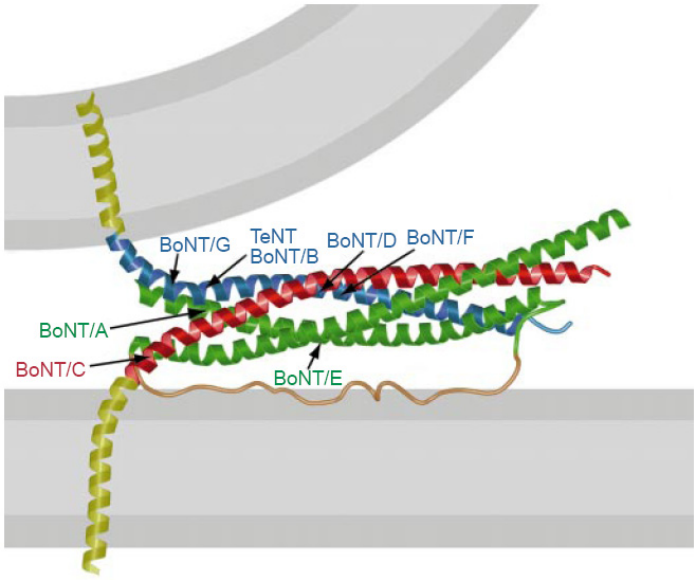

Fig. 1.9. Location of neurotoxin-mediated cleavage sites on the hypothetical model of the synaptic fusion complex as it joins two membranes. The synaptobrevin (blue) neurotoxin-mediated cleavage site for tetanus toxin (TeNT) and botulinum toxin (BoNT) type B (BoNT/B) is between Gln76 and Phe77; for BoNT/F, between Gln58 and Lys59; for BoNT/G, between Ala81 and Ala82; and for BoNT/D, between Lys59 and Leu60. The syntaxin (red) BoNT/C cleavage site is between Lys253 and Ala254. Cleavage sites in SNAP-25 (green) are between Asp193 and Glu194 for BoNT/E, and between Arg176 and Gln177 for BoNT/A (Sutton *et al.*, 1998).

In the case of SNAP-25, three neurotransmission-blocking botulinum toxins can cleave the protein: botulinum neurotoxin type A (BoNT/A) (Blasi *et al.*, 1993a), type C (BoNT/C) (Foran *et al.*, 1996), and type E (BoNT/E) (Schiavo *et al.*, 1993). Considering the mouse sequence, BoNT/A cleaves SNAP-25 at position 197, precisely nine residues from the C-terminus; BoNT/E cleaves at position 180, in the middle of the second a-helix which interacts with the other three a-helixes of the SANREs; BoNT/C cleaves at position 198 (Vaidyanathan *et al.*, 1999). While the substrate of BoNT/A and E is SNAP-25, BoNT/C cleaves also syntaxin (Blasi *et al.*, 1993b).

A striking feature of the action of different BoNTs within nerve terminals is the large difference in the duration of their inhibitory action both *in vitro*, in neuronal cultures (Keller *et al.*, 2004), and also *in vivo*, on the mouse NMJ (Montecucco *et al.*, 2005). BoNT/A and BoNT/C have a longer inhibitory effect on the nerve terminal, while BoNT/E causes a shorter paralysis. Moreover, in the mouse NMJ, cleavage of only 10% of SNAP-25 by BoNT/A is sufficient to block glycine release; in the case of BoNT/E almost a complete cleavage is needed to have the same inhibition on neurotransmitter release (Fig. 1.10).

BoNT/A cleaved SNAP-25 seems to act as a negative dominant isoform, suggesting that the C-terminal region of SNAP-25 may play a central role in the function of the proper

neuroexocytosis machinery. These findings lead to the suggestion that several SNARE complexes may bind together and cooperate to allow the formation of a functional fusion pore (Montecucco *et al.*, 2005).

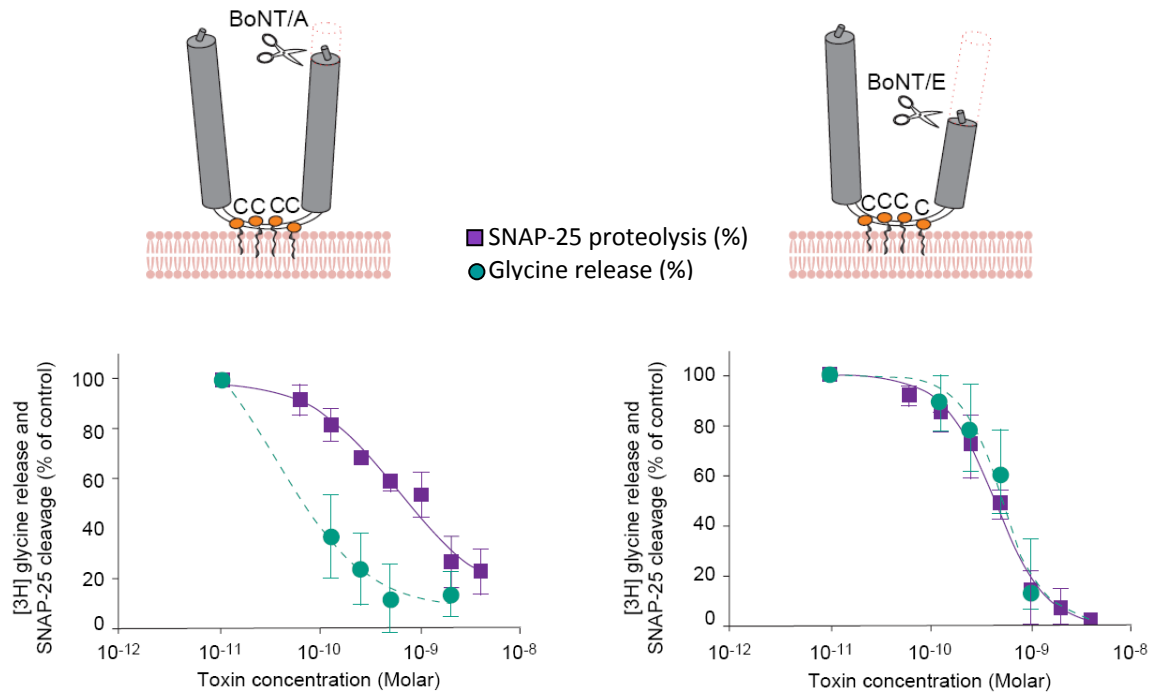

Fig. 1.10. On the top, cartoon of SNAP-25 and the position of BoNT/A and BoNT/E cleavages. On the bottom, dose response curves for the effects of the two botulinum neurotoxins on SNAP-25 proteolysis (purple squares, continuous line) and glycine release (green circles, broken line). The vertical bars indicate the values (C/KSD) for SNAP-25 proteolysis (purple) and glycine release (green).

A sequence conservation analysis was performed on neuronal SNAP-25 amino acid sequences among different species to investigate which amino acids might be involved in contacts between the SNARE complex and other proteins or lipids. This approach highlighted an arginine residue which is highly conserved even if it is not involved in the contacts between the α-helices of the molecular components of the complex (Fig. 1.11). This arginine (at position 189 in mammals) points outside the complex and, due to its positive charge, it is thought to interact with an amino acid, with a negative charge, on the adjacent SNARE complex in order to stabilize the formation of a SNARE supercomplex.

Currently, there are only few scattered pieces of evidence in favor of the hypothesis of a multimeric SNARE supercomplex as a necessary structure involved in the exocytosis of synaptic vesicles. Therefore the kinetics of the vesicle fusion process has been characterized from the energetic and temporal points of view.

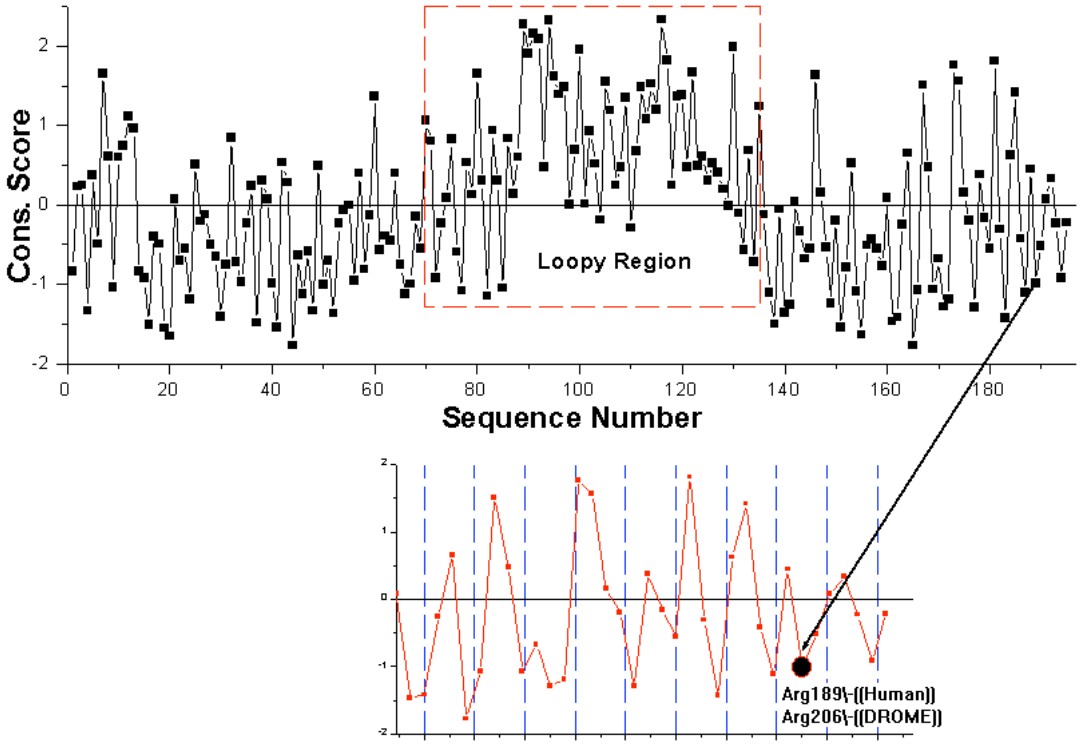

Fig. 1.11. Consensus diagram of SNAP-25 amino acid sequence. The conserved residues have a negative score; the unconserved ones have a positive score (i.e. in the loopy region). The N-terminus sequence of the protein is highlighted. Dashed lines indicate the α-helix steps and the amino acids overlapping those positions are highly conserved due to their interaction with syntaxin and synaptobrevin α-helices. Arg189 (human numeration), which corresponds to Arg206 (*Drosophila* numeration), has a negative score even if it is not involved in contacts with the other SNARE proteins within the single complex (Pantano 2007, data not published).

On the basis of the energetic requirement for membrane fusion, it has been estimated that the formation of three or more SNARE complexes provides sufficient free energy to drive the process (Cohen and Melikyan, 2004). Considering that the time delay between the cytosolic Ca^{2+} trigger and the fusion of docked and ready-to-fuse synaptic vesicles is around 100 microseconds (Kasai, 1999), even if it varies for different types of synapses (Sudhof and Malenka, 2008), it has been proposed that the docked vesicles may be in a state of hemifusion with the presynaptic membrane (Chernomordik and Kozlov, 2008). This would require that the ready-to-fuse vesicles should be actually stably juxtaposed on the cytosolic face of the plasma membrane and this appears to entail the involvement of several SNARE complexes at the same site (Montecucco *et al.*, 2005).

In the last decade, the SNARE supercomplex model has been supported by many biochemical and *in vitro* experiments. Moreover, the precise stoichiometry of the supercomplex has not been established yet. However, the necessity for a multimeric SNARE supercomplex has not been demonstrated *in vivo* yet.

2. AIMS of the RESEARCH

Recently, Montecucco and collaborators (Montecucco *et al.*, 2005) highlighted the key role of the C-terminus of SNAP-25 by performing experiments on the mouse NMJ using different types of botulinum neurotoxins. They proposed that several SNARE complexes should be present at the same site to allow the fusion of a synaptic vesicle with the presynaptic membrane: the assembly of a rosette-shaped oligomer of SNARE complexes, which binds together and cooperate to origin a functional fusion pore, may constitute a crucial event in neuroexocytosis.

Performing sequence conservation analysis on neuronal SNAP-25 protein sequences among different species, a single amino acid which is highly conserved in the protein's C-terminal region was identified, even if this residue does not face the α-helices of syntaxin and synaptobrevin, but instead appears to point outside the complex. In the murine sequence this amino acid is an arginine in position 198. This amino acid is at the first position of the peptide bond cleaved by BoNT/A and it is predicted to not to be involved in the contacts necessary for the formation of the SNARE complex.

To prove the experimental hypothesis and to demonstrate that Arg198 is fundamental for the proper function of the neuroexocytosis apparatus, we decided to introduce non functional SNARE complexes within the rosette in order to interrupt the interactions within the adjacent SNARE complexes.

Drosophila was used as an animal model to test the key role of Arg198 in the process of vesicle fusion. In *Drosophila* the homolog of murine Arg198 is the arginine at the position 206. We performed site-directed substitution in order to replace Arg206 with alanine, a neutral amino acid that should not alter the α-helix structure of SNAP-25 C-terminus or the assembly of single SNARE complexes. We hypothesized that the site-directed substitution could interfere, *in vivo*, preventing the cooperation between the SNARE complexes. As a result we expected an impairment of vesicle fusion with the consequent decrease of neurotransmitter release at the NMJ.

We generated two constructs carrying different isoforms of *SNAP-25* under the UAS promoter: *UAS-SNAP-25*^{WT}, a vector carrying the *wild-type* isoform, our control; and *UAS-SNAP-25*^{R206A}, a vector carrying the point mutated isoform of the protein, our mutant.

The plasmids were microinjected to generate several transgenic lines in a *SNAP-25* wild-type background. The *Elav-GAL4* diver was used to direct the expression of the transgenes within the nervous system. The expression levels of the transgenes were analyzed, the electrophysiological profiles were recorded from the larval NMJ, the morphology and the morphometry of the synapse was measured, and the behavior of the larvae and the adults was characterized. Moreover, we verified, *in vitro*, the assembly of the SNARE complex in the presence of mutated SNAP-25.

3. METHODS

3.1. Site-directed mutagenesis: first generation plasmids

Four isoforms of SNAP-25 (three mutants and one *wild-type*) were produced by polymerase chain reaction (PCR) using primers carrying the required point mutations. The ORF coding for SNAP-25 was amplified from the full-length cDNA derived from w^{1118} flies using the following oligonucleotides (5'-3' orientation):

NAME	SEQUENCE
sense SNAP-25	CGGAATTCATGCCAGCGGATCCATCTGAAG
antisense SNAP-25^{WT}	CTCTCGAGTTACTTTAATAGTTGATGTGCC
antisense SNAP-25^{R206A}	CTCTCGAGTTACTTTAATAGTTGATGTGCCGCTTGATTAGC
antisense SNAP-25^{R199A}	CTCTCGAGTTACTTTAATAGTTGATGTGCCCTTTGATTAGCAACTGCTA TCGCCGCTTCATTAG
antisense SNAP-25^{R199A,R206A}	CTCTCGAGTTACTTTAATAGTTGATGTGCCGCTTGATTAGCAACTGCTA TCGCCGCTTCATTAG

Sense and antisense primers have at their 5' ends the restriction sites for *Eco*RI (GAATTC) and *Xho*I (CTCGAG), respectively (underlined nucleotides). Mutated sites are highlighted.

PCRs were performed in a 50-µl reaction mixture containing:

- 1X Expand High Fidelity Buffer
- 1.5 mM $MgCl_2$
- 10 pmol each pair of primers
- 1 mM dNTPs
- 50 ng cDNA
- 2.6 U Expand High Fidelity enzyme mix (Roche, USA)

Amplification program:

- first denaturation step: 4' at 94°C
- 35 rounds of amplification:
  94°C for 30''(denaturation), 68°C for 30'' (annealing), 72°C for 1' (elongation)
- final incubation step: 72°C for 10'

A further incubation step at 72°C for 15' was necessary with GoTaq DNA polymerase (Promega, USA) to add an adenine (A) at the 3'-term of each PCR product.

The obtained 655 bp PCR products were ligated into the pCR2.1-TOPO vector (Invitrogen, USA) (Fig. 3.1) which was used to transform One Shot TOP10 *E. coli* cells (Invitrogen, USA). Positive clones were detected by β-galactosidase screening and sequencing (BRM Genomics, Italy).

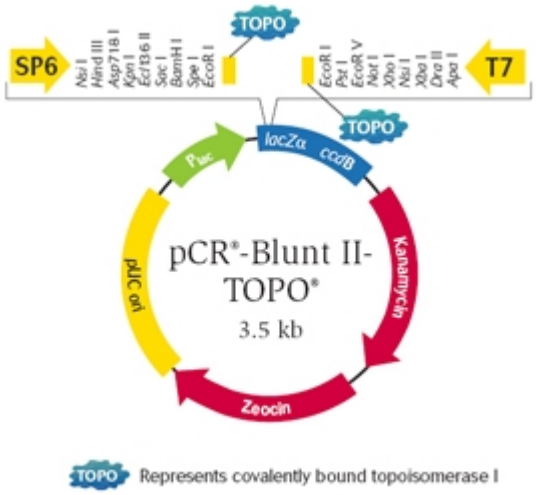

Fig. 3.1. pCR2.1-TOPO Map. The map below shows the features of pCR®2.1-TOPO® and the sequence surrounding the TOPO® Cloning site. Restriction sites are labeled to indicate the actual cleavage site. The arrow indicates the start of transcription for T7 polymerase. The plasmid consists in 3931 nucleotides and it contains:

- LacZα fragment: bases 1-547;
- M13 reverse priming site: bases 205-221;
- Multiple cloning site : bases 234-357 ;
- T7 promoter/priming site : bases 364-383 ;
- M13 Forward (-20) priming site : bases 391-406;
- F1 origin: bases 548-985;
- Kanamycin resistance ORF: bases 1319-2113;
- Ampicillin resistance ORF : bases 2131-2991;
- pUC origin : bases 3136-3809.

Using conventional restriction enzyme digestion techniques, sequences were extracted with *Eco*RI and *Xho*I and ligated into the pUAST *Drosophila* transformation vector (Fig. 3.2).

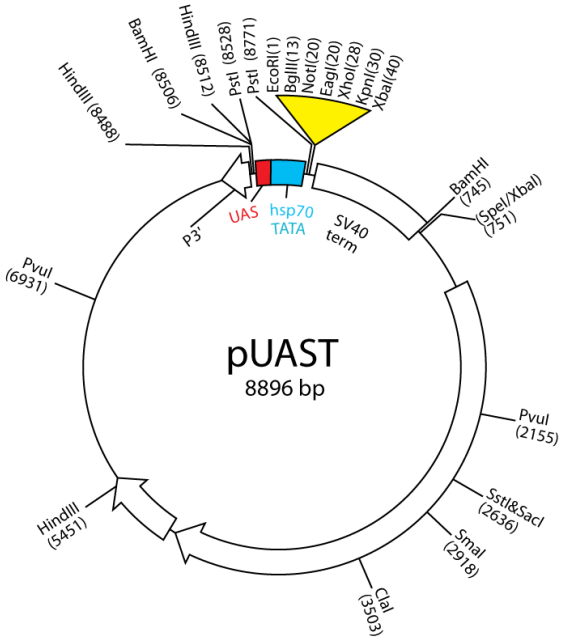

Fig. 3.2. pUAST Map. The plasmid consists of five tandemly arrayed optimized GAL4 binding sites followed by the hsp70-TATA box and transcriptional start, a polylinker containing unique restriction sites for *Eco*RI, *Bgl*II, *Not*I, *Xho*I, *Kpn*I and *Xba*I, and the SV40 small T intron and polyadenylation site. These features are included in a P-element vector (pCaSpeR3) containing the P element ends (P3' and P5') and the miniwhite gene which acts as a marker for successful incorporation into the *Drosophila* genome (Brand and Perrimon, 1993).

The resulting plasmids, pUAS-SNAP-25^{WT}, pUAS-SNAP-25^{R206A}, pUAS-SNAP-25^{R199A} and pUAS-SNAP-25^{R199A,R206A} were again sequenced (BRM Genomics, Italy) to ensure that the mutation

occurred only at the position of interest and to verify the proper orientation inside the vector of each ORF (open reading frame).

These plasmids were then used for embryo transformation. P-element-mediated germline transformation was done using a *Drosophila* embryo injection service (Best Gene Inc, CA, USA). Briefly, the constructs with the *miniwhite*$^{+}$ marker were injected into *w*^{1118} embryos. *FM7* (X chromosome), *CyO* (chromosome 2) and *TM6(sb)* (chromosome 3) balancers were used to balance these lines.

3.2. Site-directed mutagenesis: second generation plasmids

Two isoforms of syntaxin, one *wild-type* and the D253A, were produced by PCR using primers carrying point mutations as necessary. The ORFs coding for the two genes were amplified from the full-length cDNA derived from *w*^{1118} flies using the following oligonucleotides (5'-3' orientation):

NAME	SEQUENCE
sense SYX	CCGCGGCCGCATGACTAAAGACAGATTAGCCGCTC
antisense SYX^{R253A}	CCTTCTTGGTGGCCTGAGTTG
sense SYX^{R253A}	CAACTCAGGCCACCAAGAAGG
antisense SYX	GGCTCGAGTTACATGAAATAACTGCTAACATATGAGG

The restriction sites for *Not*I (GCGGCCGC) and *Xho*I (CTCGAG) are underlined. Mutated sites are highlighted.

For the generation of *syx*^{WT} gene we proceeded as explained in the previous paragraph. In order to introduce the point mutation D253R we performed two sequential PCRs reaction because the amino acid to substitute is in a central position; so we generated two fragments of the gene, one from the 5'-terminus to the region of Asp253 and the other one form this region to the 3'-terminus, that we combine together to generate the sy*x*^{D253R} gene.

Cloning, screening and sequencing were performed as previously described.

The plasmids pUAST-SYX^{WT} and pUAST-SYX^{D253R} were used for embryo transformation and P-element-mediated germline transformation was done by the TransFlyer (Ferrara, Italy), a *Drosophila* embryo injection service. Also in this case, the two constructs with the *miniwhite*$^{+}$ marker were injected into *w*^{1118} embryos. *FM7* (X chromosome), *CyO* (chromosome 2) and *TM3* (chromosome 3) balancers were used to balance the transgenic lines.

3.3. Site-directed mutagenesis: third generation plasmid

Finally, one more mutant isoforms of SNAP-25 (R206D) and syntaxin (D253R) were produced. The ORFs coding for the two genes were amplified from the full-length cDNA derived from w^{1118} flies using the following oligonucleotides (5'-3' orientation):

NAME	SEQUENCE
sense SNAP-25	CGGAATTCATGCCAGCGGATCCATCTGAAG
antisense SNAP-25^{R206D}	GGACGCGTTTACTTTAATAGTTGATGTGCGTCTTGATTAGCAACTG
sense SYX	CCGCGGCCGCATGACTAAAGACAGATTAGCCGCTC
antisense SYX^{D253R}	CCTTCTTGGTGCGCTGAGTTG
sense SYX^{D253R}	CAACTCAGCGCACCAAGAAGG
antisense SYX	GGCTCGAGTTACATGAAATAACTGCTAACATATGAGG

Restriction sites for *Eco*RI (GAATTC), *Mlu*I (ACGCGT) and *Xho*I (CTCGAG), are underlined. Mutated sites are highlighted.

PCRs, cloning, screening, sequencing and microinjection followed as described in the previous paragraphs.

3.4. Double-pUAST generation

A new expression plasmid was generated by the duplication of a region of the pUAST vector (Brand and Perrimon, 1993) containing an hsp70-TATA box, transcriptional start, a polylinker, the SV40 small T intron and polyadenylation site. The polylinker was substituted to introduce new unique restriction sites for enzymes different from those already present in the original polylinker.

By PCRs were generated two regions: one containing hsp70 TATA box, transcriptional start and a new polylinker (introduced by the primer), the other containing the SV40 small T intron and polyadenylation site. The following oligonucleotides (5'-3' orientation) were used:

NAME	SEQUENCE
sense UAS+hsp70	CCAGATCTCTCTCCGGATCCAAGCTTGC
antisense UAS+hsp70	GGGCGGCCGCCCAATTCCCTATTCAGAGTTCTCTTC
sense polylinker+SV40	GGGAATTCACGCGTGGCCCGCGGGGCCACTAGTATTTAAATGGATCTTTGT GAAGGAACCTTAC
antisense SV40	GGAGATCTGAATTAGGCCTTCTAGTGGATCC

Restriction sites for *Bgl*II (AGATCT), *Not*I (GCGGCCGC) and *EcoR*I (GAATTC) are underlined. The new polylinker is highlighted.

As showed in Fig. 3.3, first, the fragment polylinker+SV40 was cloned in pUAST using *EcoR*I and *Bgl*II sites; then, the fragment UAS+hsp70 was cloned using *Bgl*II and *Not*I sites.

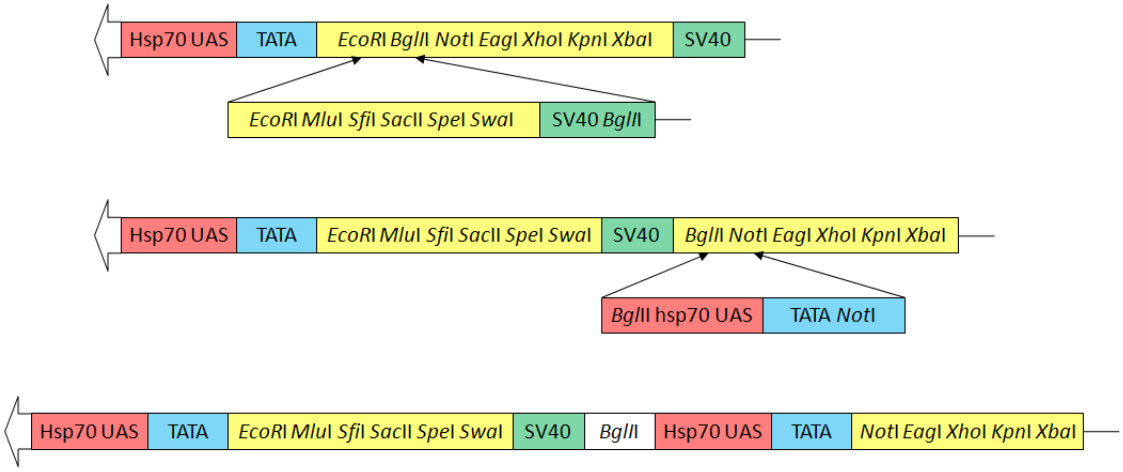

Fig. 3.3. Scheme describing the generation of double-pUAST.

3.5. Fluorescent proteins cloning

The two fluorescent proteins, EGFP and dsRED.T4.NLS, were amplified by PC using the following oligonucleotides (5'-3' orientation):

NAME	SEQUENCE
sense EGFP	GGCCGCGGCCGCGAATTCATGGTGAGCAAGGGCGAGGAGCT
antisense EGFP	CCGGCTCGAGACGCGTTTACTTGTACAGCTCGTCCATGC
sense dsRED	CGCCGCGGCCGCGAATTCATGGCCTCCTCCGAGGACGTCAT
antisense dsRED	CCGGCTCGAGACGCGTCTAGAGTCGCGGCCGGCCGCTGT

Sense primers have the restriction sites for both *Not*I and *Eco*RI. Antisense primers have the restriction sites for both *Mlu*I *Xho*I. This will allow the cloning of the two genes in both the polylinkers of the double-pUAST using *Eco*RI-*Mlu*I and *Not*I-*Xho*I enzyme pairs.

3.6. Transgenes expression

These new alleles of *SNAP-25* were expressed in flies with a *SNAP-25 wild-type* background using the GAL4/UAS system (Brand and Perrimon 1993). This system consists of two parts: the *GAL4* gene, encoding the yeast transcription activator protein Gal4, and the UAS (Upstream Activation Sequence), a short part of the promoter region, to which Gal4 specifically binds to activate gene transcription.

ElavGAL4 (pan-neuronal promoter) virgin females were crossed to homozygous *UAS-SNAP-25^{WT}*, *UAS-SNAP-25^{R206A}* and *UAS-SNAP-25^{R199A,R206A}* males. Experiments were carried on the F1 progeny.

Flies were raised on a standard yeast-glucose-agar medium and were maintained at 22°C, 70% relative humidity, in a 12 hours light:12 hours dark cycle.

3.7. Viability assay

100 male transgenic flies, carrying the different isoforms of SNAP-25, were crossed with 200 virgin female *ElavGAL4/ElavGAL4* and placed in an egg-laying chamber that consists in a small agar plate with a dab of live yeast covered by a plastic beaker with tiny holes to allow fresh air exchange. Flies were incubated at 22°C to allow egg laying on the agar plate.

After 1 hour the flies were removed from the chambers and the agar plates were photographed; the number of embryos were counted. The plates were reattached to the beakers and the embryos were allowed to develop.

After 5 days the number of pupae on the walls of the tubes were counted. Finally, after 5 more days, the number of adults was counted.

3.8. Larva dissection technique

Third instar larvae were dissected in Ca^{2+}-free haemolymph-like saline-3 (HL3) (Stewart *et al.*, 1994) and pinned on the silicone coated surface (Sylgard 184; Dow Corning, USA) of a 35 mm Petri dish using fine insect forceps, scissors and pins (FST, Germany) (Jan and Jan, 1976b).

HL3 solution: (in mM) 70 NaCl, 5 KCl, 0.2 $CaCl_2$, 20 $MgCl_2$, 10 $NaHCO_3$, 5 trehalose, 115 sucrose, and 5 HEPES, pH 7.3.

Dissection procedure:

1. 500 µl of cold HL3 was placed on the dissection plate;
2. the selected third instar larva was placed in the drop of HL3;
3. first, a pin was placed squarely in the head of the larva near the mouth hooks, then another pin between the posterior spiracles. The animal was stretched out lengthwise;
4. using the scissors, a vertical cut along the dorsal side of the larva was made, just from the anterior pin to the posterior one;
5. the flaps were pinned, stretching the body wall both horizontally and vertically;
6. the organs were removed taking extra care not to damage the muscles. First, the tracheal system was removed. Then, the rest of the organs were grabbed using the forceps and removed using the scissors. Finally, if needed, the nerves were cut at the base of the brain and removed;
7. the body wall preparation was washed with fresh HL3.

3.9. Electrophysiology

Following dissection, third instar larval body walls were washed two times with 1 mM Ca^{2+} HL3 and left to incubate in fresh 1 mM Ca^{2+} HL3 solution for at least 15' before experiment onset.

Electrophysiological recordings were performed on fibres 6 or 7 of abdominal segment 3 or 4 using intracellular glass microelectrodes (1.2 mm o.d.; 0.69 mm i.d.; 10-12 MW resistance; Science Products, Germany) filled with a 1:2 solution of 3 M KCl and 3 M CH_3CO_2K. Fibres with a membrane resting potential lower than -60 mV were discarded. In each fibre both spontaneous and evoked neurotransmitter release were recorded. No more than one fibre for each larval body wall was utilized for electrophysiological recording.

In all experiments, particular care was taken to avoid the microelectrode exiting from the fibre or fibre membrane damage. Because evoked release can influence spontaneous neurotransmitter release, each activity was recorded in a separate set of experiments. The experiments lasted maximum 60' to prevent shift of resting membrane potential or fibre alterations due to tissues degeneration.

For quantifying Ca^{2+} dependence of both spontaneous and evoked neurotransmitter release, after dissection, body walls were first incubated in 1 mM Ca^{2+} HL3 for at least 15'. After the spontaneous or evoked release was recorded, the bathing solution was replaced with one containing 3 mM Ca^{2+} HL3, taking particular care to maintain in place the intracellular microelectrode and that resting membrane potential remained substantially unchanged (apart from the physiological shift due to the different extracellular Ca^{2+} concentrations). After an additional 15' incubation, spontaneous or evoked release was recorded again, and the bathing solution was changed to one containing 5 mM Ca^{2+} HL3; following a further 15' incubation, a new recording of spontaneous or evoked release from the same fibre was performed.

3.10. Intracellular recording of spontaneous neurotransmitter release

Spontaneous neurotransmitter release was analyzed by intracellularly recording miniature end-plate potentials (MEPPs) under current-clamp conditions. Resting membrane potential was clamped at -70 mV.

Spontaneous neurotransmitter release was also analyzed by intracellularly recording miniature end-plate currents (MEPCs) under current-clamp conditions. In this case, microelectrode series resistances were corrected to 95%.

3.11. Intracellular recording of evoked neurotransmitter release

Evoked junction potentials (EJPs) were intracellularly recorded under current-clamp conditions. Resting membrane potential was clamped at -70 mV. The single segmental nerve innervating abdominal segment A3 or A4 was stimulated (stimulus duration 0.1 milliseconds, 1.5 threshold voltage (Wu and Haugland, 1985)) using a suction microelectrode, filled with extracellular bathing solution and connected to a stimulator (S88, Grass, USA) via a stimulus isolation unit (SIU5, Grass, USA).

A protocol was used to perform intracellular recordings of neurotransmitter release at several frequencies of stimulation:

- 4': no stimulation;
- 2': stimulation at 0.5 Hz;

- 40'': stimulation at 10 Hz;
- 2': stimulation at 0.5 Hz;
- 5 series of paired pulse stimulation, which consists on the application of 2 stimuli in close succession; the spacing intervals used were: 100 ms, 75 ms, 50 ms and 25 ms;
- 10': stimulation at 30 Hz.

Signals were amplified in current-clamp mode by a patch-clamp amplifier (Axopatch 200, Axon, USA).

3.12. Data analysis

Amplified signals were digitized using a digital A/C interface (National Instruments, USA) and then fed to a PC for both on-line visualization and off-line analysis using an appropriate software (WinEDR, Starthclyde University; pClamp, Axon, USA).

Stored data, were analyzed off-line using appropriate software (pClamp, Axon, USA). Statistical analysis and graph construction were carried out using Prism software (GraphPad, USA).

3.13. NMJ immunohistochemistry

NMJ axon terminals and synaptic boutons of A3-A4 fibres 6 and 7 were stained in body-wall preparations using the neuronal membrane marker anti-HRP antibody. During the dissection the central nervous system was not removed to maintain intact the nerve organization of the body wall.

PBS solution: 137 mM NaCl, 2.7 mM KCl, 10 mM sodium phosphate dibasic, 2 mM potassium phosphate monobasic, pH of 7.4.

The coloration of the nervous system followed a procedure performed at RT. The body wall preparation was:

1. washed with phosphate buffered saline (PBS);
2. incubated with 4% Paraformaldehyde (Sigma, USA) in PBS;
3. washed with 0.2% Triton X-100 (Sigma, USA) in PBS;
4. washed 3 times for 5' with 0.1% Tween 20 (Sigma, USA) in PBS;

5. incubated 30’ with 0.1% Bovine Serum Albumin (BSA) (Sigma, USA) in PBS;
6. incubated 2 hours with the primary anti-HRP and anti-NC82 antibodies (dilution 1:300 in PBS) (Cappel MP Biomedicals, USA);
7. washed with 0.2% Triton X-100 in PBS;
8. Washed 3 times for 5’ with 0.1% Tween 20 in PBS;
9. incubated 2 hours with the secondary FITC-conjugated rabbit anti-goat IgG antibodies and TRITC-conjugated rabbit anti-mouse IgG (dilution 1:300 in PBS) (Sigma-Aldrich, USA);
10. washed with 0.2% Triton X-100 in PBS;
11. washed 3 times for 5’ with 0.1% Tween 20 in PBS;
12. briefly washed in fresh H_2O milliQ.

Lastly, the pins were remove from the body wall preparation and the sample was mounted using Mowiol 4-88 medium (Polysciences Inc., USA).

Images were acquired with a video-confocal microscope (VCM; Mangoni Biomedica, Pisa, Italy). Briefly, in VC microscopy an arc lamp is used as a multi-point excitation source and a CCD camera as an image detector. Confocal performance is achieved using an original processing method (US patent 6.016.367), which allows high spatial resolution and spectral flexibility.

Optical sections of 0.5 µm were acquired using a 20X/0.75 NA dry objective (Nikon Instruments, Japan). Acquired images were then collapsed into a single image with a maximum intensity projection algorithm. Bouton diameter was measured with NIS AR software (Nikon Instruments, Japan). Bouton area was measured on digital images, using ImageJ software. Statistical analysis of bouton areas and diameters was performed with Prism software.

3.14. RNA extraction

Total RNA was extracted from approximately 10 larvae and 30 larval brains with Trizol Reagent (Invitrogen) following the manufacturer’s instruction:

Homogenization:

- animal tissue samples (~100mg) were grinded in 1 ml of Trizol Reagent using a power homogenizer;
- samples were incubate at RT for 5‘.

Phase separation:

- 0.2 ml of chloroform were added; samples were vigorously mixed, using the vortex for 15'' , and incubated at RT for 3';
- samples were centrifuged at 12,000 x g for 15' at 4°C;
- following centrifugation, the mixture separated into lower red, phenol-chloroform phase, an interphase, and a colorless upper aqueous phase which contains the RNA.

RNA precipitation:

- without disturbing the interphase, the aqueous phase was carefully transferred into fresh tube containing 0.5 ml of isopropyl alcohol;
- samples were incubated at RT for 10';
- samples were centrifuged at 12,000 x g for 10'. The RNA precipitate formed a pellet on the side and bottom of the tube.

RNA wash:

- the supernatant was completely removed;
- the RNA pellet was washed once with 1 ml of 75% ethanol;
- samples were mixed by vortexing and centrifuged at 7,500 x g for 5' at RT;
- all leftover ethanol was removed.

Redissolving RNA:

- the RNA pellet was air-dry for 10' at RT;
- the RNA was dissolved in DEPC (DiEthyl PyroCarbonate)-treated water by passing solution a few times through a pipette tip. DEPC is an efficient, nonspecific inhibitor of RNases;
- the RNA was resuspended in 10 µl of DEPC-treated water.

Spectophotometric analysis:

- dilute 1 µl of RNA with 999 µl of DEPC-treated water (1:1000 dilution);
- using the spectrophotometer (Beckman-Coulter DU530) take OD at 260 nm and 280 nm to determine sample concentration and purity. The A_{260}/ A_{280}ratio should be between 1.6 and 2. Apply the convention that 1 OD at 260 equals 40 µg/ml RNA to calculate the RNA concentration using the formula: [RNA] µl/ml = 40*A_{260}

3.15. RT-PCR

The first-strand of cDNA was synthesized by reverse transcription (RT)-PCR on mRNA, employing SuperScript II (Invitrogen, USA) according to the manufacturer's instructions. Reaction mix placed in 12 µl volumetric flask with DEPC-treated water:

- 1 µg RNA
- 1 mM dNTPs
- 1 µM oligo-dT (17 polyT)

Samples were incubated 5' at 65°C to denature RNA hairpins and other secondary structures, then the following reagents were add in a total volume of 20 µl of DEPC-treated water:

- 1X First-Strand Buffer
- 0.1 M DiThioThreitol (DTT) (Invitrogen, USA)
- 40 U RNaseOUT^{TM} (Invitrogen, USA)
- 100 U Superscript II

Samples were incubated 1 hour at 42°C. Afterwards the enzyme was inactivated by a following incubation of 15' at 75°C.

3.16. Semi-quantitative PCR

In each PCR reaction, a fragment of the constitutively expressed *rp49* (ribosomal protein 49KDa) mRNA and the 3'-term portion of one SNAP-25 isoform were amplified, using the following oligonucleotides (5'-3' oriented):

NAME	SEQUENCE
sense SNAP-25	GGATAACGAACGACGCTAGAGA
antisense SNAP-25^{WT}	TACTTTAATAGTTGATGTGCCCT
antisense SNAP-25^{R206A}	TACTTTAATAGTTGATGTGCCGC
sense *rp49*	ATCGGTTACGGATCGAACAA
antisense *rp49*	GACAATCTCCTTGCGCTTCT

Antisense SNAP-25^{WT} and antisense SNAP-25^{R206A} are different in the last 2 nucleotides at the 3'-term (underlined), which determine the specificity of each primer for the corresponding isoform.

PCRs were performed in a 50 µl reaction mixture containing:

- 1X Expand High Fidelity Buffer
- 1.5 mM $MgCl_2$
- 10 pmol each pair of primers
- 1 mM dNTPs
- 50 ng cDNA
- 2.6 U Expand High Fidelity enzyme mix (Roche, USA)

Amplification program:

- first denaturation step: 4’ at 94°C
- 35 rounds of amplification:
  94°C for 30’’(denaturation), 65°C for 30’’ (annealing), 72°C for 45’ (elongation)
- final incubation step: 72°C for 7’

The sizes of the PCR products were 210 bp in the case of the *SNAP-25* isoforms and 164 bp in the case of *rp49*. The PCR products were analyzed by 1% agarose gel electrophoresis and the resultant digital image of the gel was captured using a UV transilluminator.

The intensity of the bands was quantified using Image Pro Plus 6.0 (Media Cybernetics, USA). WT and mutant SNAP-25 isoforms expression was calculated relative to the median values of the *rp49* housekeeping mRNA.

3.17. Analysis of locomotor behavior

- *Larvae*

The locomotor activity of a single third instar larva inside an arena was recorded for a 10’’ period using a video tracking system.

Third instar wandering larvae emerging from the food of a vial were selected, briefly washed with water and put in the middle of the arena. The arena consisted in a Petri dish (5 cm in diameter) covered by a thin layer of agar gel 1%. If the larva did not start to move, it was stimulated using a drop of water on the dorsal surface.

The Petri dish was placed inside a box, the internal walls of which were painted black, containing a ring of ultrabright white leads to generate a uniform illumination. After having closed the box, the movement of the larva inside the arena was video recorded using a Canon digital video camera (10 frames per second). Video signals were fed online to a PC through a video-interface. A specific software (AnyMaze, Stoelting, USA) was utilized to track the path covered by the moving animal during the recording time period of 10’’. The software calculated the total length of the path, the average speed and the maximum speed of the larvae. A total number of 50 larvae were analyzed for each genotype. The tests were performed at the same time interval of the day for all strains.

- *Adults*

The locomotor activity of adult flies was analyzed by recording with a video tracking system as in the case of the larvae. In this case movements of single adult flies inside an arena were recorded for a 10' period.

Adult flies collected 3-5 days after pupal eclosion, were anaesthetized under CO_2 and single adult flies were collected and placed into small transparent vials (4.5 cm in length and 1.5 cm in diameter) with no food and water ad libitum (provided by a piece of wet paper inserted under the cotton plug). Each vial contained a single fly. Flies were then left to rest overnight (at least 10 hours) in order to have a complete recovery from CO_2 anesthesia. Five minutes before the experiment, the wet paper was removed from each vial. The vial was then placed inside a box with the uniform and ultrabright white illumination. After having closed the box, the movement of the fly inside the vial (the arena) was video recorded. Every time the animal stopped moving for more than 2'', the pause was considered an immobility episode. During the immobility episode, the animal body did not change its coordinates inside the arena, even if it was moving its legs or wings. The tracking software automatically analyzed the number of immobility episodes and their total time duration (sum of the time duration of each immobile episode). The software calculated also the time spent during active movement together with the average speed during active movement and the total distance covered. It was impossible to analyze the maximum speed because the adults can jump inside the vial, skewing the data. A total number of 24 flies were analyzed for each genotype. Again, the tests were performed at the same time interval of the day for all strains.

3.19. Bang test

Flies were collected under CO_2 at 3-5 days after eclosion and kept at 6 animals/vial for 1 day before behavioral analysis in order to have a complete recovery from CO_2 anesthesia. Vials were transparent, 15 cm in length and 1.2 cm in diameter, with no food inside and water ad libitum through a piece of wet paper that was removed 5 minutes before the experiment. Each vial was mechanically stimulated by placing on a bench-top vortex for 10'' at the maximum setting. After the stimulation, the vial was allowed to drop into a graduated cylinder (with marks at 28, 56, 84 and 112 mm) so that the flies would all fall on the bottom. Subsequently a webcam recorded the movements of the flies for 30'' at 10 frames per second. Video signals were fed online to a PC through a video-interface. Video recordings were analyzed using Image Pro Plus 6.0 (Media Cybernetics, USA). Different phenotypes

were defined as follow: flies that were lying on the bottom of the vial unable to right themselves; flies that remained on the bottom of the vial but were able to stand on their legs; and flies able to climb the wall of the vial, reaching the different marks. The number of flies in each group was counted. Moreover, within the group of the flies able to climb the wall of the vial, the time needed to reach the different marks was also measured.

4. RESULTS

4.1. Site-directed mutagenesis

In order to destabilize the multimeric SNARE complex, we mutated the key arginine residue. As already anticipated, the *Drosophila* protein is longer than the mouse one, respectively 212 and 206 amino acids, and it presents one more α-helix turn at the N-terminus. From a predicted three-dimensional structure of the fly protein we identified two homologs of the murine Arg198: the Arg199 and the Arg206; these two aminoacids faces the same side of the α-helix and are close together in the predicted three-dimensional structure (the crystallographic analysis of the *Drosophila* SNAP-25 is not reported in any database).

We decided to substitute the arginine, which has a positive charge, with alanine, which is a neutral amino acid often present in α-helix structures so it should not produce alteration in the structure of the protein. Moreover, alanine has a small apolar side chain which should not introduce steric hindrance in SNARE complex formation or change the surface charge of the complex. This is important, because several other proteins (e.g. synaptotagmin, complexin) bind to the surface of the SNARE complex through polar interactions.

We decided also to not attach a tag to the transgenic protein in order not to risk altering the interactions between SNAP-25 and other regulatory elements, protein or lipids.

Several independent transformant lines were established for each construct except pUAS-SNAP-25^{R199A} which was not injected due to technical problems. We thus obtained:

- 5 lines carrying *UAS-SNAP-25^{WT}*
- 7 lines carrying *UAS-SNAP-25^{R206A}*
- 6 lines carrying *UAS-SNAP-25^{R199A,R206A}*

Lines carrying the *UAS-SNAP-25^{WT}* transgene, the *UAS-SNAP-25^{R206A}* transgene and the *UAS-SNAP-25^{R199A,R206A}* transgene on the 2nd or the 3rd chromosome were chosen on the basis of their homozygous viability.

We focused our investigation only on the R206A mutation because preliminary results carried out the *UAS-SNAP-25^{R199A,R206A}* were almost the same as the ones obtained with the

UAS-SNAP-2^{R206A} and also because a further comparison between the human and the fly SNAP-25 sequences indicated Arg206 as the most probable candidate as shown in Fig. 4.1.

```
human     MPADPSEEVAPQVPKTELEELQINAQGVADESLESTRRMLALCEESKEAGIRTLVALDDQ 60
fly       MAEDAD-------MRNELEEMQRRADQLADESLESTRRMLQLVEESKDAGIRTLVMLDEQ 53
          *. *..        :.****:* .*: :************ * ****:******* **:*

Human     GEQLDRIEEGMDQINADMREAEKNLSGMEKCCGICVLPCNKSQSFKEDDGTWKGNDDGKV 120
fly       GEQLERIEEGMDQINKDMKEAEKNLTDLGKFCGLCVCPCNKLKSSDAYKKAWGNNQDG-V 112
          ****:********** **:******:.: * **:** **** :* .  . :* .*:** *

human     VNNQPQRVMDDRNGMMAQAGYIGRITNDAREDEMEENMGQVNTMIGNLRNMALDMGSELE 180
fly       VASQPARVVDEREQMAISGGFIRRVTNDARENEMDENLEQVSGIIGNLRHMALDMGNEID 172
          * .** **:*:*: *  ..*:* *:******:**:**: **. :*****:******.*::

human     NQNRQIDRINRKGESNEARIAVANQRAHQLLK-- 212
fly       TQNRQIDRIMEKADSNKTRIDEANQRATKMLGSG 206
          .******** .*.:**::**  ***** ::*
```

Fig. 4.1. Clustal v.2.0.12 alignment of human (Swiss-Prot: P60880.1) and fly (Swiss-Prot: P36975.1) SNAP-25 sequences.

4.2 - The expression of the SNAP-25 isoforms does not affect the viability

First of all we analyzed if the presence of the mutant protein and the overexpression of the *wild-type* one in the nervous system had any effect on the life cycle of the animals.

Homozygous *ElavGAL4* virgin females were crossed to males homozygous for either the *UAS-SNAP-25*^{WT} or the *UAS-SNAP-25*^{R206A} constructs. The F1 animals produced the SNAP-25 *wild-type* protein, encoded by the corresponding endogenous gene, as well as either of also the transgenic SNAP-25 proteins (*wild-type* or mutant), encoded by the transgenes.

The *elav* (*embryonic lethal abnormal vision*) gene of *Drosophila* is necessary for the proper development of the embryonic and adult nervous systems. *in situ* RNA localization data showed that *elav* is transcribed exclusively within the central nervous system as well as the peripheral nervous system during the whole life cycle of the fly, from the embryonic stage (6 hours post fertilization) till the adult stage (Robinow and White, 1988).

To verify if the expression of the transgenes affected the vitality of the animals, we counted the number of adults which developed from the embryos. The results are shown in Fig. 4.2, while the absolute numbers obtained were as follows:

GENOTYPE	N° EMBRYOS	N° ADULTS
w^{1118}	111	109
UAS-SNAP-25^{WT}	182	159
UAS-SNAP-25^{R206A}	182	159
ElavGAL4/ UAS-SNAP-25^{WT}	165	154
ElavGAL4/ UAS-SNAP-25^{R206A}	347	324

We found that almost the totality of the F1 embryos *ElavGAL4/UAS-SNAP-25*^{WT} and *ElavGAL4/UAS-SNAP-25*^{R206A} reached adulthood. No lethality was observed in the transgene expressing animals if compared with the parental lines *UAS-SNAP-25*^{WT} and *UAS-SNAP-25*^{R206A} (controls). We observed limited mortality in the parental lines during the pupal stage, probably because they are homozygous for the transgene insertion while the transgene expressing lines are heterozygous for the insertions. It could thus be possible that the transgene has been inserted in a genome region interrupting a gene necessary for the proper development of the animals, resulting in a slightly deleterious recessive mutation.

Only a delay (about 24 hours) in the pupal eclosion was observed for the *ElavGAL4;UAS-SNAP-25*^{R206A}/+ line but we did not investigate the possible mechanisms for this developmental delay.

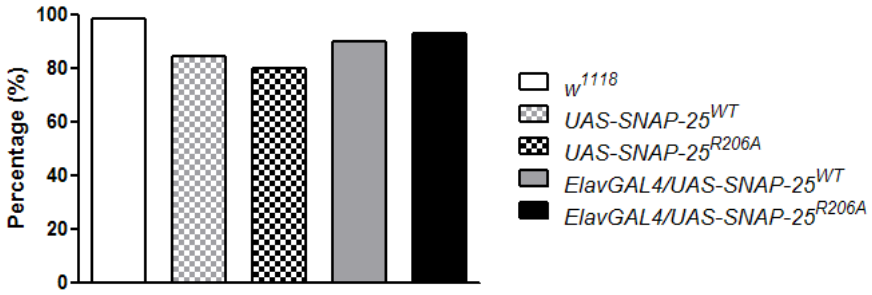

Fig. 4.2. Percentage of embryos which developed to adulthood.

The presence of a mutant isoform of SNAP-25 does not produce lethality at any of the life stages of the fly. Moreover, also the overexpression of the *wild-type* protein has no effect on the animals. This is in contrast of the data previously presented by Babcock and collaborators (Babcock *et al.*, 2004) showing that, of the two lines, overexpressing SNAP-25 in the nervous system, analyzed by them, one resulted in embryonic lethality, while the other presented no defects except wing inflation defects. They explained this severe phenotype as a consequence of the secretion inhibition produced by SNAP-25 overexpression. In our hands SNAP-25 overexpression was not toxic and did not lead to any phenotypical alterations neither in larvae nor adults.

4.3. Expression of the different SNAP-25 isoforms in the nervous system

Due to the impossibility of detecting the different protein isoforms, which differ for only one amino acid, using specific antibodies, the level of SNAP-25^{WT} and SNAP-25^{R206A} expression was estimated by semi-quantitative PCR performed on RNA extractions obtained from third instar larval body-walls or brain. The neuronal expression levels of *Snap-25^{WT}* and *Snap-25^{R206A}* mRNAs are illustrated in Fig. 4.3, which shows a representative semi-quantitative PCR performed on third instar larval brain and entire body-wall: average (± s.d.) relative percentage expression levels of SNAP-25 isoforms (WT or R206A), relative to constitutive SNAP-25 expression in control *w^{1118}*. In this case *w^{1118}* is the control, which is the line used as the genetic background for the generation of the transgenic lines.

Considering the whole body of the larvae, the relative percentage expression of the *SNAP-25^{WT}* isoform was 148.1±29.6 in *ElavGAL4/UAS-SNAP-25^{WT}* and 97.0±3.7 in *ElavGAL4/UAS-SNAP-25^{R206A}*, whereas for the *SNAP-25^{R206A}* isoform it was 2.3±4.0 in *ElavGAL4/UAS-SNAP25^{WT}* and 212.0±58.9 in *ElavGAL4/UAS-SNAP-25^{R206A}* larval brains (*n*=4 for each line and for the control *w^{1118}* line). On average, *SNAP-25^{R206A}* transgene expression, in a *wild-type* background, was 2 times the expression of *SNAP-25^{WT}*.

Within the nervous system, the relative percentage expression of the *SNAP-25^{WT}* isoform was 136.0±17.3 in *ElavGAL4/UAS-SNAP-25^{WT}* and 106.0±26.3 in *ElavGAL4/UAS-SNAP-25^{R206A}*, whereas for the *SNAP-25^{R206A}* isoform it was 4.8±3.6 in *ElavGAL4/UAS-SNAP25^{WT}* and 256.0±113.3 in *ElavGAL4/UAS-SNAP-25^{R206A}* larval brains (*n*=4 for each line and for the control *w^{1118}* line). Also in this set of experiments, on average, *SNAP-25^{R206A}* transgene expression was 2.5 times the expression of *SNAP-25^{WT}*.

While the *ElavGAL4/UAS-SNAP-25^{WT}* line expresses only the WT isoform, the *ElavGAL4/UAS-SNAP-25^{R206A}* line co-expresses the R206A isoform, due to the transgene, and also the WT, due to the endogenous gene.

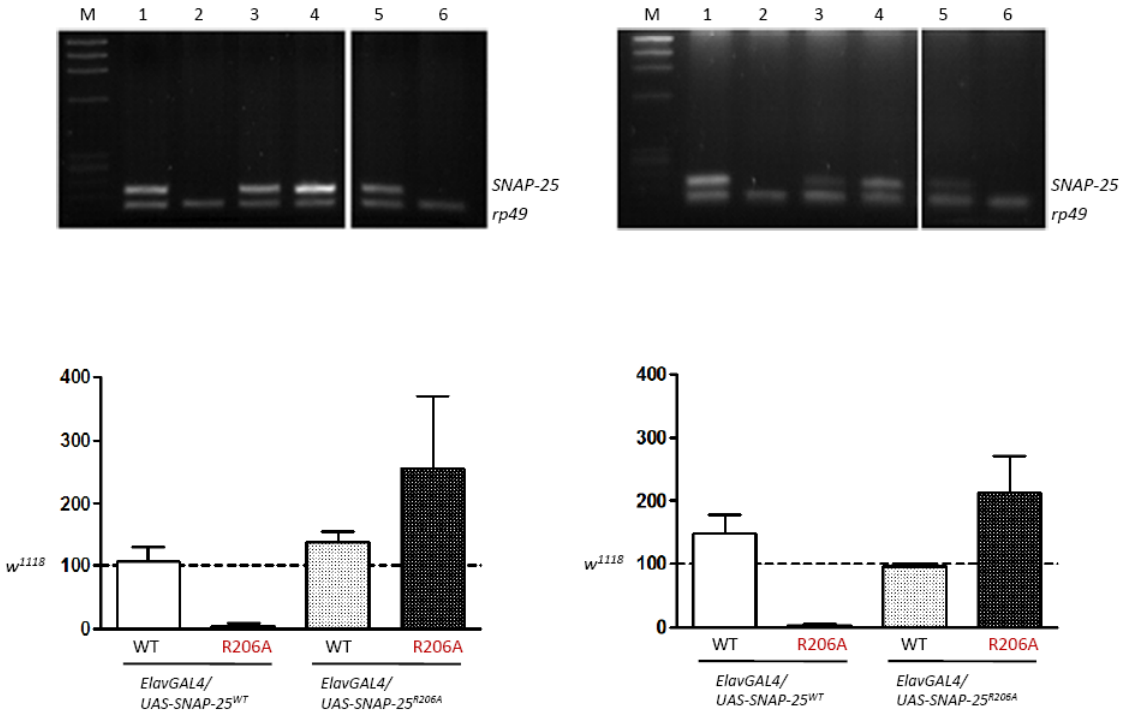

Fig. 4.3. Semi-quantitative PCR analysis of *wild-type* (WT) and mutant (R206A) SNAP-25 isoforms in third instar larvae brains. Agarose gel electrophoresis of PCR-amplified fragments produced on cDNA from (A) brain total RNA and (B) body wall total RNA. Lane M is the molecular mass marker (*FX174/Hae*III). The bottommost band in lanes 1-6 is the housekeeping gene *rp49* (164 bp); the other bands are *SNAP-25* fragments (WT in lanes 1, 3 and 5; R206A in lanes 2, 4 and 6; 210 bp). Average (± s.d.) relative percentage expression levels of SNAP-25 isoforms (WT or R206A) in *ElavGAL4/UAS-SNAP-25*^{WT} and *ElavGAL4/UAS-SNAP-25*^{R206A} (C) larval brains (*n*=4 for each line) and (D) whole larval body (*n*=4 for each line), relative to constitutive SNAP-25 (=100%; dotted line) expression in control w^{1118} larval brains (*n*=4).

4.4. Morphology and morphometry of the NMJ

As other *Drosophila* synaptic mutants with alteration in synaptic function were reported to show a morphological change at the level of the NMJ, we analyzed the morphology and morphometry of the NMJ after staining with the neuronal-membrane-specific anti-HRP antibody. The enzyme horseradish peroxidase (HRP) recognizes a carbohydrate epitope that is selectively expressed in the insect nervous system; a large number of neuronal glycoproteins and cell adhesion molecules that may be involved in axon outgrowth and guidance process bear the HRP carbohydrate epitope (Desai *et al.*, 1994).

To analyze synaptic changes in the *ElavGAL4/UAS-SNAP-25*^{R206A} mutant we investigated the projections of motorneurons (axon 1 and axon 2) onto of abdominal segment 3 muscle 6 and 7 in third instar larvae. These neurons form type-I synaptic terminals and use glutamate as their major neurotransmitter (Hoang and Chiba, 2001; Johansen *et al.*, 1989a).

Fig. 4.4 shows representative confocal images of the NMJ of muscles 6 and 7 in the abdominal segment 3 of *ElavGAL4/UAS-SNAP-25*^{WT} and *ElavGAL4/UAS-SNAP-25*^{R206A} larvae stained with anti-HRP to visualize neural projections, and anti-NC82 to visualize active zones.

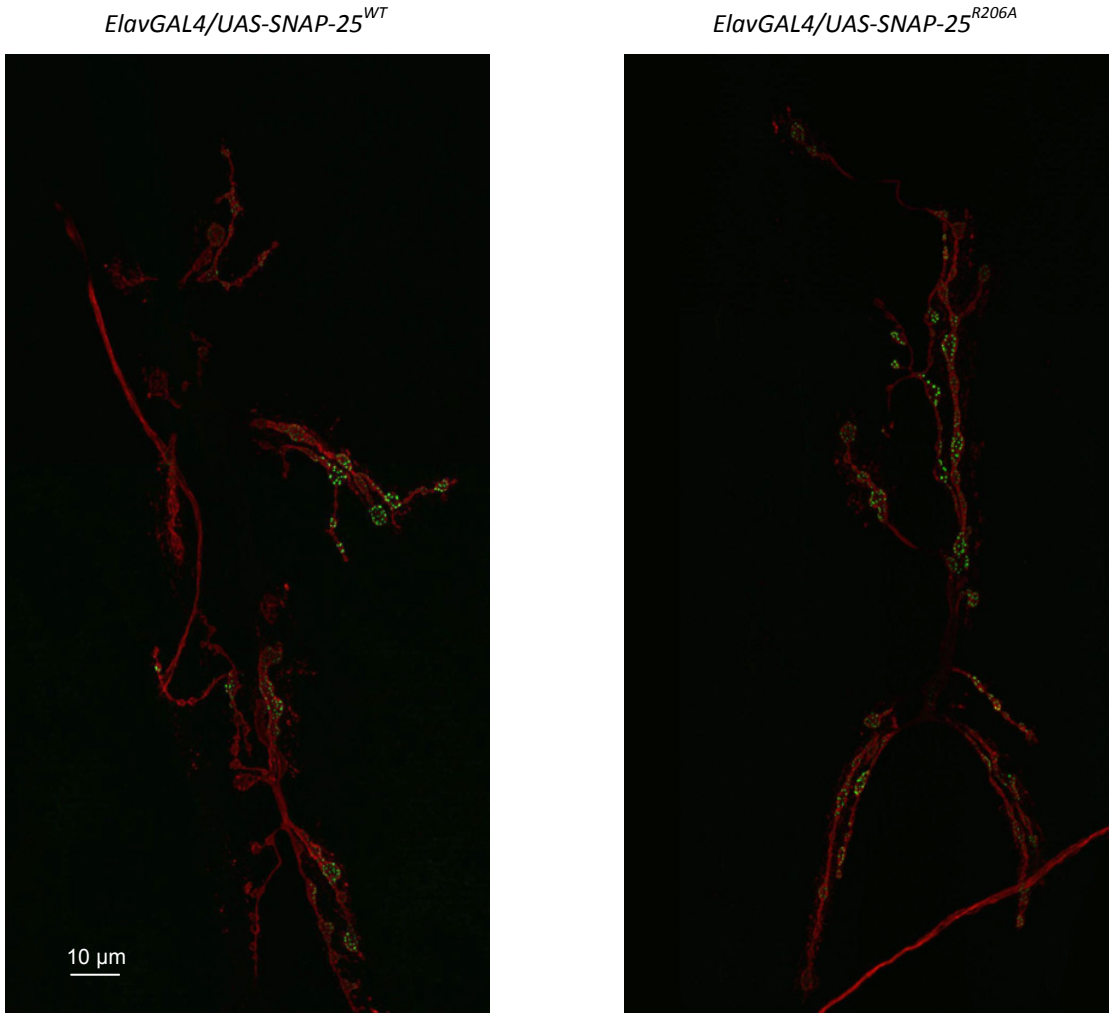

Fig. 4.4. Immunohistochemical staining of abdominal segment 3 fibres 6 and 7 NMJ of control (left) and mutant (right) larva. The neuronal membrane marker anti-HRP antibody (red) and the active zone marker anti-NC82 (green) were used for the staining.

The innervation of muscles 6/7 in SNAP-25^{R206A} mutants did not differ from the typical morphology of SNAP-25^{WT} control neurons; mutants presented a well developed NMJ in which the synapses appeared correctly harborized in order to cover and stimulate the maximum surface of the muscles with their secondary branches. To determine how long the axon was expanded in SNAP-25^{R206A} mutants, we measured the synaptic spans of all branches. In *ElavGAL4/UAS-SNAP-25*^{R206A} larvae, the NMJ length was extended as the one in *ElavGAL4/UAS-SNAP-25*^{WT}. The morphological observation was confirmed by morphometrical data (Fig. 4.5B) showing no differences between control and mutant NMJ; indeed the average extension of *ElavGAL4/UAS-SNAP-25*^{R206A} is 656.3±126.4 µm^2 while in the case of *ElavGAL4/UAS-SNAP-25*^{WT} it was 639.9±121.4 µm^2. These results suggest that SNAP-

25^{R206A} is not involved in alteration of bouton number or length of synaptic innervation at the NMJ.

To quantify the SNAP-25^{R206A} phenotype, we counted the number of type-I boutons. When compared to controls, *ElavGAL4/UAS-SNAP-25^{R206A}* larvae had approximately the same number of boutons.

It has been reported that muscle size can be correlated with the size of the NMJ (Schuster *et al.*, 1996). But, because the expression of the transgenes is localized within the nervous system, and, as consequence, the muscle surface area should not differ between mutants and controls.

If compared with a other synaptic mutant previously characterized in the lab, the *Sply^{null}* mutant, the structure of the *ElavGAL4/UAS-SNAP-25^{R206A}* NMJ seemed to be not altered. *Sphingosine-1-phosphate lyase* (*Sply*) gene codes for an enzyme involved in sphingolipid metabolism. The mutant lacks Sphingosine-1-phosphate, a sphingolipid metabolite which regulates cell proliferation, migration and apoptosis, and which is important for adult muscle development and integrity, reproduction and larval viability (Herr *et al.*, 2003). *Sply^{null}* larvae display a severe alteration in the architecture of the NMJ, affecting both the axon terminal arborization, synaptic boutons size, and the muscle apparatus (Magnabosco, PhD thesis and personal communication). Otherwise, at the *ElavGAL4/UAS-SNAP-25^{R206A}* NMJ the boutons were easily recognizable, well bound and determined with the characteristic round shape, not aggregated or fused together

To test whether type-Is and Ib boutons might be altered in the mutant in general, the average number (Fig. 4.5A) and diameter (Fig. 4.5D) of each group of boutons was measured. The average number of type-Is and Ib boutons counted in mutants and controls were, respectively, 39.2±4.9 and 37.1±4.5. The bouton diameter distribution of *ElavGAL4/UAS-SNAP-25^{R206A}* overlaps the *ElavGAL4/UAS-SNAP-25^{WT}* one; the first peak, at around 1.5-2 µm, corresponds to type-Is boutons, while the second peak, at around 3-4 µm, corresponds to type-Ib boutons. Those values are comparable to the ones reported in literature (Hoang and Chiba, 2001).

Morphometrical analysis indicates that neither the total number of boutons per NMJ nor the diameter of type-Ib and Is boutons were changed in *ElavGAL4/UAS-SNAP*-25^{R206A} compared with *ElavGAL4/UAS-SNAP-25^{WT}*. Mutants displayed a normal architecture of the NMJ at this resolution level.

To analyze more in detail the boutons architecture, we determined the number of putative active zones in control and mutant larvae. The NMJ was labeled with an antibody against the active zone specific marker Bruchpilot, a presynaptic active zone protein which promotes active zone assembly, Ca^{2+} channel clustering, and vesicle release in the larval nervous system (Kittel *et al.*, 2006).

It has been reported that the number of active zones increases in proportion to bouton size (Atwood *et al.*, 1993). Therefore, the number of active zones in the type-Is and Ib boutons were counted for the fibres 6 and 7 synapse of a abdominal segment 3 (Fig. 4.5C). We found that this parameter was slightly increased in mutants; the *ElavGAL4/UAS-SNAP-*25^{R206A} larvae had, on average, 452.6±86.6 active zones per NMJ, while controls presented 348.9±56.0 anti-NC82-positive spots.

Analysis of several *Drosophila* mutants suggests that bouton number and size might be regulated by separate signaling processes. The synaptic growth of neurons during the development and adult life of an animal is a very dynamic and highly regulated process, especially during larval development. In this period new boutons and branches are added at the glutamatergic NMJ until a balance between neuronal activity and morphological structures is reached (Budnik, 1996). It can be possible that the increase active zone number of about 22% in mutants respect to controls can be a sort of compensation for the impairment of vesicle fusing process determined by the presence of SNAP-25^{R206A}. So, the increase in active zone number may correlate with a change in synaptic transmission determining an increase in the vesicle fusion events in order to compensate the impairment caused by the presence of mutant SNAP-25 isoform at the synaptic terminal.

Thus the presence of SNAP-25^{R206A} did not alter the morphometry of the synapse, at least not at the level of analysis performed, but instead it produced a slight structure rearrangement at the bouton terminals, i.e. the increase in active zone number.

Experiments performed with murine spinal cord cultures have shown that the removal on the part of BoNT/A of the SNAP-25 C-terminal segment beginning with Arg198 did not change either the appearance of the synaptic terminal or the number and distribution of synaptic terminals (Neale *et al.*, 1999). Also in the *Drosophila SNAP-*25^{ts} mutant, the synapses in the larvae appeared to be grossly normal at both the permissive and non-permissive temperatures even if, in this case, the mutation produced more severe effects than the ones studied by us (i.e. altering the structure of the protein and its interaction with the other SNAREs, synaptobrevin and syntaxin (Rao *et al.*, 2001)). On the basis of these

considerations, we did not extend our morphological analysis to the electron microscopic level.

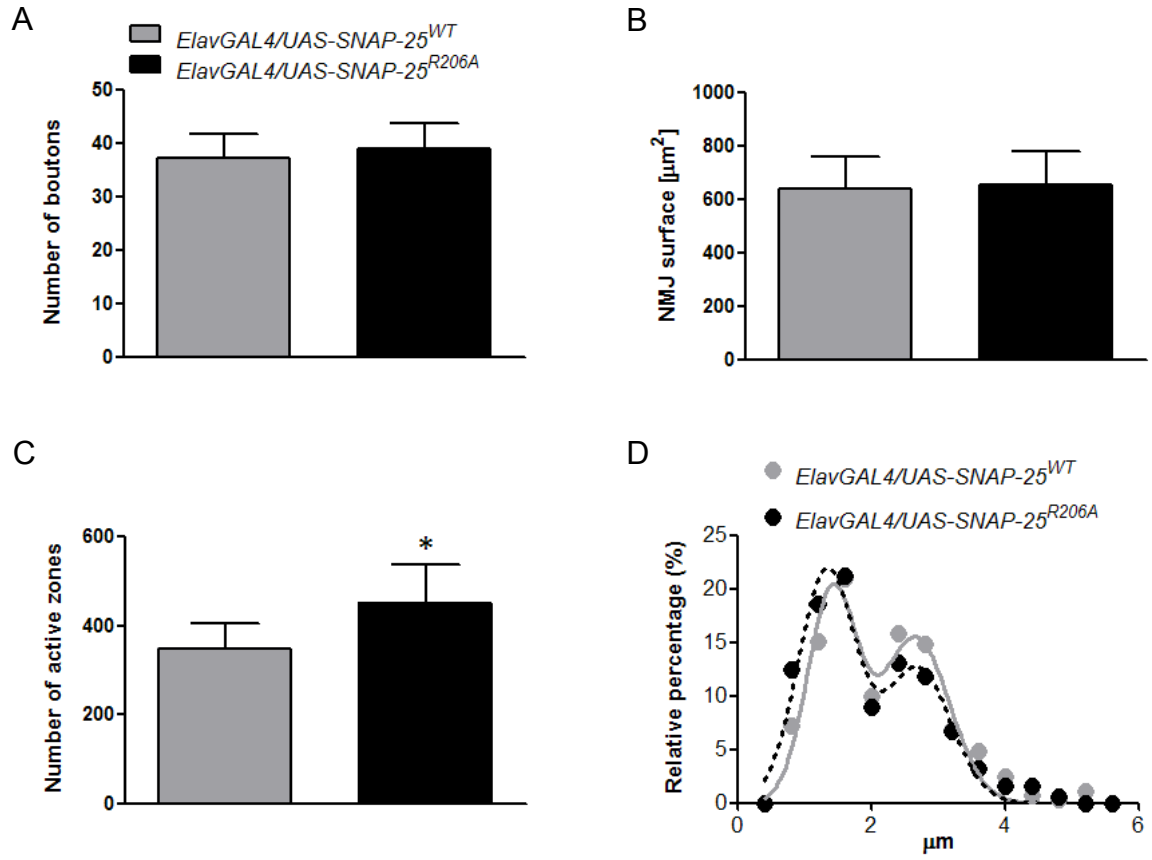

Fig. 4.5. Third instar larvae NMJ morphological and morphometrical analyses. (A) Mean (± s.e.m.) number of NMJ type-Ib and Is boutons from abdominal segment 3 fibre 6/7 of controls and mutants (*n*=8). (B) Mean (± s.e.m.) of the surface covered by the synapse (*n*=8). (C) Mean (± s.e.m.) number of active zones (*n*=8). (D) Relative percentage frequency distribution of type-Ib and Is bouton diameters. Data were fitted with a double Gaussian function (R^2=0.95 and 0.94 for *ElavGAL4/UAS-SNAP-25*^{WT} and *ElavGAL4/UAS-SNAP-25*^{R206A} data, respectively) showing the presence of a double peak corresponding to type-Ib and type-Is bouton diameters.

4.5. Locomotor behavior

Locomotion is an integral component of most animal behaviors. This behavior presents extreme variation in nature which is attributable to multiple interacting quantitative trait loci whose expression is influenced by the environment (Jordan *et al.*, 2006). Insects have long proven to be popular subject for the study of both innate and adaptative behavior. Insects have elaborated a sensory systems, are affected by internal state, and exhibit a wide array of stereotyped and nonstereotyped behaviors; they display several phenomena that, from our point of view, can be described as thirst, hunger, lust, aggression, attention, sleep,

and learning and memory. Even if the genetic basis of such complex behavior is largely uncharacterized (Jordan *et al.*, 2007), studying *Drosophila* can indeed inform us of the driving forces involved (Zhang *et al.*, 2010).

At the larval stage the animal are photophobic and escape light, so locomotion is required for localization of food and dark environments. The D*rosophila* larva's forward and backward movements are produced by peristaltic waves of contraction of the body wall musculature. The rhythmic contractions of the body segments are coordinated by a central pattern generator (Jordan *et al.*, 2007). Larvae have a simpler nervous system than adults, they have a less elaborate repertoire of behaviors and their behavior is unavoidably linked to ongoing development. Both the body and the nervous system continuously grow as the animal transitions through the three instars and prepares for pupariation (Zhang *et al.*, 2010). At the adult stage the flies are no longer photophobic but they are attracted by light sources. Locomotion is required for localization of food and mates, escape from predators, and response to stress (Jordan *et al.*, 2006).

The locomotor behavior of *ElavGAL4/UAS-SNAP-25*^{R206A} larvae was characterized to verify if the impairment of the vesicle fusion at the NMJ resulted in an altered locomotor phenotype. To evaluate the condition of the animals we measured the total distance covered, the average speed and the maximum speed. In all the three parameter considered the mutants appeared to perform worse than the controls (Fig. 4.6).

In 10 seconds *ElavGAL4/UAS-SNAP-25*^{R206A} larvae covered, on average, 4 mm more than the controls (which corresponds to the length of a third instar larvae). This is probably due to the fact that the mutant larvae move slowly; in fact their average and maximum speed are respectively 15% and 17% lower than *ElavGAL4/UAS-SNAP-25*^{WT} larvae. Moreover the mutant larvae appeared to be less active and they needed to be stimulated to move (i.e. by using a drop of water placed on the dorsal abdomen) more often than controls.

To complete the characterization, adult flies were also tested to verify if the presence of the mutated SNAP-25 produced any effects on adult locomotion. For this analysis other parameters were considered; in addition to the total distance covered and the average speed, the time spent resting was considered.

Also in adulthood (Fig. 4.7) the mutants exhibited the same sluggish behavior already seen at the larval stage; the phenotype persists in both sexes. Indeed, in ten minutes, control males and females covered, on average, 338.9 and 348.1 cm respectively, while the mutants walked for 238.7 and 287.5 cm; there is a difference of about one meter between the

distance covered by SNAP-25 mutant transgene expressing line and the corresponding controls, irrespective of sex.

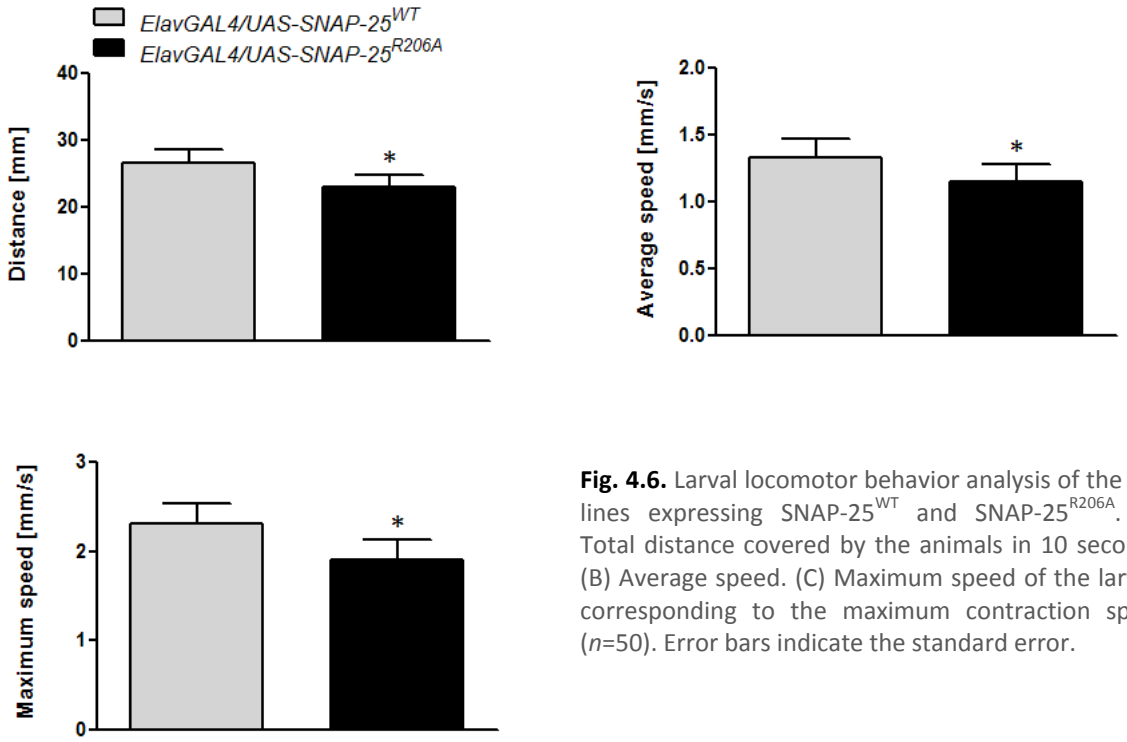

Fig. 4.6. Larval locomotor behavior analysis of the two lines expressing SNAP-25^{WT} and SNAP-25^{R206A}. (A) Total distance covered by the animals in 10 seconds. (B) Average speed. (C) Maximum speed of the larvae, corresponding to the maximum contraction speed (*n*=50). Error bars indicate the standard error.

Moreover, the mutants tended to rest longer than controls. The difference was significant in both sexes, and it appeared stronger for males with respect to females: on average, the control males remained immobile for 141.6 s, while the mutant males rested for 258.4 s; the latter's resting time was almost two minute longer. In the case of females the difference was less remarkable: controls rested for 158.3 s, mutants for 206.8 s; the latter's resting time was less than one minute longer.

The last parameter analyzed was the effective average speed of the animals; this parameter was calculated as the ratio between distance and walking time (distance/walking time). The mutants were slower than controls and, as observed before, the difference is more evident for males in which *ElavGAL4/UAS-SNAP-25*^{R206A} animals moved at 0.577 cm/s while *ElavGAL4/UAS-SNAP-25*^{WT} at 0.823 cm/s. Mutant males are 30% slower than controls. In the case of females the difference was finer: mutants moved at the speed of 0.667 cm/s, controls at 0.723 cm/s.

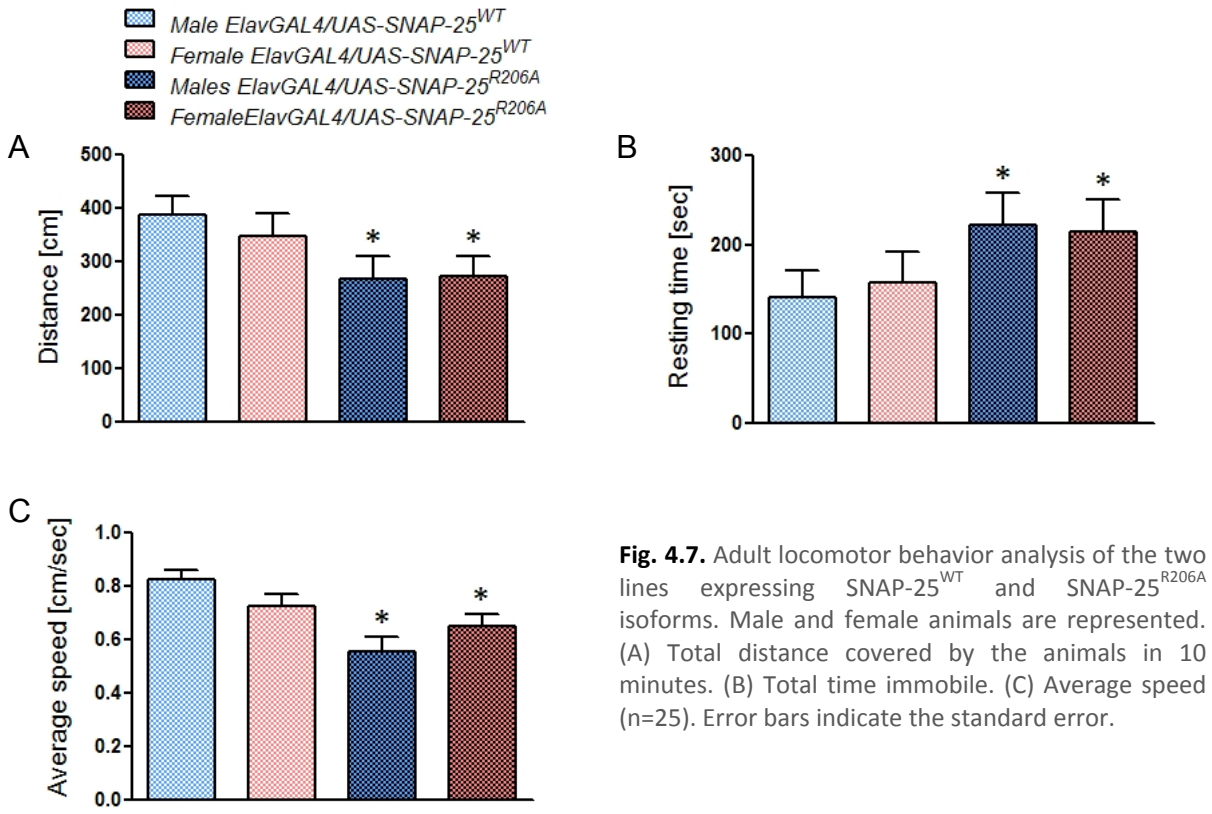

Fig. 4.7. Adult locomotor behavior analysis of the two lines expressing SNAP-25^{WT} and SNAP-25^{R206A} isoforms. Male and female animals are represented. (A) Total distance covered by the animals in 10 minutes. (B) Total time immobile. (C) Average speed (n=25). Error bars indicate the standard error.

The neuromodulatory function of dopamine (DA) is an inherent feature of nervous systems of all animals. Despite the evolutionary distance between mammals and the fly, functional and molecular parallels exist between their dopaminergic systems. In the fly, DA neurons in the fly brain are involved in the regulation of specific behaviors (e.g. locomotor activity, sexual function, and response to drugs of abuse). These neurons show cluster-specific, stereotypical projection patterns with terminal arborization in target areas which include the mushroom bodies, involved in memory formation and motivation, and the central complex, involved in the control of motor behavior. The circuit from the dopamine system to mushroom bodies is crucial for choice behavior in Drosophila; mutants lacking DA biosynthesis showed reduced activity, extended sleep time, negative geotaxis, abolished olfactory learning and they are hypophagic (Riemensperger *et al*., 2011; White *et al*., 2010). It can be possible that *ElavGAL4/UAS-SNAP-25*^{R206A} animals had an altered modulation of the dopaminergic system which resulted in defects in motor behavior, deficit with characterize many human health problems (e.g. Parkinson's disease, Huntington's disease, activity disorders and depression). The *ElavGAL4/UAS-SNAP-25*^{R206A} mutant may represent a model to investigate neuropsychiatric and neurological disorders related to alterations in SNAP-25 function.

4.6. Electrophysiology recordings: spontaneous neurotransmitter release

Two modes of vesicular release of transmitter occur at a synapse: spontaneous release, in the absence of a stimulus, and evoked release, that is triggered by Ca^{2+} influx. Evoked and spontaneous release occur in a quantal manner. These modes often have been presumed to represent the same exocytotic apparatus functioning at different rates in different Ca^{2+} concentrations. Spontaneous discharges consisted of events which were randomly distributed in time and of bursts of temporally ordered events (Budnik and Ruiz-Cañada, 2006). To investigate the mechanism of transmitter release in *ElavGAL4*/*UAS-SNAP-25*^{R206A} and *ElavGAL4/UAS-SNAP-25*^{WT} third instar larvae, the neurotransmitter release was monitored at the NMJ of ventrolateral muscles 6 and 7.

Fig. 4.8A and Fig. 4.9A show that the co-expression of SNAP-25^{R206A} with SNAP-25^{WT} led to a significant (P<0.05) reduction in spontaneous neurotransmitter release. The mean (± s.e.m.) frequency values of spontaneous release were: 1.85±0.35 Hz in *ElavGAL4/UAS-SNAP-25*^{WT} and 1.01±0.11 Hz in *ElavGAL4/UAS-SNAP-25*^{R206A} under current-clamp conditions.

To be more precise, the spontaneous neurotransmitter release was analyzed also under voltage-clamp conditions. This technique was used for the accuracy of minis detection (low signal to noise ratio) and the possibility, due to 3rd instar larval muscle fiber biophysical properties, to utilize only one microelectrode for voltage-clamping muscle fibre. This particular advantage is lost when larger currents (for instance evoked excitatory junctional currents) must be clamped, making necessary to use the more complex two-electrode voltage clamp (Wu and Haugland, 1985). Using this configuration the average miniature end-plate current (MEPC) amplitude values were: 1.61±0.05 Hz in *ElavGAL4/UAS-SNAP-25*^{WT} and 1.07±0.04 Hz in *ElavGAL4/UAS-SNAP-25*^{R206A}.

The average miniature end-plate potential (MEPP) amplitudes (in current-clamp conditions) were: 0.97±0.06 mV and 0.94±0.02 mV in *ElavGAL4/UAS-SNAP-25*^{WT} and *ElavGAL4/UAS-SNAP-25*^{R206A}, respectively (Fig. 4.8B). Data were not significantly different (Student's *t*-test for unpaired samples). Fig. 4.8C shows that the cumulative MEPP amplitudes distributions were not significantly different (Kolmogorov-Smirnov D=0.069; P=NS).

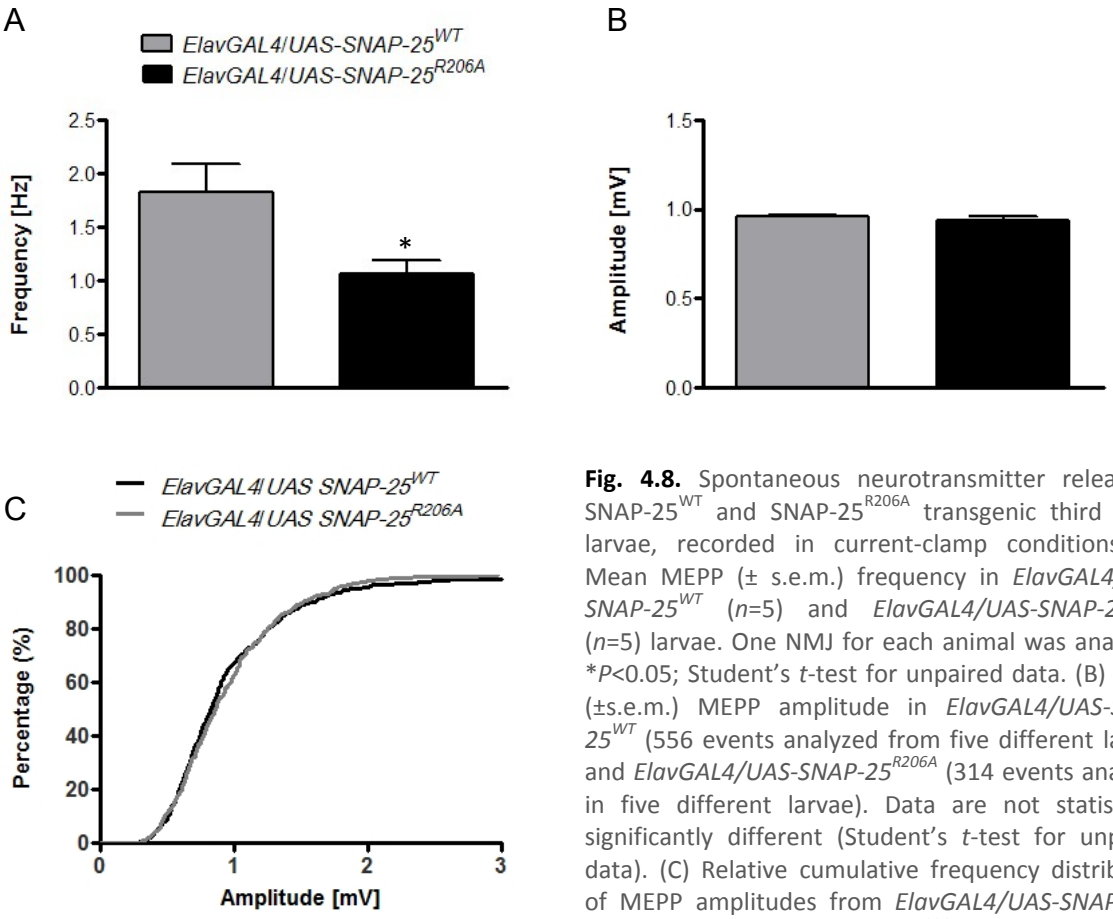

Fig. 4.8. Spontaneous neurotransmitter release in SNAP-25^{WT} and SNAP-25^{R206A} transgenic third instar larvae, recorded in current-clamp conditions. (A) Mean MEPP (± s.e.m.) frequency in *ElavGAL4/UAS-SNAP-25^{WT}* (*n*=5) and *ElavGAL4/UAS-SNAP-25^{R206A}* (*n*=5) larvae. One NMJ for each animal was analyzed. **P*<0.05; Student's *t*-test for unpaired data. (B) Mean (±s.e.m.) MEPP amplitude in *ElavGAL4/UAS-SNAP-25^{WT}* (556 events analyzed from five different larvae) and *ElavGAL4/UAS-SNAP-25^{R206A}* (314 events analyzed in five different larvae). Data are not statistically significantly different (Student's *t*-test for unpaired data). (C) Relative cumulative frequency distribution of MEPP amplitudes from *ElavGAL4/UAS-SNAP-25^{WT}* and *ElavGAL4/UAS-SNAP-25^{R206A}*. Data are not statistically different (Kolmogorov-Smirnov test).

By contrast, the average miniature end plate current (MEPC) amplitude (under voltage-clamp conditions) was significantly reduced in *ElavGAL4/UAS-SNAP-25^{R206A}* (132.6±2.2 pA; mean ± s.e.m.) with respect to *ElavGAL4/UAS-SNAP-25^{WT}* (167.8±2.5 pA; mean ± s.e.m.; Fig. 4.9B). And this is reflected in the cumulative MEPC amplitudes distributions, showing a shift towards smaller amplitudes in the case of *ElavGAL4/UAS-SNAP-25^{R206A}* (Kolmogorov-Smirnov *D*=0.186; *P*=0.001; Fig. 4.9C).

Because concentration of neurotransmitter is the same in all synaptic vesicles, the volume of the vesicle determines how much transmitter is released. Thus, variation in vesicular volume may contribute to observed variance of synaptic quantal unit size. Spontaneous fusions occur in a random manner, each event being independent from the previous and next one (Kim *et al.*, 2000). Accordingly, the frequency distribution of MEPCs inter-event intervals is well described by a Poisson distribution in both controls and SNAP-25 mutants (Fig. 4.9D), indicating that the random nature of spontaneous fusion was not altered by the presence of SNAP-25^{R206A}.

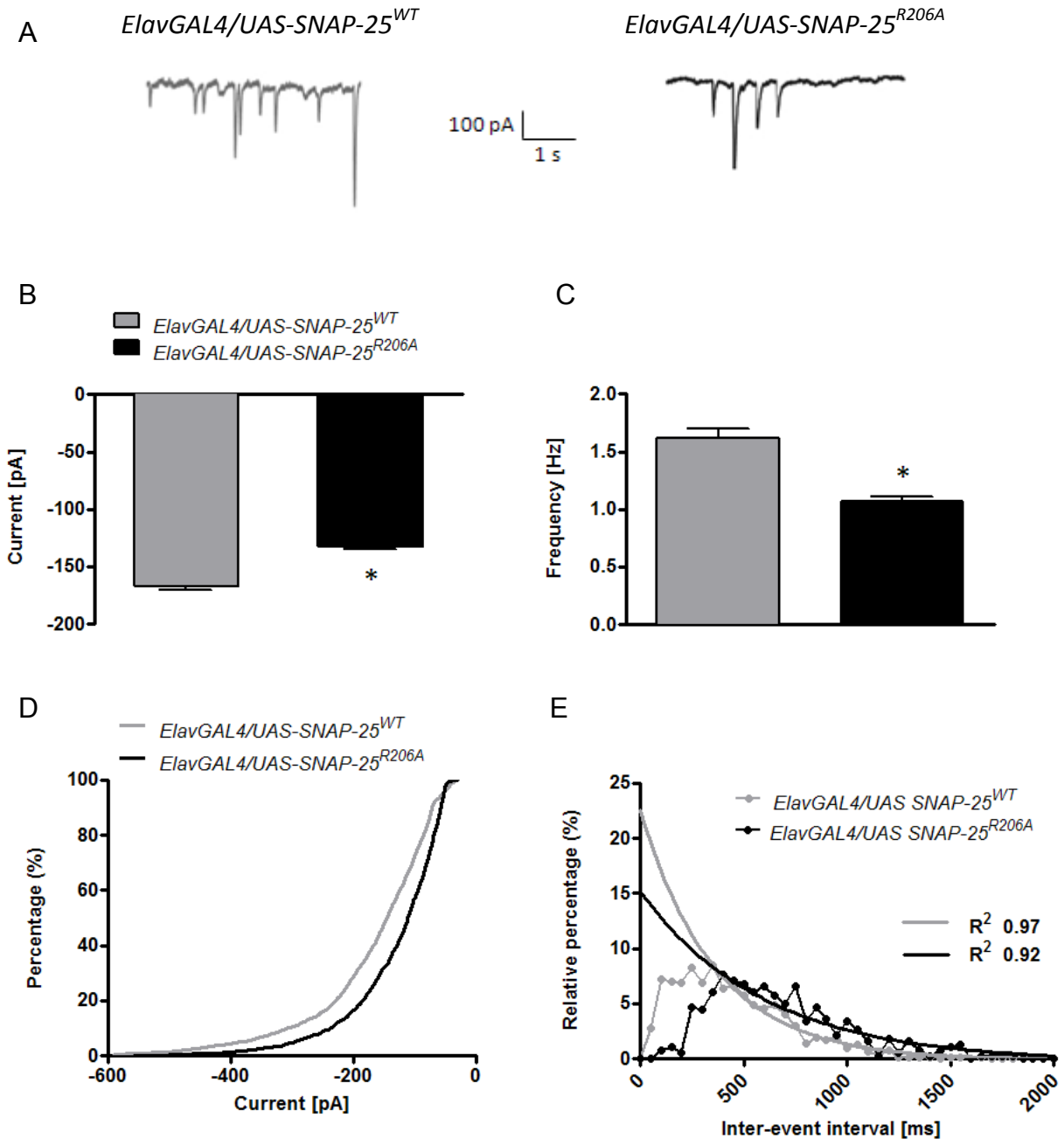

Fig. 4.9. Spontaneous neurotransmitter release in SNAP-25^{WT} and SNAP-25^{R206A} transgenic third instar larvae, recorded in voltage-clamp conditions. (A) Representative traces of MEPCs recorded in control and mutant (black line) larvae. (B) Mean MEPC (± s.e.m.) frequency in *ElavGAL4/UAS-SNAP-25^{WT}* (*n*=7) and *ElavGAL4/UAS-SNAP-25^{R206A}* (*n*=6) larvae; *n* indicates the number of NMJ analyzed. One neuromuscular junction for each animal was analyzed. *Data are statistically different (P<0.05; Student's *t*-test for unpaired data). (C) Mean (± s.e.m.) MEPC amplitude in *ElavGAL4/UAS-SNAP-25^{WT}* (2616 events analyzed in seven different NMJs) and *ElavGAL4/UAS-SNAP-25^{R206A}* (1539 events analyzed in six different NMJs). *Data are statistically different (P<0.05; Student's *t*-test for unpaired data). (D) Relative cumulative frequency distribution of MEPC amplitudes from *ElavGAL4/UAS-SNAP-25^{WT}* and *ElavGAL4/UAS-SNAP-25^{R206A}*. Data are statistically different (Kolmogorov-Smirnov test). (E) Percentage relative frequency distribution of inter-event intervals (gray dots: *ElavGAL4/UAS-SNAP-25^{WT}*; black dots: *ElavGAL4/UAS-SNAP-25^{R206A}*). Black and grey lines are the monoexponential curve fitting of *ElavGAL4/UAS-SNAP-25^{WT}* and *ElavGAL4/UAS-SNAP-25^{R206A}* data, respectively. The good R^2 of each curve fit indicates the random behavior of spontaneous release.

4.7. Electrophysiology recordings: evoked neurotransmitter release

To complete the characterization of the electrophysiological profile of the *ElavGAL4/UAS-SNAP-25^{R206A}* and *ElavGAL4/UAS-SNAP-25^{WT}* NMJ, the evoked release of quanta form the synaptic terminals has been examined. To fully investigate the mechanism of transmitter release, the records were performed stimulating the nerve at different frequencies.

- *Low frequency stimulation*

Initially, to not stress the NMJ, the nerve was stimulated at low frequency; synapses do not display fatigue at this frequency, the RRP pool results not depleted, and, as consequence, the vesicle cycle is not accelerated. During the low frequency stimulation only the vesicles of the RRP, generally thought to be docked to the presynaptic active zone and primed, fuse with the target membrane and release the neurotransmitter into the synaptic cleft (Rizzoli and Betz, 2005).

Fig. 4.10B shows that the mean amplitude of EJPs recorded at third instar larva NMJ following segmental nerve stimulation at 0.5 Hz, was clearly (P<0.05) reduced in *ElavGAL4/UAS-SNAP-25^{R206A}* mutants, with respect to the controls (33.7±0.6 mV in *ElavGAL4/UAS-SNAP-25^{WT}* and 26.0±0.3 mV in *ElavGAL4/UAS-SNAP-25^{R206A}*; mean ± s.e.m.; n=6 and 11, respectively).

On the same fibres we recorded the EJPs after a period higher frequency (10 Hz) of stimulation of the nerve; Fig. 4.10C shows that the mean amplitude of EJPs recorded. Values were 35.0±0.5 mV in *ElavGAL4/UAS-SNAP-25^{WT}* and 28.6±0.3 mV in *ElavGAL4/UAS-SNAP-25^{R206A}* (mean ± s.e.m.; n=6 and 11, respectively). The 10 Hz stimulation of the nerve determined the rise of postsynaptic membrane potential of a value of 2 mV in both mutants and controls. This event is described as short term plasticity, a phenomenon, lasting a few seconds, which synaptic enhancement results from an increase in the probability that synaptic terminals will release transmitters in response to presynaptic action potentials.

Synapses strengthen for a short time due to either an increase in size of the readily releasable pool of packaged transmitter or an increase in the amount of packaged neurotransmitter released in response to each action potential (Stevens and Wesseling, 1999).

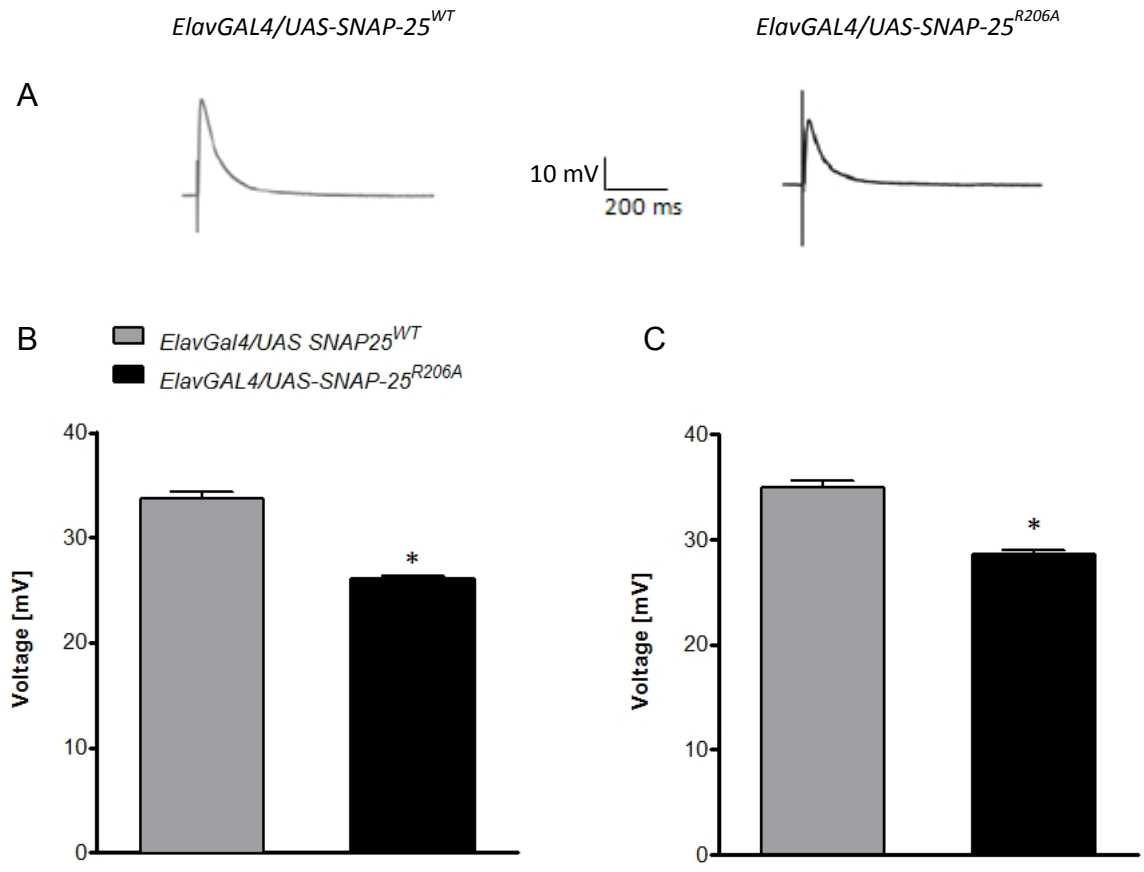

Fig. 4.10. Evoked neurotransmitter release recordings: 0.5 Hz frequency stimulation. (A) Representative traces of MEPCs recorded in individual *ElavGAL4/UA-SNAP-25^{WT}* (grey line) and *ElavGAL4/UAS-SNAP-25^{R206A}* (black line) larvae. (B) Mean ± s.e.m. amplitude of EJPs (stimulation pre 10 Hz frequency stimulation). (C) Mean ± s.e.m. amplitude of EJPs (stimulation post 10 Hz frequency stimulation). All records were performed in fibre 6 or 7 NMJ by stimulation of the nerve of abdominal segmental 3 in *ElavGAL4/UAS-SNAP-25^{WT}* (*n*=6) and *ElavGAL4/UAS-SNAP-25^{R206A}* (*n*=11) third instar larvae. Extracellular Ca^{2+} concentration was 1 mM. *P<0.05; Student's t-test for unpaired data.

In both current-clamp and voltage-clamp recordings the probability of vesicle fusion was reduced, as already seen for the spontaneous events. As results, fewer vesicles fused with the presynaptic plasma membrane leading to reduced EJPs.

- *Moderate frequency stimulation*

Stimulating the nerve at the frequency of 10 Hz, the RRP starts to be depleted and it is refilled by newly recycled vesicle. The recycling pool is the pool of vesicles that maintain release on moderate stimulation; physiological frequencies of stimulation cause it to recycle continuously, but not by recruitment from the RP. Even if the endocytic way is prominent,

the synapse can respond to this stimulation without displaying fatigue (Rizzoli and Betz, 2005).

The only remarkable effect is the short-term synaptic depression (STD), one of several phenomena underlying synaptic plasticity, a propriety which allows the synaptic connection functional strength to be modified by neuronal activity . When stimulated repetitively under physiological conditions, many synapses exhibit rapid depression that progresses to a steady-state level and recovers in seconds after stimulation. Many forms of STD reflect activity-dependent changes in neurotransmitter release (Zucker and Regehr, 2002).

Stimulating the nerve at 10 Hz frequency, the first few spikes presented an increased EJP value if compared to the others recorded subsequently in a row. The STD effect occurred in both *ElavGAL4/UAS-SNAP-25*^{WT} and *ElavGAL4/UAS-SNAP-25*^{R206A} NMJs.

In Fig. 4.11 the mean amplitude of EJPs, recorded during 10 Hz nerve stimulation, are shown. The neurotransmitter release quantal size was clearly (P<0.05) reduced in *ElavGAL4/UAS-SNAP-25*^{R206A} mutants, with respect to the controls as previously observed in the case of low frequency stimulation. EJPs mean amplitude values were 36.2±0.3 mV in *ElavGAL4/UAS-SNAP-25*^{WT} and 25.2±0.2 mV in *ElavGAL4/UAS-SNAP-25*^{R206A}; mean ± s.e.m.; n=6 and 11, respectively. The difference between mutants and controls in case of moderate stimulation (Δ_{10Hz}=11 mV) is increased respect to the difference observed in case of low frequency stimulation ($\Delta_{0.5HzPRE}$ =7.7 mV, $\Delta_{0.5HzPOST}$ =6.4 mV).

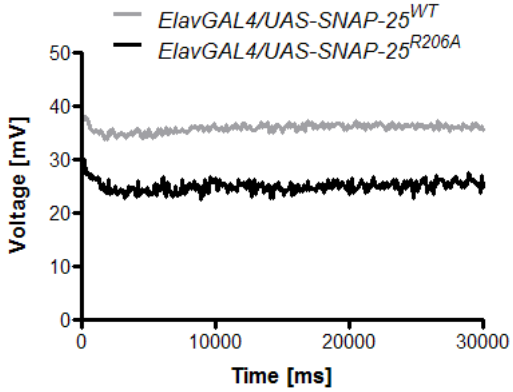

Fig. 4.11. Evoked neurotransmitter release recordings: 10 Hz frequency stimulation. Mean amplitude of EJPs. Records were performed in fibre 6 or 7 NMJ by stimulation of the nerve of abdominal segmental 3 in *ElavGAL4/UAS-SNAP-25*^{WT} (n=6) and *ElavGAL4/UAS-SNAP-25*^{R206A} (n=11) third instar larvae. Extracellular Ca^{2+} concentration was 1 mM.

- *Paired pulse stimulation*

Synaptic plasticity is the ability of the synapse to change in strength in response to either use or disuse of transmission over synaptic pathways (Hughes, 1958). There are several

underlying mechanisms that cooperate to achieve synaptic plasticity, including changes in the quantity of neurotransmitters released into a synapse (Gaiarsa *et al.*, 2002).

Facilitation of membrane electrical excitability is the ability of chemical synapses to change their strength; this effects consists in the increasing in postsynaptic potential evoked by a second impulse. The mechanism of facilitation involves the inactivation of an early, fast, transient outward current by prior membrane depolarization. During the facilitated state, the Ca^{2+}-dependent spike-like response has a decreased current and voltage threshold. The facilitated state persists for around 1 second after a membrane active response (Salkoff and Wyman, 1980). Because a single nerve-driven spike is sufficient to facilitate membrane excitability for a short time, with the paired pulse stimulation we induced facilitation in the synapse and we recorded the EJPs of the second response of the muscular fibre. Not only the amplitude of the events but also the ability of the NMJ to respond to the second stimulus were characterized in *ElavGAL4/UAS-SNAP-25^{R206A}* and *ElavGAL4/UAS-SNAP-25^{WT}* NMJs. The nerve was stimulated by paired pulses differing for the interval time; 20, 30, 50, 75 and 100 ms intervals were chosen for the analysis (Fig. 4.12A).

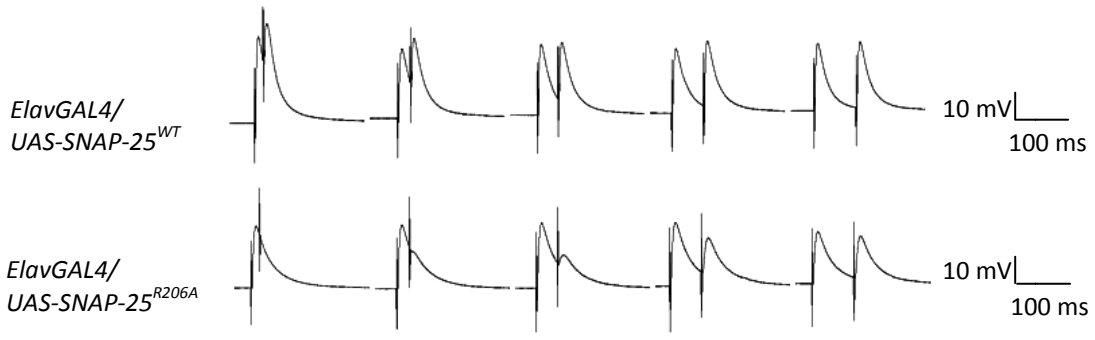

Fig. 4.12. Paired pulses recordings performed on *ElavGAL4/UA-SNAP-25^{WT}* and *ElavGAL4/UAS-SNAP-25^{R206A}* larval NMJ. Representative recordings of paired pulses in control and mutant NMJ; paired pulse intervals were: 20, 30, 50, 75 and 100 ms.

The differences in paired pulse responses between mutants and controls were remarkable; while the control NMJ was able to respond to all stimulation series, the mutants did not display a response to them all. Values were as follows:

Paired pulse Interval [ms]	20	30	50	75	100
Response to the second pulse in *ElavGAL4/UAS-SNAP-25^{WT}* [fails/total events]	0/33	0/34	0/33	0/35	0/37
Response to the second pulse in *ElavGAL4/UAS-SNAP-25^{R206A}* [fails/total events]	69/144	52/139	25/134	17/142	3/172

The number of EJP failures is maximum when the interval is 20 ms. Increasing the distance between the two stimuli, the *ElavGAL4/UAS-SNAP-25*^{R206A} reacquired the ability to respond to the second pulse. At 100 ms the mutant phenotype is comparable to the control one, and the failure events occurred only few times.

- *4.7.4. Tetanic stimulation*

To complete our electrophysiological characterization of the mutant we analyzed the EJPs at high frequency stimulation (30 Hz), called tetanic stimulation (Fig. 4.13). It consisted in a high-frequency sequence of individual stimulations of a neuron which results in a depletion of both RRP and recycling vesicle pool. This high-frequency stimulation causes the mobilization of the RP, which is called into action only upon strong, often unphysiological stimulation (Rizzoli and Betz, 2005).

Only a qualitative analysis of the EJPs was performed. The results showed that the mutants failed to respond more frequently than controls during the stimulation. *ElavGAL4/UAS-SNAP-25*^{WT} NMJs were able to maintain the stimulation for few minutes while *ElavGAL4/UAS-SNAP-25*^{R206A} NMJs became unable to respond earlier, in some cases within the first minute of stimulation. Reducing the frequency of stimulation the mutants became able to respond to the stimuli, showing that the phenotype was not caused by a depletion of the ready releasable pool of synaptic vesicles.

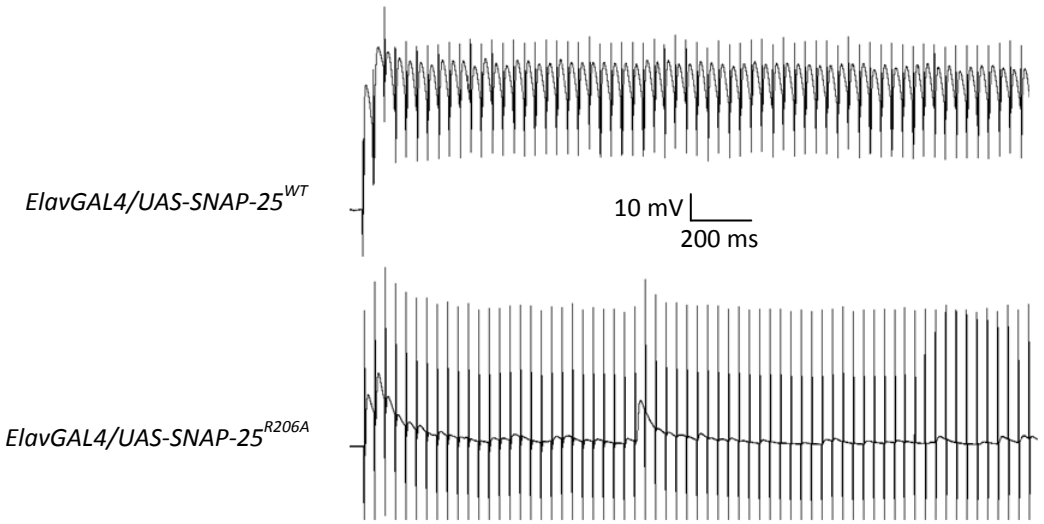

Fig. 4.12. Representative records 30 Hz stimulation recordings performed on *ElavGAL4/UA-SNAP-25*^{WT} and *ElavGAL4/UAS-SNAP-25*^{R206A} larval NMJ.

4.8. Ca^{2+} dependency of neuroexocytosis

At the synapse, neurotransmitter release is triggered physiologically by Ca^{2+} influx through voltage-gated Ca^{2+} channels which origins high calcium concentration microprofiles at the axon terminal. The control of transmitter release at the neuromuscular synapse is achieved also by intracellular calcium; while membrane-bound organelles, such as mitochondria and the endoplasmic reticulum, regulate Ca^{2+} homeostasis intracellularly, performing electrophysiological experiments on the larval NMJ it is possible to alter the extracellular Ca^{2+} concentration of the bath solution.

It is known that calcium ions trigger the final step of vesicle fusion (Katz and Miledi, 1967) but also regulate other steps in the synaptic vesicle cycle, such as vesicle priming, vesicle-pool refilling, and endocytosis (Burgoyne and Morgan, 1995; Sudhof, 2004). It has been demonstrated that SNAP-25 is involved in the control of Ca^{2+} dynamics (close to) at the active zone (Pozzi *et al.*, 2008) and interacts with the voltage gated Ca^{2+} channel via its C-terminus (Catterall, 1999; Zhong *et al.*, 1999). Moreover, it has been well documented that high external Ca^{2+} concentrations can partially rescue the neuroexocytosis blocking effect of BoNT/A which cleaves SNAP-25 at the Gln198-Arg199 peptide bond; the paralysis caused by BoNT/A, but not that caused by BoNT/E, can be partially reversed by raising intracellular calcium (Binz *et al.*, 1994; Capogna *et al.*, 1997; Schiavo *et al.*, 1993). To test for the possibility that the Arg-Ala replacement affects the Ca^{2+} sensitivity of neuroexocytosis, the Ca^{2+} dependence of evoked neurotransmitter release was measured.

EJPs were recorded on the same fibre increasing the external Ca^{2+} concentration. We observed a reduced Ca^{2+} sensitivity in *ElavGAL4/UAS-SNAP-25^{R206A}* compared with *ElavGAL4/UAS-SNAP-25^{WT}* (Fig. 4.12A) with no change in the slope of the linear fit to the data of voltage change recorded at different extracellular Ca^{2+} concentrations (Fig. 4.12B). This result suggests that the Ca^{2+} cooperativity of the process is unchanged between *ElavGAL4/UAS-SNAP-25^{R206A}* and *ElavGAL4/UAS-SNAP-25^{WT}* transgenic lines.

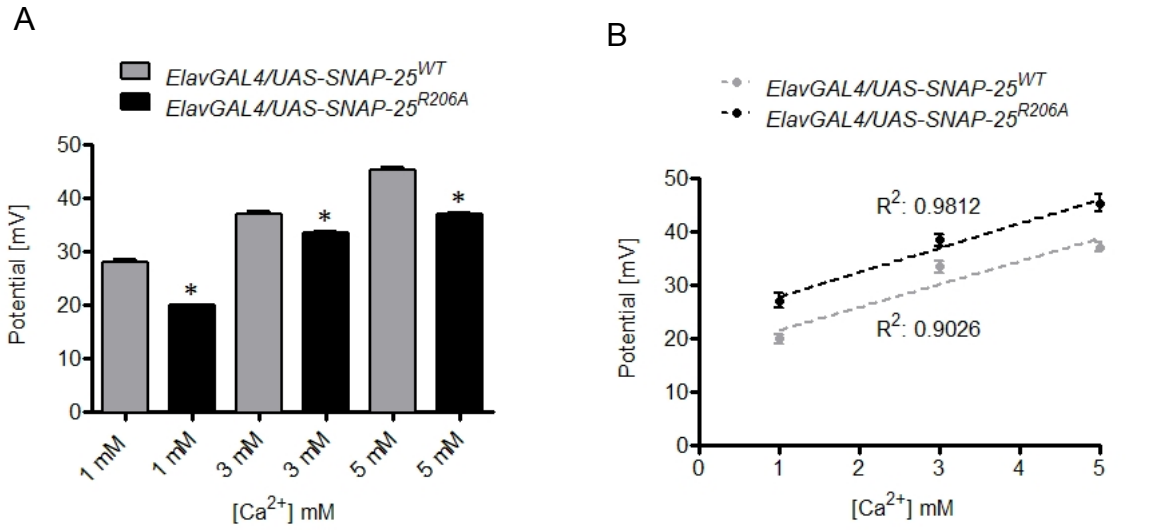

Fig. 4.12. Calcium sensitivity of evoked release. (A) Mean ± s.e.m. amplitude of EJPs evoked in fibre 6 or 7 NMJ by stimulation of the nerve of abdominal segment 3 or 4 fibre at different extracellular Ca^{2+} concentrations in *ElavGAL4/UAS-SNAP-25*^{WT} (*n*=8; grey bars) and *ElavGAL4/UAS-SNAP-25*^{R206A} (*n*=9; black bars) third instar larvae. Only fibres in which it was possible to maintain the intracellular recording throughout the whole experiments (i.e. at different external Ca^{2+} concentrations) were considered for analysis. *Statistically significant (*P*<0.05) difference at each Ca^{2+} concentration tested (Student's *t*-test for unpaired data). (B) Linear regression of the same data as in A. R^2 for each linear regression is indicated for the *wild-type* SNAP-25 (grey) and mutated SNAP-25 (black) samples.

4.9. Bang test

Due to the potential implications of SNAP-25, together with other genes, in the pathologies of neuropsychiatric and neurological disorders (e.g. schizophrenia, ADHD and epilepsy), we also tested the functionality of central neuronal circuits in the *ElavGAL4/UAS-SNAP-25*^{R206A} flies by performing the bang sensitivity assay on adult flies.

The bang test (Ganetzky and Wu, 1982b) consists in a hyper stimulation of the animals that promote the fusion of a large number of SVs of the RRP pool in the neurons. As results the animals can show different phenotypes: they can show a sustained paralysis after a brief seizure, such as occurs in the case of the *easily shocked* (*eas*) mutant do; the can temporally lose the climbing ability (*wild-type* flies normally show negative geotaxis), as happens in the case of the *shibire*^{ts} mutant; they can show a positive geotaxis phenotype or they can briefly recover and show a normal phenotype, as *wild-type* individuals normally do.

Males and females were distinguished in this test to pick out any possible sexual dimorphism. In general, males are more active than females, and the bang sensitivity assay reflected this difference (Fig. 4.13). Within the same sexual class, *ElavGAL4/UAS-SNAP-*

25^{R206A} flies needed more time to recover after the hyperstimulation. As a consequence, they reached the different marks later that corresponding controls (i.e. the *ElavGAL4*/*UAS-SNAP-25*^{WT} animals). The worse behavior of the mutant was significant for the first two marks, 28 and 56 mm respectively, where the animals showed, on average, a delay of about 4 seconds with respect to the concurrent controls.

Furthermore, few animals showed short seizures, defined as transient signs and/or symptoms of abnormal, excessive or synchronous neuronal activity in the brain (Fisher *et al.*, 2005). During the epileptic transient they performed uncontrolled bursts of wing flappings. As soon as the seizure ended, few animals were not able to stand stably on their legs (Fig. 4.13B and 4.13D, columns KO), and some others tended to remain in the same area of the test arena (Fig. 4.13B and 4.13D, columns 0) showing a phenotype that can be related to the defective behavioral activity observed in the *coloboma* mutant mouse (Hess *et al.*, 1992b), in which, SNAP-25 is partially lacking.

After the recovery, the mutant flies usually displayed negative geotaxis as also observed in controls; these animals climbed the walls of the vial passing the four climbing marks to reach the top. The proportion of flies reaching the different marks was lower in the *ElavGAL4*/*UAS-SNAP-25*^{R206A} line than the *ElavGAL4*/*UAS-SNAP-25*^{WT} line, because not only the mutants moved more slowly, as previously observed in the locomotor assay, but also the delay in the post-stimulation recovery time was longer (5 seconds more on average, with respect to the concurrent controls).

It has been proposed that, in the case of human neuropsychiatric disorders associated with SNAP-25 defects, the effects on SNAP-25 expression could be downstream and secondary to maintaining synaptic homeostasis, resulting from altered neural circuits or network function. In fact it is probable that each of the candidate genes thought to be involved in neuropsychiatric disease, among which *Snap-25,* appear to contribute only a small effect towards the overall phenotype of disability (Corradini *et al.*, 2009). This is in keeping with the lack of a severe phenotype in the case of the overexpression of the mutant isoform described in this work.

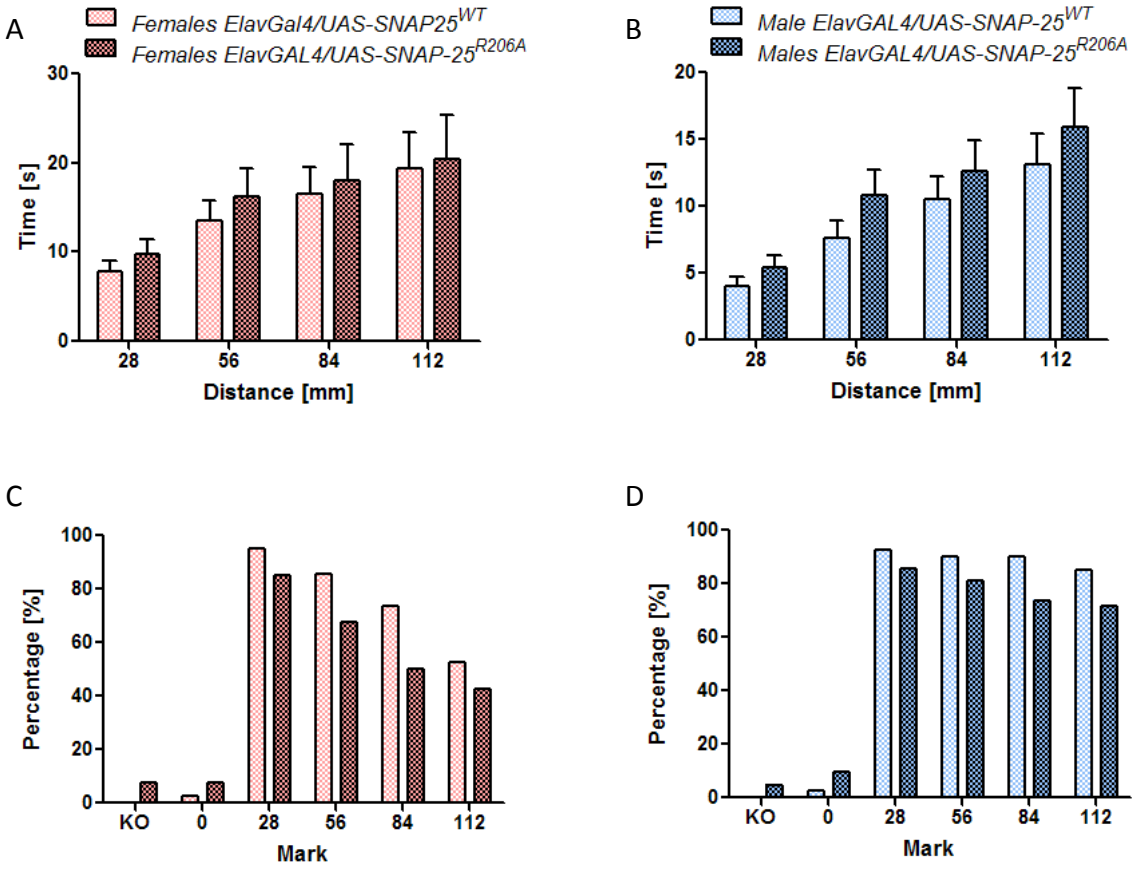

Fig. 4.13. Bang sensitivity of adults. Female data are reported in red, male data in blue. Light color refers to *ElavGAL4/UAS-SNAP-25*^{WT}, dark refers to *ElavGAL4/UAS-SNAP-25*^{R206A}. (A and B) Average time needed by the animals to reach the marks positioned on the vial at 28, 56, 84 and 112 mm from the bottom. (C and D) Percentage of animals which reached the different marks. KO refers to animals unable to recover after the epileptic seizure. 0 refers to animals which did not present the typical climbing ability, by remaining instead at the bottom of the testing vial.

4.10. SNARE in vitro assembly

To verify if the presence of the mutated SNAP-25 could prevent the assembly of single SNARE complexes, *in vitro* experiments were performed in our laboratory in order to assay the extent and time-course of the formation of SNARE complexes. Mouse GST-SNAP-25^{WT} or the mutant mouse GST-SNAP-25^{R198A} were in turn incubated together with the cytoplasmic domains of VAMP and syntaxin and the capacity to form complexes *in vitro* determined (Fasshauer *et al.*, 1998).

Fig. 4.14A shows that no difference in the formation of SNARE complexes *in vitro* was detected between the *wild-type* and mutated proteins.

Furthermore, a more sensitive and relevant end point was also determined by assaying the time-course of SNARE complexes formation.

Fig. 4.14B shows that both wild-type and mutated SNAP-25 very rapidly formed a SNARE complex with VAMP and syntaxin as found previously (Fasshauer *et al.*, 2002) with no difference in the time course.

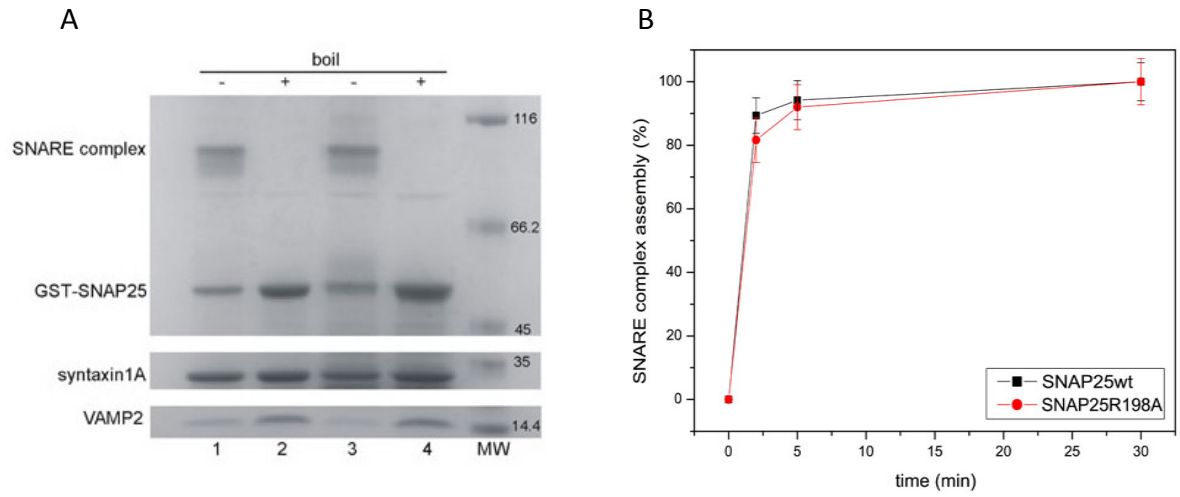

Fig. 4.14. The point mutation R198A of GST–SNAP-25 does not prevent SNARE complex assembly. SNARE complex formation was analyzed using recombinant VAMP2 1-96, syntaxin1A 1-261 and GST-SNAP-25WT (lanes 1, 2) or the mutant R198A (lanes 3, 4). Reactions were stopped at 30 minutes (A) or at the indicated time points (B) by adding SDS-containing sample buffer. Samples were then subjected to SDS-PAGE with or without boiling. Protein were visualized by Coomassie staining (A). Panel B shows the time course of the formation of the SNARE complexes quantified by densitometry of the SDS-PAGE gels (n=3) (Megighian *et al.*, 2010).

It has been show that mutations affecting the properties of core complex formation and vesicular fusion, such BoNT/A cleaved SNAP-25, do not affect the capability of forming the in vitro complex but rather the thermostability of this complex (Zhang *et al.*, 2002). The results obtained in these important control experiments confirmed our expectation since, as pointed out, the mutated residue points outward in the crystallographic structure of the SNARE complex (Brunger *et al.*, 2009; Sutton *et al.*, 1998) and C-terminal mutations of SNAP-25 have been shown not to affect SNARE assembly (Sorensen *et al.*, 2006).

5. DISCUSSION

5.1. SNAP-25^{R206A} reduced the probability of vesicle fusion

The probability of fusion of a synaptic vesicle is strictly dependent on the correct formation of SNARE complexes (Sorensen, 2009; Sudhof and Rothman, 2009). The fact that BoNT/A is known to cleave nine amino acid residues from the COOH-terminus of SNAP-25 indicates that this part of the molecule must play an essential role in the assembly of the exocytotic machinery. Performing sequence conservation analysis on neuronal SNAP-25 protein sequences among different species, a single amino acid which is highly conserved in the protein's C-terminal region was identified: the arginine in position 206. This amino acid is at the first position of the peptide bond cleaved by BoNT/A. Using site-directed mutagenesis, the conserved Arg206 was replaced with alanine. The results obtained by the *in vivo* expression of SNAP-25^{R206A} within the *Drosophila* nervous system reflect defective SNARE complex assembly. As consequence, the probability of neurotransmitter release at the larval NMJ was reduced, leading to the decrease of the frequency of the spontaneous fusion events and the amplitude of evoked events.

Nowadays it is debated if the two forms of neurotransmitter liberation involve the same molecular machinery. Regarding to the spontaneous vesicle fusion, the phenomenon occurs both in the absence of action potentials and without any apparent stimulus and is hence thought to be Ca^{2+}-independent. However, increasing evidence shows that this form of neurotransmitter release can be modulated by changes in intracellular Ca^{2+} concentration, suggesting that it is not fully spontaneous (Glitsch, 2008). For example, synaptotagmin-1 (SYT-1) (Perin *et al.*, 1990), a protein of a family of transmembrane proteins containing tandem Ca^{2+}-binding C2 domains, plays the role as sensor which trigger Ca^{2+}-induced exocytosis. The protein, localized to synaptic vesicles, is involved in the vesicle fusion as well as recycling. When the Ca^{2+} concentration increases within the axon terminal, the two C2 domains, after binding Ca^{2+} ions, induce membrane curvature bringing the two membranes destined to fuse into close proximity, increasing the probability of vesicle fusion. Genetic studies in *Drosophila* and mice have demonstrated that loss of *syt-1* specifically eliminates the fast synchronous component of release, without removing the slow asynchronous component (Geppert *et al.*, 1994; Loewen *et al.*, 2001; Yoshihara and Littleton, 2002).

Also the presence of SNAP-25^{R206A} led to an alteration in the frequency of spontaneous vesicle fusion, supporting the idea that spontaneous release is not an independent process but can be modulated, for example, by interfering with a protein involved in the exocytotic process.

As seen for the *syt-1^{null}* mutants, modulation of spontaneous discharge at the level of the release machinery is not always accompanied by corresponding modulation of action potential-evoked release, suggesting that two independent processes may exist for spontaneous and evoked exocytosis. For this reason, also the electrophysiological profile of the evoked neurotransmitter release has been characterized in the transgene expressing SNAP-25^{R206} isoform.

Action potential-evoked potentials recorded at *ElavGAL4/UAS-SNAP-25^{R206A}* third instar larva NMJ were reduced if compared to controls both at low and high frequency stimulation, respectively 0.5 and 10 Hz. Assuming that the concentration of neurotransmitter is the same in all synaptic vesicles, the volume of the vesicle determines how much transmitter is released. Thus, the presence of SNAP-25^{R206A} determined a decrease in fusion event number in response to a stimulus. As a consequence of the depletion of vesicle fusion with the plasma membrane, the amplitude of the peaks recorded in current-clamp condition is reduced, if compared with controls.

From voltage-clamp recordings it was possible to appreciate that the vesicles pool which fused with the plasma membrane was enriched in small diameter vesicles; a possible explanation for this can be correlated to the different energetic requirement to fuse big and small vesicles. If a big vesicle require more energy to fuse, probably more SNARE complexes have to mediate the process; on the other hand, a small vesicle may require less SNARE complexes. For this reason the presence of the SNAP-25^{R206A} isoform may be more probable at the big vesicles, and less probable at the small vesicles.

Moreover, the tetanic stimulation (30 Hz) showed a more severe electrophysiological phenotype: the expression of SNAP-25^{R206A} had repercussion on the origin of action potentials. The *ElavGAL4/UAS-SNAP-25^{R206A}* NMJ did not respond to the stimulation already after a few minutes of stimulation, while *ElavGAL4/UAS-SNAP-25^{WT}* synapses were able to sustain the strong stimulation for several minutes before displaying a failure in the response. Also this results reflects an impairment of vesicle fusion, as observed for the lower frequency stimulation experiments.

Lastly, from the paired pulse recordings it appeared clear that the presence of SNAP-25^{R206A} affected the probability of fast vesicle fusion. In fact, when the *ElavGAL4/UAS-SNAP-25^{R206A}*

synapse has been stimulated with temporally closed spaced pulses, the synapse was not able to respond to the second stimulus; while, by increasing the temporal spacing of the stimuli, the *ElavGAL4/UAS-SNAP-25*^{R206A} synapse could respond to both pulses, reacquiring a phenotype similar to the controls. This result can be explained assuming that when the first action potential invaded the axon terminal, all the fusion-competent vesicles fused with the plasma membrane, while the fusion of vesicles presenting a non-functional SNARE complex is prevented. When the second action potential arrives, the active zone may be still enriched in vesicles which have a SNAP-25^{R206A} isoform in their SNARE complex, vesicles which are not able to fuse; thus, in these conditions, the number of fusion events is strongly reduced. Nothing is known about the turnover rate of SNARE proteins but it is plausible that barely any vesicles were able to fuse and collapse; as consequence, the neurotransmitter released in the synaptic cleft may not be sufficient to activate all the channels on the muscle membrane, resulting in no post synaptic potential arising.

These results prove the experimental hypothesis demonstrating that Arg198 is fundamental for the proper functioning of the neuroexocytosis apparatus. Because the amino acid does not face the α-helices of syntaxin and synaptobrevin, but instead points outside the complex, it appears plausible that this residue might be involved in contacts with lipids or other proteins which regulate and/or modulate the synaptic vesicle fusion process.

5.2. Evidences of the SNARE supercomplex

Currently it is still debated whether assembly of one SNARE complex generates sufficient energy to initiate vesicle fusion. Several biochemical studies have been performed to identify the minimum number of complexes necessary to promote vesicle fusion (Lu *et al.*, 2008). While the energy profile of SNARE complex assembly reaction and the thermodynamic properties of the SNARE complex are almost clarified, just how the energy is transferred from the complex across lipid bilayers is still obscure (Wiederhold and Fasshauer, 2009). Models of specific kinetics, interaction and assembly/dissociation forces of the SNAREs harnessed for membrane fusion remain speculative (Yersin *et al.*, 2003).

It was recently reported that *in vitro* liposomes can fuse with the help of a single SNARE complex, albeit with low speed (van den Bogaart *et al.*, 2010). It was hypothesized that vesicles resident at the plasma membrane have time to form several SNARE complexes in the absence of stimulation, achieving faster speeds of fusion when triggered by calcium.

However, vesicles arriving during conditions of sustained high calcium concentrations might fuse using fewer (or possibly only a single SNARE complex) (Mohrmann *et al.*, 2010).

In vitro experiments, using liposomes or isolated synaptic vesicles, gave only ambiguous proof that one SNARE is sufficient for the fusion process. Even in the fastest reconstituted biochemical systems, the fusion process is still at least 20 times slower than fusion of synaptic vesicles in neurotransmission; in these *in vitro* systems, also the docking occurs stochastically over many tens of minutes (Domanska *et al.*, 2009). Moreover, all these models do not consider that neuronal docking and calcium-dependent secretion are tightly regulated, both spatially and temporally, by a multitude of proteins. Thus the *in vivo* complexity, where many regulatory proteins, such as Munc18, complexin and synaptotagmin, interact with the SNAREs, is vastly increased compared to *in vitro* systems. It is conceivable that binding of these proteins siphons away some of the energy of SNARE assembly and that under these conditions one SNARE complex may no longer suffice to bring about fusion (van den Bogaart *et al.*, 2010).

The membrane-bridging assembly of the neuronal SNARE complex is central in exocytosis of secretory cells (Jahn and Scheller, 2006). Even if the SNARE proteins are responsible for the mechanism of fusion in the both chromaffin cells and nerve terminals, the differences between neuroexocytosis and neurosecretion are several: the two processes differ in many parameters, such as the vesicle dimension and density in the cytosol, the fusion timeline, and the recycling process.

To become available for exocytosis, granules must move from the cytosol to the plasma membrane and dock there. In chromaffin cells, a layer of filamentous actin covers the internal side of the plasma membrane (Steyer and Almers, 1999). This “cortical” actin layer appears to be a barrier to granules on their way to the plasma membrane (Nakata and Hirokawa, 1992), reducing the mobility of isolated chromaffin granules *in vitro* (Miyamoto *et al.*, 1993), although whether cortical actin helps or hinders the motion of granules to the plasma membrane remains unresolved. At the axonal terminal this structure is not present.

Furthermore, neuroendocrine cells that release hormones and peptides typically contain vesicles of larger diameters than those at classical synapses: at the *Drosophila* NMJ, vesicles have a mean diameter of about 40 µm (Zhang *et al.*, 1998) while chromaffin granules have a diameter between 330 and 360 µm (Plattner *et al.*, 1997), almost 10 times larger than synaptic vesicles.

Although dense-cored vesicles which contain peptides are found within nerve terminals of non-neuroendocrine cells, they occur with lower frequency than the clear-cored vesicles which contain neurotransmitter (Kupfermann, 1991).

Lastly, different types of cells present different types of presynaptic Ca^{2+} signals. 'Nanodomains' arise from local diffusion from single open Ca^{2+} channels, 'microdomains' from multiple open Ca^{2+} channels, and 'radial gradients' from long-distance movements of Ca^{2+} away from the channels. On the basis of this classification, very local, nanodomain Ca^{2+} signals are used when optimizing for speed, microdomains are used at slightly slower synapses, and radial shells mediate the delayed secretion of peptides (Augustine, 2001). Not only the Ca^{2+} signals are different in neuroexocytosis and neurosecretion but also the fusion processes follow different time courses. Probably granules do not attain exocytic competence immediately after docking, and the docking complex must undergo subsequent maturation. Moreover, once at the plasmalemma, a granule evidently reaches fusion competence within minutes (Steyer *et al.*, 1997). The chromaffin cells present two distinct populations of granules, a readily releasable pool and a slowly releasable pool, which follow two distinct secretory pathways (Liu *et al.*, 2010): at high intracellular Ca^{2+} concentration (>10 μM) a fast secretion occurs; at low intracellular Ca^{2+} concentration (between 5 and 10 μM) a slow one occurs (Kasai *et al.*, 1996). On the other hand, in the presynaptic cell, the time course of the local, rapidly decaying Ca^{2+} concentration at the release site or intrinsic kinetics of the fusion apparatus does not control the timing of action potential-evoked release. Moreover, in the chromaffin cells, the maximal rate constant of the fast exocytosis is larger than 30 ms (Kasai *et al.*, 1996), while in the axon terminal a synaptic vesicle takes only 2-3 ms to fully fuse with the plasma membrane (Heidelberger *et al.*, 1994).

After a high frequency stimulation to deplete the RRP, the plasmalemmal granule population is partially replenished with a time constant of 6 min in the chromaffin cells (Steyer *et al.*, 1997). This is >10-fold slower than at neuronal synapses, where endocytic vesicles become release-ready synaptic vesicles in only 15-30 s (frog neuromuscular junction) (Betz and Wu, 1995).

All these evidences suggest that the two processes may differ for the number of SNARE complexes and/or for the interactions between the molecular partners involved. These elements can distinguish between the fast vesicle fusion of the nerve and the slow vesicle fusion of the chromaffin cells. So, although the chromaffin granule has been a good model to study the basic mechanism of membrane fusion, currently it cannot be considered a precise model reflecting the tonic vesicle fusion process which occurs at the neuronal synapse.

In spite of all above limitations, multimers containing a variable number of SNARE complexes have been observed under various circumstances *in vitro* (Antonin *et al.*, 2000; Fasshauer *et al.*, 1998). SNARE complexes were also isolated from detergent-treated squid synaptosomes (Tokumaru *et al.*, 2001). The Ca^{2+}-cooperativity of neurotransmitter release was found to be linked to the number of SNARE proteins (Stewart *et al.*, 2000). Remarkably, star-shaped oligomers, comprising three to four SNARE complexes, were isolated from detergent-treated homogenized bovine brain with a monoclonal antibody directed toward the acetylated N-terminus of SNAP-25 (Rickman *et al.*, 2005). *In vitro* experiments performed with different biophysical approaches have led to the suggestion that 5 to 11 SNARE complexes might be involved in faster modes of fusion (Karatekin *et al.*, 2010; Lu *et al.*, 2008; Yersin *et al.*, 2003). Another study, performed using a peptide that inhibits granule fusion in a chromaffin cell line, estimated that a minimum of three SNARE complexes is sufficient to support exocytosis; in this case it was proposed that SNARE complexes form an 'heterogeneous' fusion pore together with the lipids (Hua and Scheller, 2001). In the same PC12 cells, mutagenesis of the transmembrane domain of the SNARE presynaptic membrane protein syntaxin led to an estimate of 5 to 8 syntaxin molecules being involved in catecholamine release (Han *et al.*, 2004). However, careful experiments performed with mouse spinal cord motorneurons and with the frog NMJ intoxicated with botulinum neurotoxins suggested a higher number (Keller *et al.*, 2004; Keller and Neale, 2001; Montecucco *et al.*, 2005; Raciborska *et al.*, 1998).

The involvement of multi SNARE complexes in neuroexocytosis also accounts for the strikingly long duration of BoNT/A poisoning (>3 months in human skeletal muscles) (Eleopra *et al.*, 1998; Meunier *et al.*, 2003) and for the fact that transfection of BoNT/A-truncated SNAP-25 inhibits exocytosis (Fang *et al.*, 2008; Huang *et al.*, 1998; Wei *et al.*, 2000).

Our data suggests that the SNAP-25^{R206A} isoform formed a stable and inhibitory SNARE complex; several SNARE complexes assembled together and formed a multimeric SNARE ring, which is ultimately responsible of the exocytic event; and the truncated SNAP-25^{R206A} prevented the assembly of the multimer SNARE ring or might gave rise to a non-functional SNARE ring. A similar mechanism of function was hypothesized for BoNT/A-truncated SNAP-25 protein, which acts as a dominant-negative factor of exocytosis reducing the quantal release as observed at the NMJ in the presence of SNAP-25^{R206A} (Montecucco *et al.*, 2005).

5.3. Model of SNARE supercomplex

On the basis of this rich set of data indicating the role of an oligomeric SNARE supercomplex in exocytosis, we have modeled here a ten-SNARE complex rosette and have run molecular dynamics simulations (Fig 5.1). Such modeling is justified by the fact that the three SNARE proteins are sufficient to promote membrane fusion *in vitro* and can, therefore provide relevant information on protein-protein contacts among SNARE complexes in membranes (Karatekin *et al.*, 2010; Sudhof and Rothman, 2009). The number of SNARE complexes used here (ten) derives from analysis of different experiments performed with botulinum neurotoxins type A and E on the frog NMJ (Raciborska *et al.*, 1998) and on mouse spinal cord motorneurons (Keller *et al.*, 2004). Moreover, the steric effects of the proteins involved has been considered and, in particular, the ten-SNARE complex model calculates one synaptotagmin protein every two SNARE complexes. Clearly, the number ten is an approximate value, but it should be noted that using 8 to 13 complexes does not significantly change the position of the SNAP-25 Arg with respect to the neighboring partner.

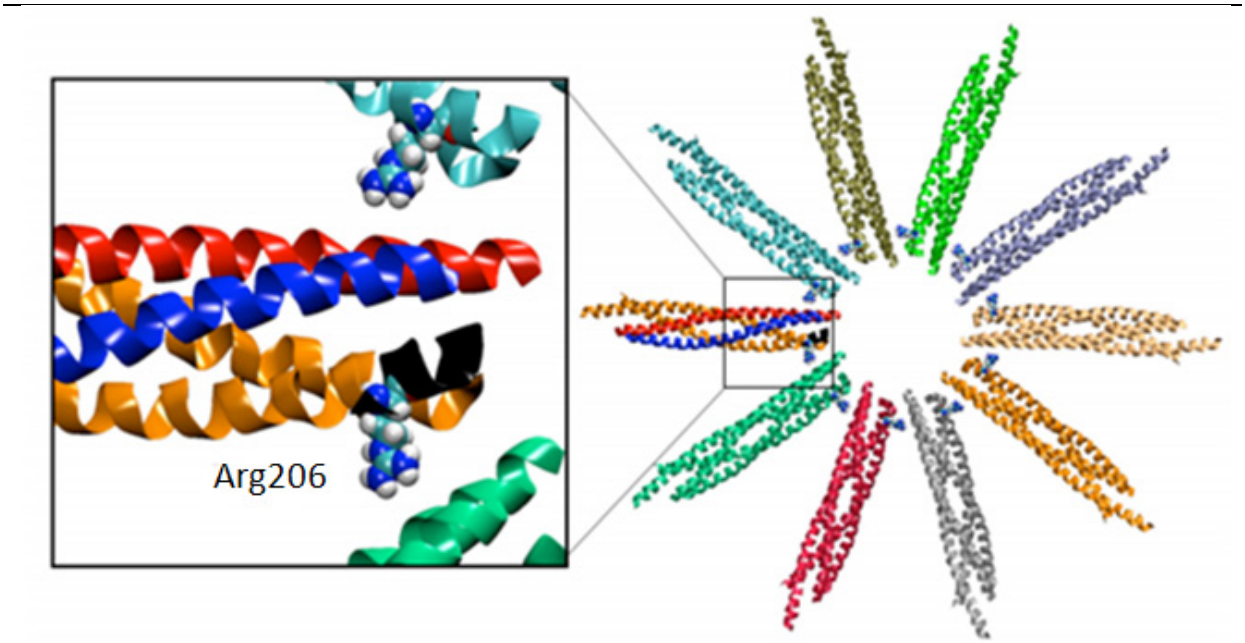

Fig. 5.1. Model of the SNARE complex rosette apparatus of neuroexocytosis. In the highlighted frame, the dark α-helix turns at the end of the orange protein (SNAP-25 C-terminus) corresponds to the peptide cleaved by BoNT/A. SNAP-25 Arg206 is represented with its specific R chain (Megighian *et al.*, 2010).

Given the necessity of forming a ring of 'petals' to define a central area where membrane fusion may take place, such an approach shows that few protein-protein contacts between SNARE complexes are involved, and Arg206 is at the centre of the contact areas between the petals of the rosette. Changing the number of petals of the rosette between 8 and 13 results

in little alteration in the amount of protein-protein contacts between each SNARE complex, while Arg206 remains in a central position within the area of contact.

The simple replacement of this charged residue with a helix-promoting, but uncharged, alanine residue does not appear to change the secondary structure, and indeed we did not find any effect of the alanine replacement in the rate and extent of assembly of the SNARE complex *in vitro*. However, this single mutated SNAP-25 is sufficient to decrease the number of MEPPs events as well as EJPs. It is even more remarkable that it does so in a *wild-type* SNAP-25 background at the *Drosophila* larva NMJ.

Although further analysis with expression of the mutant SNAP-25 in a null background is required to substantiate the present results, the consistency of the data reported here suggests that the presence of a single mutant SNARE complex in the very critical region of protein-protein contact between the petals of the rosette is sufficient to block the activity of the rosette. This does explain the dominant negative nature of the mutation introduced here with respect to neuroexocytosis, and fits well with the specific action of BoNT/A and BoNT/C which cleave SNAP-25 just before and after Arg206, respectively, causing a dominant-negative effect with the characteristic long duration of action of these two neurotoxins (Eleopra *et al.*, 1998; Eleopra *et al.*, 1997; Meunier *et al.*, 2003).

The present model also explains the remarkable findings that the replacements of Lys201 and Leu203 (human numeration) with a negatively charged glutamate residue do not affect SNARE assembly but inhibits exocytosis in chromaffin cells (Criado *et al.*, 1999; Gil *et al.*, 2002) as these changes are disturbing the protein-protein contacts between adjacent SNARE complexes, causing their repulsion.

5.3. Fusion pore hypothesis

Within the scientific community, there are two schools of thought, with different explanations concerning the main determinants involved in the origin of the fusion pore: the lipidic school and the protein school. In one view, the fusion pore is purely lipidic, and the pathway to fusion passes through the stalk intermediate (hemifusion); the SNAREs, perhaps in concert with additional proteins, serve as catalysts that lower the intrinsic barrier to bilayer fusion. In the other view, the fusion pore is formed by the cylindrical stacking of a ring of several SNARE complexes which anchor the vesicle to the plasma membrane.

The involvement of a SNARE supercomplex highlights not only the functional but also the structural role of the SNARE proteins during the fusion process. The ionic interactions between adjacent SNARE complexes may coordinate the single complexes pushing them close together. This model supports the protein fusion pore hypothesis, not excluding the participation of lipids in the stalk intermediate.

6. CONCLUSIONS and FUTURE PERSPECTIVES

The replacement of the conserved Arg206 residue of *Drosophila* SNAP-25 with alanine affects the *in vivo* probability of neurotransmitter release, reducing the frequency of the spontaneous fusion events and the amplitude of evoked release.

The present finding is highly relevant because it identifies a key residue in the process of vesicle exocytosis which is of paramount importance for the function of the nervous system. However, as the process is a complex one, the end result is open to different interpretations. We provided evidence against the possibilities that:

- this change might have affected the assembly of the SNARE complex;
- the calcium concentration dependence of the phenomenon could have been altered;
- the morphology and/or morphometry of the NMJ were changed (i.e. developmental processes involved in synaptic formation were not affected).

Molecular modeling suggests that the Arg206 residue is not involved in protein-protein interactions between the three SNARE proteins, and points outward from the complex, suggesting that it may be involved in the interaction with other proteins of the neuroexocytosis machinery.

The presence of the mutant SNAP-25 isoform affects also the behavior of the animals at both larval and adult stages. Locomotor activity is reduced, due to a decrease in the speed of the animals, most likely as a consequence of impairment in the NMJ. The animals also appears less active and less reactive, suggesting a more generalized malfunctioning of neuronal circuits involved in motivating (i.e. decision making) and eliciting locomotion. So the presence of the point-mutated isoform seems to produce a widespread effect on the nervous system.

Although, this is not a direct evidence of the assembly of the SNARE supercomplex, there are, however, several pieces of evidence in favor of the hypothesis of a rosette of SNARE complexes as a necessary structure involved in the exocytosis of synaptic vesicles *in vivo*.

In *Drosophila*, we believe we have identified the amino acid with which SNAP-25 Arg206 takes contact: this should be syntaxin Asp253. The two amino acids present opposite charges

and are probably involved in an ionic interaction, specifically of the salt bridge type, which could be involved in the binding together of adjacent SNARE complexes.

To prove that Asp253 plays a key role in the assembly of the SNARE complex, we have already generated two constructs expressing different isoforms of neuronal syntaxin:

- pUAST-syntaxin^{WT}, our control;
- pUAST-syntaxin^{D253A}, a mutant isoform with an alanine instead of the aspartate.

Transgenic *Drosophila* lines were generated carrying the two transgenes in a syntaxin *wild-type* background. We are planning to express the transgenes pan-neuronally as in the case of the SNAP-25 transgenes. Also in this case, we expect that the co-expression of the endogenous *wild-type* isoform together with the mutant form should result in a reduction of the probability of neurotransmitter release. More precisely, in this situation the specific SNAP-25 arginine in position 206 should not be able to interact with the syntaxin alanine in position 253, so we expect to see similar effects to the ones observed in the presence of SNAP-25^{R206A}.

But to prove that the two residues have the leading role and bind together, we also generated another set of constructs carrying other mutant isoforms of the two SNAREs:

- pUAST-SNAP-25^{R206D}
- pUAST-syntaxin^{D253R}

These plasmids will be respectively injected in a SNAP-25 and syntaxin *wild-type* background in order to generate a repulsion of adjacent SNARE complexes. In this case, two amino acids with the same charge will face each other, so we expect to have a more severe phenotype than the one observed in the case of the isoforms having a neutral amino acid in the respective positions.

In the light of the above experimental approaches, we are also planning definitive proof of principle experiments in which SNAP-25^{R206D} and syntaxin^{D253R} will be co-expressed in a SNAP-25 and syntaxin double null background. This experiment entails the swapping of the charges involved in the ionic interaction between adjacent SNARE complexes: the inversion of the charges should maintain the formation of the hypothesized salt bridge. For this purpose we have designed a new tool allowing the cloning of two different genes in the same plasmid, a double-pUAST vector, in which SNAP-25^{R206D} and syntaxin^{D253R} will be inserted. Before cloning the cDNA of the two SNARE genes, the functionality of the cloning sites and the expression levels of the two UAS units contained in the plasmid will be

characterized. For this purpose a green fluorescent protein with a cytoplasmic localization (EGFP) and a red one with a nuclear localization signal (dsRED.T4- NLS) will be cloned into the double-pUAST vector. The resulting plasmid will then be used to transform a Drosophila S2 cell line together with a pGAL4 plasmid, and the fluorescent intensity level of the two fluorophores will be measured using fluorescent and/or confocal microscopy. Once the *in vitro* tests have been successfully concluded, the characterization of the plasmid will be carried out also *in vivo*.

In conclusion, all the previously described SNAP-25 mutants present mutations which alter the association with syntaxin and/or synaptobrevin, thus preventing the proper formation of a functional SNARE complex. The mutant generated and characterized in this work is the only one which carries a mutation which does not affect the formation of the SNARE complex itself, but, nonetheless, acts as a dominant negative. In this case the phenotype observed is similar to the one observed in the presence of BoNT/A cleaved SNAP-25. Our data support the hypothesis that several SNARE complexes are involved in the formation of a supercomplex necessary for neuroexocytosis. In this supercomplex SNAP-25 Arg206 plays a key role as suggested by computer molecular dynamic simulations. Finally, in relation to the issue concerning the potential involvement of SNAP-25 in neuropsychiatric and neurological disorders, other experiments should be performed in the future to more specifically address central nervous system function in our animal model. This issue could be tackled by implementing assays specifically designed to test for learning and memory abilities (i.e. courtship conditioning test (Mehren and Griffith, 2004)) together with approaches such as the proboscis extension reflex assay, designed to test conditioning in a central nervous system reflex circuit (DeJianne *et al.*, 1985).

7. REFERENCES

Adams, M.D., Celniker, S.E., Holt, R.A., Evans, C.A., Gocayne, J.D., Amanatides, P.G., Scherer, S.E., Li, P.W., Hoskins, R.A., Galle, R.F*., et al.* (2000). The genome sequence of Drosophila melanogaster. Science *287*, 2185-2195.

An, S.J., and Almers, W. (2004). Tracking SNARE complex formation in live endocrine cells. Science *306*, 1042-1046.

Anderson, M.S., Halpern, M.E., and Keshishian, H. (1988). Identification of the neuropeptide transmitter proctolin in Drosophila larvae: characterization of muscle fiber-specific neuromuscular endings. J Neurosci *8*, 242-255.

Andretic, R., Chaney, S., and Hirsh, J. (1999). Requirement of circadian genes for cocaine sensitization in Drosophila. Science *285*, 1066-1068.

Antonin, W., Holroyd, C., Fasshauer, D., Pabst, S., Von Mollard, G.F., and Jahn, R. (2000). A SNARE complex mediating fusion of late endosomes defines conserved properties of SNARE structure and function. EMBO J *19*, 6453-6464.

Atwood, H.L., Govind, C.K., and Wu, C.F. (1993). Differential ultrastructure of synaptic terminals on ventral longitudinal abdominal muscles in Drosophila larvae. J Neurobiol *24*, 1008-1024.

Augustine, G.J. (2001). How does calcium trigger neurotransmitter release? Curr Opin Neurobiol *11*, 320-326.

Aunis, D., and Langley, K. (1999). Physiological aspects of exocytosis in chromaffin cells of the adrenal medulla. Acta Physiol Scand *167*, 89-97.

Babcock, M., Macleod, G.T., Leither, J., and Pallanck, L. (2004). Genetic analysis of soluble N-ethylmaleimide-sensitive factor attachment protein function in Drosophila reveals positive and negative secretory roles. J Neurosci *24*, 3964-3973.

Bai, J., Wang, C.T., Richards, D.A., Jackson, M.B., and Chapman, E.R. (2004). Fusion pore dynamics are regulated by synaptotagmin*t-SNARE interactions. Neuron *41*, 929-942.

Bajjalieh, S.M., and Scheller, R.H. (1995). The biochemistry of neurotransmitter secretion. J Biol Chem *270*, 1971-1974.

Bark, I.C. (1993). Structure of the chicken gene for SNAP-25 reveals duplicated exon encoding distinct isoforms of the protein. J Mol Biol *233*, 67-76.

Bark, I.C., and Wilson, M.C. (1994). Human cDNA clones encoding two different isoforms of the nerve terminal protein SNAP-25. Gene *139*, 291-292.

Barker, L.A., Dowdall, M.J., and Whittaker, V.P. (1972). Choline metabolism in the cerebral cortex of guinea pigs. Stable-bound acetylcholine. Biochem J *130*, 1063-1075.

Bate, M. (1993). The mesoderm and its derivatives. In “The Development of Drosophila melanogaster” (ed. Bate, M. and Martinez-Arias, A.), pp 1013-1090. Cold Spring Harbor Laboratory Press, Plainview, NY.

Bennett, M.K., Garcia-Arraras, J.E., Elferink, L.A., Peterson, K., Fleming, A.M., Hazuka, C.D., and Scheller, R.H. (1993). The syntaxin family of vesicular transport receptors. Cell *74*, 863-873.

Bennett, M.K., and Scheller, R.H. (1993). The molecular machinery for secretion is conserved from yeast to neurons. Proc Natl Acad Sci U S A *90*, 2559-2563.

Bennett, M.K., and Scheller, R.H. (1994). Molecular correlates of synaptic vesicle docking and fusion. Curr Opin Neurobiol *4*, 324-329.

Bertherat, J., and Gimenez-Roqueplo, A.P. (2005). New insights in the genetics of adrenocortical tumors, pheochromocytomas and paragangliomas. Horm Metab Res *37*, 384-390.

Betz, W.J., and Wu, L.G. (1995). Synaptic transmission. Kinetics of synaptic-vesicle recycling. Curr Biol *5*, 1098-1101.

Binz, T., Blasi, J., Yamasaki, S., Baumeister, A., Link, E., Sudhof, T.C., Jahn, R., and Niemann, H. (1994). Proteolysis of SNAP-25 by types E and A botulinal neurotoxins. J Biol Chem *269*, 1617-1620.

Blasi, J., Chapman, E.R., Link, E., Binz, T., Yamasaki, S., De Camilli, P., Sudhof, T.C., Niemann, H., and Jahn, R. (1993a). Botulinum neurotoxin A selectively cleaves the synaptic protein SNAP-25. Nature *365*, 160-163.

Blasi, J., Chapman, E.R., Yamasaki, S., Binz, T., Niemann, H., and Jahn, R. (1993b). Botulinum neurotoxin C1 blocks neurotransmitter release by means of cleaving HPC-1/syntaxin. EMBO J *12*, 4821-4828.

Bracher, A., Perrakis, A., Dresbach, T., Betz, H., and Weissenhorn, W. (2000). The X-ray crystal structure of neuronal Sec1 from squid sheds new light on the role of this protein in exocytosis. Structure *8*, 685-694.

Brand, A.H., and Perrimon, N. (1993). Targeted gene expression as a means of altering cell fates and generating dominant phenotypes. Development *118*, 401-415.

Brunger, A.T., Weninger, K., Bowen, M., and Chu, S. (2009). Single-molecule studies of the neuronal SNARE fusion machinery. Annu Rev Biochem *78*, 903-928.

Budnik, V. (1996). Synapse maturation and structural plasticity at Drosophila neuromuscular junctions. Curr Opin Neurobiol *6*, 858-867.

Budnik, V., and Ruiz-Cañada, C. (2006). The Fly Neuromuscular Junction: Structure and Function, Volume 75: Second Edition (International Review of Neurobiology). Academic Press.

Budnik, V., Zhong, Y., and Wu, C.F. (1990). Morphological plasticity of motor axons in Drosophila mutants with altered excitability. J Neurosci *10*, 3754-3768.

Burgess, R.W., Deitcher, D.L., and Schwarz, T.L. (1997). The synaptic protein syntaxin1 is required for cellularization of Drosophila embryos. J Cell Biol *138*, 861-875.

Burgess, T.L., and Kelly, R.B. (1987). Constitutive and regulated secretion of proteins. Annu Rev Cell Biol *3*, 243-293.

Burgoyne, R.D., and Morgan, A. (1995). Ca2+ and secretory-vesicle dynamics. Trends Neurosci *18*, 191-196.

Cantera, R., and Nassel, D.R. (1992). Segmental peptidergic innervation of abdominal targets in larval and adult dipteran insects revealed with an antiserum against leucokinin I. Cell Tissue Res *269*, 459-471.

Capogna, M., McKinney, R.A., O'Connor, V., Gahwiler, B.H., and Thompson, S.M. (1997). Ca2+ or Sr2+ partially rescues synaptic transmission in hippocampal cultures treated with botulinum toxin A and C, but not tetanus toxin. J Neurosci *17*, 7190-7202.

Cardno, A.G., and Gottesman, II (2000). Twin studies of schizophrenia: from bow-and-arrow concordances to star wars Mx and functional genomics. Am J Med Genet *97*, 12-17.

Catsicas, S., Larhammar, D., Blomqvist, A., Sanna, P.P., Milner, R.J., and Wilson, M.C. (1991). Expression of a conserved cell-type-specific protein in nerve terminals coincides with synaptogenesis. Proc Natl Acad Sci U S A *88*, 785-789.

Catterall, W.A. (1999). Interactions of presynaptic Ca2+ channels and snare proteins in neurotransmitter release. Ann N Y Acad Sci *868*, 144-159.

Ceccarelli, B., Hurlbut, W.P., and Mauro, A. (1973). Turnover of transmitter and synaptic vesicles at the frog neuromuscular junction. J Cell Biol *57*, 499-524.

Cerezo, J.R., Jimenez, F., and Moya, F. (1995). Characterization and gene cloning of Drosophila syntaxin 1 (Dsynt1): the fruit fly homologue of rat syntaxin 1. Brain Res Mol Brain Res *29*, 245-252.

Chernomordik, L.V., and Kozlov, M.M. (2008). Mechanics of membrane fusion. Nat Struct Mol Biol *15*, 675-683.

Cohen, F.S., and Melikyan, G.B. (2004). The energetics of membrane fusion from binding, through hemifusion, pore formation, and pore enlargement. J Membr Biol *199*, 1-14.

Corradini, I., Verderio, C., Sala, M., Wilson, M.C., and Matteoli, M. (2009). SNAP-25 in neuropsychiatric disorders. Ann N Y Acad Sci *1152*, 93-99.

Criado, M., Gil, A., Viniegra, S., and Gutierrez, L.M. (1999). A single amino acid near the C terminus of the synaptosomeassociated protein of 25 kDa (SNAP-25) is essential for exocytosis in chromaffin cells. Proc Natl Acad Sci U S A *96*, 7256-7261.

Crossley, A.C. (1978). The morphology and development of the Drosophila muscular system. In “The Genetics and Biology of Drosophila” (ed. Ashburner, M., and Wright, T. R. F.), vol. 2b, pp. 499-560. Academic Press, NY.

Davletov, B., and Montecucco, C. (2010). Lipid function at synapses. Curr Opin Neurobiol *20*, 543-549.

de Haro, L., Ferracci, G., Opi, S., Iborra, C., Quetglas, S., Miquelis, R., Leveque, C., and Seagar, M. (2004). Ca2+/calmodulin transfers the membrane-proximal lipid-binding domain of the v-SNARE synaptobrevin from cis to trans bilayers. Proc Natl Acad Sci U S A *101*, 1578-1583.

DeJianne, D., McGuire, T.R., and Pruzan-Hotchkiss, A. (1985). Conditioned suppression of proboscis extension in Drosophila melanogaster. J Comp Psychol *99*, 74-80.

Desai, C.J., Popova, E., and Zinn, K. (1994). A Drosophila receptor tyrosine phosphatase expressed in the embryonic CNS and larval optic lobes is a member of the set of proteins bearing the "HRP" carbohydrate epitope. J Neurosci *14*, 7272-7283.

Domanska, M.K., Kiessling, V., Stein, A., Fasshauer, D., and Tamm, L.K. (2009). Single vesicle millisecond fusion kinetics reveals number of SNARE complexes optimal for fast SNARE-mediated membrane fusion. J Biol Chem *284*, 32158-32166.

Eleopra, R., Tugnoli, V., Rossetto, O., De Grandis, D., and Montecucco, C. (1998). Different time courses of recovery after poisoning with botulinum neurotoxin serotypes A and E in humans. Neurosci Lett *256*, 135-138.

Eleopra, R., Tugnoli, V., Rossetto, O., Montecucco, C., and De Grandis, D. (1997). Botulinum neurotoxin serotype C: a novel effective botulinum toxin therapy in human. Neurosci Lett *224*, 91-94.

Fang, Q., Berberian, K., Gong, L.W., Hafez, I., Sorensen, J.B., and Lindau, M. (2008). The role of the C terminus of the SNARE protein SNAP-25 in fusion pore opening and a model for fusion pore mechanics. Proc Natl Acad Sci U S A *105*, 15388-15392.

Fasshauer, D., Antonin, W., Subramaniam, V., and Jahn, R. (2002). SNARE assembly and disassembly exhibit a pronounced hysteresis. Nat Struct Biol *9*, 144-151.

Fasshauer, D., Eliason, W.K., Brunger, A.T., and Jahn, R. (1998). Identification of a minimal core of the synaptic SNARE complex sufficient for reversible assembly and disassembly. Biochemistry *37*, 10354-10362.

Fatt, P., and Katz, B. (1951). An analysis of the end-plate potential recorded with an intracellular electrode. J Physiol *115*, 320-370.

Fatt, P., and Katz, B. (1952). Spontaneous subthreshold activity at motor nerve endings. J Physiol *117*, 109-128.

Fisher, R.S., van Emde Boas, W., Blume, W., Elger, C., Genton, P., Lee, P., and Engel, J., Jr. (2005). Epileptic seizures and epilepsy: definitions proposed by the International League Against Epilepsy (ILAE) and the International Bureau for Epilepsy (IBE). Epilepsia *46*, 470-472.

Foran, P., Lawrence, G.W., Shone, C.C., Foster, K.A., and Dolly, J.O. (1996). Botulinum neurotoxin C1 cleaves both syntaxin and SNAP-25 in intact and permeabilized chromaffin cells: correlation with its blockade of catecholamine release. Biochemistry *35*, 2630-2636.

Fouquet, W., Owald, D., Wichmann, C., Mertel, S., Depner, H., Dyba, M., Hallermann, S., Kittel, R.J., Eimer, S., and Sigrist, S.J. (2009). Maturation of active zone assembly by Drosophila Bruchpilot. J Cell Biol *186*, 129-145.

Gaiarsa, J.L., Caillard, O., and Ben-Ari, Y. (2002). Long-term plasticity at GABAergic and glycinergic synapses: mechanisms and functional significance. Trends Neurosci *25*, 564-570.

Ganetzky, B., and Wu, C.F. (1982a). Drosophila mutants with opposing effects on nerve excitability: genetic and spatial interactions in repetitive firing. J Neurophysiol *47*, 501-514.

Ganetzky, B., and Wu, C.F. (1982b). Indirect Suppression Involving Behavioral Mutants with Altered Nerve Excitability in DROSOPHILA MELANOGASTER. Genetics *100*, 597-614.

Ganetzky, B., and Wu, C.F. (1983). Neurogenetic analysis of potassium currents in Drosophila: synergistic effects on neuromuscular transmission in double mutants. J Neurogenet *1*, 17-28.

Geppert, M., Goda, Y., Hammer, R.E., Li, C., Rosahl, T.W., Stevens, C.F., and Sudhof, T.C. (1994). Synaptotagmin I: a major Ca2+ sensor for transmitter release at a central synapse. Cell *79*, 717-727.

Gil, A., Gutierrez, L.M., Carrasco-Serrano, C., Alonso, M.T., Viniegra, S., and Criado, M. (2002). Modifications in the C terminus of the synaptosome-associated protein of 25 kDa (SNAP-25) and in the complementary region of synaptobrevin affect the final steps of exocytosis. J Biol Chem *277*, 9904-9910.

Glitsch, M.D. (2008). Spontaneous neurotransmitter release and Ca2+--how spontaneous is spontaneous neurotransmitter release? Cell Calcium *43*, 9-15.

Gorczyca, M., Augart, C., and Budnik, V. (1993). Insulin-like receptor and insulin-like peptide are localized at neuromuscular junctions in Drosophila. J Neurosci *13*, 3692-3704.

Han, X., Wang, C.T., Bai, J., Chapman, E.R., and Jackson, M.B. (2004). Transmembrane segments of syntaxin line the fusion pore of Ca2+-triggered exocytosis. Science *304*, 289-292.

Heberlein, U. (2000). Genetics of alcohol-induced behaviors in Drosophila. Alcohol Res Health *24*, 185-188.

Heidelberger, R., Heinemann, C., Neher, E., and Matthews, G. (1994). Calcium dependence of the rate of exocytosis in a synaptic terminal. Nature *371*, 513-515.

Herr, D.R., Fyrst, H., Phan, V., Heinecke, K., Georges, R., Harris, G.L., and Saba, J.D. (2003). Sply regulation of sphingolipid signaling molecules is essential for Drosophila development. Development *130*, 2443-2453.

Hess, D.T., Slater, T.M., Wilson, M.C., and Skene, J.H. (1992a). The 25 kDa synaptosomal-associated protein SNAP-25 is the major methionine-rich polypeptide in rapid axonal transport and a major substrate for palmitoylation in adult CNS. J Neurosci *12*, 4634-4641.

Hess, E.J., Collins, K.A., and Wilson, M.C. (1996). Mouse model of hyperkinesis implicates SNAP-25 in behavioral regulation. J Neurosci *16*, 3104-3111.

Hess, E.J., Jinnah, H.A., Kozak, C.A., and Wilson, M.C. (1992b). Spontaneous locomotor hyperactivity in a mouse mutant with a deletion including the Snap gene on chromosome 2. J Neurosci *12*, 2865-2874.

Heuser, J.E., and Reese, T.S. (1973). Evidence for recycling of synaptic vesicle membrane during transmitter release at the frog neuromuscular junction. J Cell Biol *57*, 315-344.

Hoang, B., and Chiba, A. (2001). Single-cell analysis of Drosophila larval neuromuscular synapses. Dev Biol *229*, 55-70.

Hong, C.S., and Ganetzky, B. (1994). Spatial and temporal expression patterns of two sodium channel genes in Drosophila. J Neurosci *14*, 5160-5169.

Hua, Y., and Scheller, R.H. (2001). Three SNARE complexes cooperate to mediate membrane fusion. Proc Natl Acad Sci U S A *98*, 8065-8070.

Huang, X., Wheeler, M.B., Kang, Y.H., Sheu, L., Lukacs, G.L., Trimble, W.S., and Gaisano, H.Y. (1998). Truncated SNAP-25 (1-197), like botulinum neurotoxin A, can inhibit insulin secretion from HIT-T15 insulinoma cells. Mol Endocrinol *12*, 1060-1070.

Hughes, J.R. (1958). Post-tetanic potentiation. Physiol Rev *38*, 91-113.

Hutt, D.M., Baltz, J.M., and Ngsee, J.K. (2005). Synaptotagmin VI and VIII and syntaxin 2 are essential for the mouse sperm acrosome reaction. J Biol Chem *280*, 20197-20203.

Jacobsson, G., and Meister, B. (1996). Molecular components of the exocytotic machinery in the rat pituitary gland. Endocrinology *137*, 5344-5356.

Jahn, R., and Hanson, P.I. (1998). Membrane fusion. SNAREs line up in new environment. Nature *393*, 14-15.

Jahn, R., Lang, T., and Sudhof, T.C. (2003). Membrane fusion. Cell *112*, 519-533.

Jahn, R., and Scheller, R.H. (2006). SNAREs--engines for membrane fusion. Nat Rev Mol Cell Biol *7*, 631-643.

Jahn, R., and Sudhof, T.C. (1999). Membrane fusion and exocytosis. Annu Rev Biochem *68*, 863-911.

Jan, L.Y., and Jan, Y.N. (1976a). L-glutamate as an excitatory transmitter at the Drosophila larval neuromuscular junction. J Physiol *262*, 215-236.

Jan, L.Y., and Jan, Y.N. (1976b). Properties of the larval neuromuscular junction in Drosophila melanogaster. J Physiol *262*, 189-214.

Jan, Y.N., and Jan, L.Y. (1978). Genetic dissection of short-term and long-term facilitation at the Drosophila neuromuscular junction. Proc Natl Acad Sci U S A *75*, 515-519.

Jeans, A.F., Oliver, P.L., Johnson, R., Capogna, M., Vikman, J., Molnar, Z., Babbs, A., Partridge, C.J., Salehi, A., Bengtsson, M.*, et al.* (2007). A dominant mutation in Snap25 causes impaired vesicle trafficking, sensorimotor gating, and ataxia in the blind-drunk mouse. Proc Natl Acad Sci U S A *104*, 2431-2436.

Jia, X.X., Gorczyca, M., and Budnik, V. (1993). Ultrastructure of neuromuscular junctions in Drosophila: comparison of wild type and mutants with increased excitability. J Neurobiol *24*, 1025-1044.

Jo, M., Gieske, M.C., Payne, C.E., Wheeler-Price, S.E., Gieske, J.B., Ignatius, I.V., Curry, T.E., Jr., and Ko, C. (2004). Development and application of a rat ovarian gene expression database. Endocrinology *145*, 5384-5396.

Johansen, J., Halpern, M.E., Johansen, K.M., and Keshishian, H. (1989a). Stereotypic morphology of glutamatergic synapses on identified muscle cells of Drosophila larvae. J Neurosci *9*, 710-725.

Johansen, J., Halpern, M.E., and Keshishian, H. (1989b). Axonal guidance and the development of muscle fiber-specific innervation in Drosophila embryos. J Neurosci *9*, 4318-4332.

Jordan, K.W., Carbone, M.A., Yamamoto, A., Morgan, T.J., and Mackay, T.F. (2007). Quantitative genomics of locomotor behavior in Drosophila melanogaster. Genome Biol *8*, R172.

Jordan, K.W., Morgan, T.J., and Mackay, T.F. (2006). Quantitative trait loci for locomotor behavior in Drosophila melanogaster. Genetics *174*, 271-284.

Karatekin, E., Di Giovanni, J., Iborra, C., Coleman, J., O'Shaughnessy, B., Seagar, M., and Rothman, J.E. (2010). A fast, single-vesicle fusion assay mimics physiological SNARE requirements. Proc Natl Acad Sci U S A *107*, 3517-3521.

Kasai, H. (1999). Comparative biology of Ca2+-dependent exocytosis: implications of kinetic diversity for secretory function. Trends Neurosci *22*, 88-93.

Kasai, H., Takagi, H., Ninomiya, Y., Kishimoto, T., Ito, K., Yoshida, A., Yoshioka, T., and Miyashita, Y. (1996). Two components of exocytosis and endocytosis in phaeochromocytoma cells studied using caged Ca2+ compounds. J Physiol *494 (Pt 1)*, 53-65.

Katz, B., and Miledi, R. (1967). The timing of calcium action during neuromuscular transmission. J Physiol *189*, 535-544.

Keller, J.E., Cai, F., and Neale, E.A. (2004). Uptake of botulinum neurotoxin into cultured neurons. Biochemistry *43*, 526-532.

Keller, J.E., and Neale, E.A. (2001). The role of the synaptic protein snap-25 in the potency of botulinum neurotoxin type A. J Biol Chem *276*, 13476-13482.

Kidokoro, Y. (2003). Roles of SNARE proteins and synaptotagmin I in synaptic transmission: studies at the Drosophila neuromuscular synapse. Neurosignals *12*, 13-30.

Kidokoro, Y. (2006). Vesicle trafficking and recycling at the neuromuscular junction: two pathways for endocytosis. Int Rev Neurobiol *75*, 145-164.

Kidokoro, Y., Kuromi, H., Delgado, R., Maureira, C., Oliva, C., and Labarca, P. (2004). Synaptic vesicle pools and plasticity of synaptic transmission at the Drosophila synapse. Brain Res Brain Res Rev *47*, 18-32.

Kim, S., Atwood, H.L., and Cooper, R.L. (2000). Assessing accurate sizes of synaptic vesicles in nerve terminals. Brain Res *877*, 209-217.

Kittel, R.J., Wichmann, C., Rasse, T.M., Fouquet, W., Schmidt, M., Schmid, A., Wagh, D.A., Pawlu, C., Kellner, R.R., Willig, K.I*., et al.* (2006). Bruchpilot promotes active zone assembly, Ca2+ channel clustering, and vesicle release. Science *312*, 1051-1054.

Kupfermann, I. (1991). Functional studies of cotransmission. Physiol Rev *71*, 683-732.

Lagow, R.D., Bao, H., Cohen, E.N., Daniels, R.W., Zuzek, A., Williams, W.H., Macleod, G.T., Sutton, R.B., and Zhang, B. (2007). Modification of a hydrophobic layer by a point mutation in syntaxin 1A regulates the rate of synaptic vesicle fusion. PLoS Biol *5*, e72.

Landgraf, M., Bossing, T., Technau, G.M., and Bate, M. (1997). The origin, location, and projections of the embryonic abdominal motorneurons of Drosophila. J Neurosci *17*, 9642-9655.

Landgraf, M., Jeffrey, V., Fujioka, M., Jaynes, J.B., and Bate, M. (2003). Embryonic origins of a motor system: motor dendrites form a myotopic map in Drosophila. PLoS Biol *1*, E41.

Li, C., Davletov, B.A., and Sudhof, T.C. (1995). Distinct Ca2+ and Sr2+ binding properties of synaptotagmins. Definition of candidate Ca2+ sensors for the fast and slow components of neurotransmitter release. J Biol Chem *270*, 24898-24902.

Li, J., and Schwarz, T.L. (1999). Genetic evidence for an equilibrium between docked and undocked vesicles. Philos Trans R Soc Lond B Biol Sci *354*, 299-306.

Lin, R.C., and Scheller, R.H. (1997). Structural organization of the synaptic exocytosis core complex. Neuron *19*, 1087-1094.

Liu, Y., Schirra, C., Edelmann, L., Matti, U., Rhee, J., Hof, D., Bruns, D., Brose, N., Rieger, H., Stevens, D.R*., et al.* (2010). Two distinct secretory vesicle-priming steps in adrenal chromaffin cells. J Cell Biol *190*, 1067-1077.

Llinas, R., Sugimori, M., and Silver, R.B. (1992). Microdomains of high calcium concentration in a presynaptic terminal. Science *256*, 677-679.

Lnenicka, G.A., and Keshishian, H. (2000). Identified motor terminals in Drosophila larvae show distinct differences in morphology and physiology. J Neurobiol *43*, 186-197.

Loewen, C.A., Mackler, J.M., and Reist, N.E. (2001). Drosophila synaptotagmin I null mutants survive to early adulthood. Genesis *31*, 30-36.

Lopez, I., Giner, D., Ruiz-Nuno, A., Fuentealba, J., Viniegra, S., Garcia, A.G., Davletov, B., and Gutierrez, L.M. (2007). Tight coupling of the t-SNARE and calcium channel microdomains in adrenomedullary slices and not in cultured chromaffin cells. Cell Calcium *41*, 547-558.

Lu, X., Zhang, Y., and Shin, Y.K. (2008). Supramolecular SNARE assembly precedes hemifusion in SNARE-mediated membrane fusion. Nat Struct Mol Biol *15*, 700-706.

Marshall, C., Hitman, G.A., Partridge, C.J., Clark, A., Ma, H., Shearer, T.R., and Turner, M.D. (2005). Evidence that an isoform of calpain-10 is a regulator of exocytosis in pancreatic beta-cells. Mol Endocrinol *19*, 213-224.

McMahon, H.T., Missler, M., Li, C., and Sudhof, T.C. (1995). Complexins: cytosolic proteins that regulate SNAP receptor function. Cell *83*, 111-119.

Megighian, A., Rigoni, M., Caccin, P., Zordan, M.A., and Montecucco, C. (2007). A lysolecithin/fatty acid mixture promotes and then blocks neurotransmitter release at the Drosophila melanogaster larval neuromuscular junction. Neurosci Lett *416*, 6-11.

Megighian, A., Scorzeto, M., Zanini, D., Pantano, S., Rigoni, M., Benna, C., Rossetto, O., Montecucco, C., and Zordan, M. (2010). Arg206 of SNAP-25 is essential for neuroexocytosis at the Drosophila melanogaster neuromuscular junction. J Cell Sci *123*, 3276-3283.

Mehren, J.E., and Griffith, L.C. (2004). Calcium-independent calcium/calmodulin-dependent protein kinase II in the adult Drosophila CNS enhances the training of pheromonal cues. J Neurosci *24*, 10584-10593.

Meunier, F.A., Lisk, G., Sesardic, D., and Dolly, J.O. (2003). Dynamics of motor nerve terminal remodeling unveiled using SNARE-cleaving botulinum toxins: the extent and duration are dictated by the sites of SNAP-25 truncation. Mol Cell Neurosci *22*, 454-466.

Miyamoto, S., Funatsu, T., Ishiwata, S., and Fujime, S. (1993). Changes in mobility of chromaffin granules in actin network with its assembly and Ca(2+)-dependent disassembly by gelsolin. Biophys J *64*, 1139-1149.

Mohrmann, R., de Wit, H., Verhage, M., Neher, E., and Sorensen, J.B. (2010). Fast vesicle fusion in living cells requires at least three SNARE complexes. Science *330*, 502-505.

Monastirioti, M., Gorczyca, M., Rapus, J., Eckert, M., White, K., and Budnik, V. (1995). Octopamine immunoreactivity in the fruit fly Drosophila melanogaster. J Comp Neurol *356*, 275-287.

Montecucco, C., Schiavo, G., and Pantano, S. (2005). SNARE complexes and neuroexocytosis: how many, how close? Trends Biochem Sci *30*, 367-372.

Nagy, G., Milosevic, I., Mohrmann, R., Wiederhold, K., Walter, A.M., and Sorensen, J.B. (2008). The SNAP-25 linker as an adaptation toward fast exocytosis. Mol Biol Cell *19*, 3769-3781.

Nakata, T., and Hirokawa, N. (1992). Organization of cortical cytoskeleton of cultured chromaffin cells and involvement in secretion as revealed by quick-freeze, deep-etching, and double-label immunoelectron microscopy. J Neurosci *12*, 2186-2197.

Neale, E.A., Bowers, L.M., Jia, M., Bateman, K.E., and Williamson, L.C. (1999). Botulinum neurotoxin A blocks synaptic vesicle exocytosis but not endocytosis at the nerve terminal. J Cell Biol *147*, 1249-1260.

Niemeyer, B.A., and Schwarz, T.L. (2000). SNAP-24, a Drosophila SNAP-25 homologue on granule membranes, is a putative mediator of secretion and granule-granule fusion in salivary glands. J Cell Sci *113 (Pt 22)*, 4055-4064.

Nolan, P.M., Peters, J., Strivens, M., Rogers, D., Hagan, J., Spurr, N., Gray, I.C., Vizor, L., Brooker, D., Whitehill, E.*, et al.* (2000). A systematic, genome-wide, phenotype-driven mutagenesis programme for gene function studies in the mouse. Nat Genet *25*, 440-443.

Nose, A., Mahajan, V.B., and Goodman, C.S. (1992). Connectin: a homophilic cell adhesion molecule expressed on a subset of muscles and the motoneurons that innervate them in Drosophila. Cell *70*, 553-567.

Oyler, G.A., Higgins, G.A., Hart, R.A., Battenberg, E., Billingsley, M., Bloom, F.E., and Wilson, M.C. (1989). The identification of a novel synaptosomal-associated protein, SNAP-25, differentially expressed by neuronal subpopulations. J Cell Biol *109*, 3039-3052.

Perin, M.S., Fried, V.A., Mignery, G.A., Jahn, R., and Sudhof, T.C. (1990). Phospholipid binding by a synaptic vesicle protein homologous to the regulatory region of protein kinase C. Nature *345*, 260-263.

Peters, A., Palay, S.L., and Webster, H.d. (1991). The fine structure of the nervous system : neurons and their supporting cells, 3rd edn (New York, Oxford University Press).

Petersen, S.A., Fetter, R.D., Noordermeer, J.N., Goodman, C.S., and DiAntonio, A. (1997). Genetic analysis of glutamate receptors in Drosophila reveals a retrograde signal regulating presynaptic transmitter release. Neuron *19*, 1237-1248.

Plattner, H., Artalejo, A.R., and Neher, E. (1997). Ultrastructural organization of bovine chromaffin cell cortex-analysis by cryofixation and morphometry of aspects pertinent to exocytosis. J Cell Biol *139*, 1709-1717.

Poodry, C.A., and Edgar, L. (1979). Reversible alteration in the neuromuscular junctions of Drosophila melanogaster bearing a temperature-sensitive mutation, shibire. J Cell Biol *81*, 520-527.

Pozzi, D., Condliffe, S., Bozzi, Y., Chikhladze, M., Grumelli, C., Proux-Gillardeaux, V., Takahashi, M., Franceschetti, S., Verderio, C., and Matteoli, M. (2008). Activity-dependent phosphorylation of Ser187 is required for SNAP-25-negative modulation of neuronal voltage-gated calcium channels. Proc Natl Acad Sci U S A *105*, 323-328.

Prokop, A. (1999). Integrating bits and pieces: synapse structure and formation in Drosophila embryos. Cell Tissue Res *297*, 169-186.

Prokop, A., and Meinertzhagen, I.A. (2006). Development and structure of synaptic contacts in Drosophila. Semin Cell Dev Biol *17*, 20-30.

Raciborska, D.A., Trimble, W.S., and Charlton, M.P. (1998). Presynaptic protein interactions in vivo: evidence from botulinum A, C, D and E action at frog neuromuscular junction. Eur J Neurosci *10*, 2617-2628.

Rao, S.S., Stewart, B.A., Rivlin, P.K., Vilinsky, I., Watson, B.O., Lang, C., Boulianne, G., Salpeter, M.M., and Deitcher, D.L. (2001). Two distinct effects on neurotransmission in a temperature-sensitive SNAP-25 mutant. EMBO J *20*, 6761-6771.

Reiff, D.F., Thiel, P.R., and Schuster, C.M. (2002). Differential regulation of active zone density during long-term strengthening of Drosophila neuromuscular junctions. J Neurosci *22*, 9399-9409.

Reiter, L.T., Potocki, L., Chien, S., Gribskov, M., and Bier, E. (2001). A systematic analysis of human disease-associated gene sequences in Drosophila melanogaster. Genome Res *11*, 1114-1125.

Rickman, C., Hu, K., Carroll, J., and Davletov, B. (2005). Self-assembly of SNARE fusion proteins into star-shaped oligomers. Biochem J *388*, 75-79.

Riemensperger, T., Isabel, G., Coulom, H., Neuser, K., Seugnet, L., Kume, K., Iche-Torres, M., Cassar, M., Strauss, R., Preat, T*., et al.* (2011). Behavioral consequences of dopamine deficiency in the Drosophila central nervous system. Proc Natl Acad Sci U S A *108*, 834-839.

Risinger, C., Deitcher, D.L., Lundell, I., Schwarz, T.L., and Larhammar, D. (1997). Complex gene organization of synaptic protein SNAP-25 in Drosophila melanogaster. Gene *194*, 169-177.

Risinger, C., and Larhammar, D. (1993). Multiple loci for synapse protein SNAP-25 in the tetraploid goldfish. Proc Natl Acad Sci U S A *90*, 10598-10602.

Rizzoli, S.O., and Betz, W.J. (2005). Synaptic vesicle pools. Nat Rev Neurosci *6*, 57-69.

Robinow, S., and White, K. (1988). The locus elav of Drosophila melanogaster is expressed in neurons at all developmental stages. Dev Biol *126*, 294-303.

Rohrbough, J., and Broadie, K. (2005). Lipid regulation of the synaptic vesicle cycle. Nat Rev Neurosci *6*, 139-150.

Salkoff, L., and Wyman, R. (1980). Facilitation of membrane electrical excitability in Drosophila. Proc Natl Acad Sci U S A *77*, 6216-6220.

Sankaranarayanan, S., and Ryan, T.A. (2000). Real-time measurements of vesicle-SNARE recycling in synapses of the central nervous system. Nat Cell Biol *2*, 197-204.

Schiavo, G., Santucci, A., Dasgupta, B.R., Mehta, P.P., Jontes, J., Benfenati, F., Wilson, M.C., and Montecucco, C. (1993). Botulinum neurotoxins serotypes A and E cleave SNAP-25 at distinct COOH-terminal peptide bonds. FEBS Lett *335*, 99-103.

Schulze, K.L., and Bellen, H.J. (1996). Drosophila syntaxin is required for cell viability and may function in membrane formation and stabilization. Genetics *144*, 1713-1724.

Schuster, C.M., Davis, G.W., Fetter, R.D., and Goodman, C.S. (1996). Genetic dissection of structural and functional components of synaptic plasticity. II. Fasciclin II controls presynaptic structural plasticity. Neuron *17*, 655-667.

Shimada, M., Yanai, Y., Okazaki, T., Yamashita, Y., Sriraman, V., Wilson, M.C., and Richards, J.S. (2007). Synaptosomal-associated protein 25 gene expression is hormonally regulated during ovulation and is involved in cytokine/chemokine exocytosis from granulosa cells. Mol Endocrinol *21*, 2487-2502.

Sollner, T., and Rothman, J.E. (1994). Neurotransmission: harnessing fusion machinery at the synapse. Trends Neurosci *17*, 344-348.

Sollner, T., Whiteheart, S.W., Brunner, M., Erdjument-Bromage, H., Geromanos, S., Tempst, P., and Rothman, J.E. (1993). SNAP receptors implicated in vesicle targeting and fusion. Nature *362*, 318-324.

Sorensen, J.B. (2009). Conflicting views on the membrane fusion machinery and the fusion pore. Annu Rev Cell Dev Biol *25*, 513-537.

Sorensen, J.B., Matti, U., Wei, S.H., Nehring, R.B., Voets, T., Ashery, U., Binz, T., Neher, E., and Rettig, J. (2002). The SNARE protein SNAP-25 is linked to fast calcium triggering of exocytosis. Proc Natl Acad Sci U S A *99*, 1627-1632.

Sorensen, J.B., Nagy, G., Varoqueaux, F., Nehring, R.B., Brose, N., Wilson, M.C., and Neher, E. (2003). Differential control of the releasable vesicle pools by SNAP-25 splice variants and SNAP-23. Cell *114*, 75-86.

Sorensen, J.B., Wiederhold, K., Muller, E.M., Milosevic, I., Nagy, G., de Groot, B.L., Grubmuller, H., and Fasshauer, D. (2006). Sequential N- to C-terminal SNARE complex assembly drives priming and fusion of secretory vesicles. EMBO J *25*, 955-966.

Stevens, C.F., and Wesseling, J.F. (1999). Augmentation is a potentiation of the exocytotic process. Neuron *22*, 139-146.

Stewart, B.A., Atwood, H.L., Renger, J.J., Wang, J., and Wu, C.F. (1994). Improved stability of Drosophila larval neuromuscular preparations in haemolymph-like physiological solutions. J Comp Physiol A *175*, 179-191.

Stewart, B.A., Mohtashami, M., Trimble, W.S., and Boulianne, G.L. (2000). SNARE proteins contribute to calcium cooperativity of synaptic transmission. Proc Natl Acad Sci U S A *97*, 13955-13960.

Steyer, J.A., and Almers, W. (1999). Tracking single secretory granules in live chromaffin cells by evanescent-field fluorescence microscopy. Biophys J *76*, 2262-2271.

Steyer, J.A., Horstmann, H., and Almers, W. (1997). Transport, docking and exocytosis of single secretory granules in live chromaffin cells. Nature *388*, 474-478.

Sudhof, T.C. (2004). The synaptic vesicle cycle. Annu Rev Neurosci *27*, 509-547.

Sudhof, T.C., Czernik, A.J., Kao, H.T., Takei, K., Johnston, P.A., Horiuchi, A., Kanazir, S.D., Wagner, M.A., Perin, M.S., De Camilli, P*., et al.* (1989). Synapsins: mosaics of shared and individual domains in a family of synaptic vesicle phosphoproteins. Science *245*, 1474-1480.

Sudhof, T.C., and Malenka, R.C. (2008). Understanding synapses: past, present, and future. Neuron *60*, 469-476.

Sudhof, T.C., and Rizo, J. (1996). Synaptotagmins: C2-domain proteins that regulate membrane traffic. Neuron *17*, 379-388.

Sudhof, T.C., and Rothman, J.E. (2009). Membrane fusion: grappling with SNARE and SM proteins. Science *323*, 474-477.

Sutton, R.B., Fasshauer, D., Jahn, R., and Brunger, A.T. (1998). Crystal structure of a SNARE complex involved in synaptic exocytosis at 2.4 A resolution. Nature *395*, 347-353.

Thompson, P.M., Sower, A.C., and Perrone-Bizzozero, N.I. (1998). Altered levels of the synaptosomal associated protein SNAP-25 in schizophrenia. Biol Psychiatry *43*, 239-243.

Tokumaru, H., Umayahara, K., Pellegrini, L.L., Ishizuka, T., Saisu, H., Betz, H., Augustine, G.J., and Abe, T. (2001). SNARE complex oligomerization by synaphin/complexin is essential for synaptic vesicle exocytosis. Cell *104*, 421-432.

Tsui-Pierchala, B.A., Encinas, M., Milbrandt, J., and Johnson, E.M., Jr. (2002). Lipid rafts in neuronal signaling and function. Trends Neurosci *25*, 412-417.

Usherwood, P.N. (1981). Glutamate synapses and receptors on insect muscle. Adv Biochem Psychopharmacol *27*, 183-193.

Vaidyanathan, V.V., Yoshino, K., Jahnz, M., Dorries, C., Bade, S., Nauenburg, S., Niemann, H., and Binz, T. (1999). Proteolysis of SNAP-25 isoforms by botulinum neurotoxin types A, C, and E: domains and amino acid residues controlling the formation of enzyme-substrate complexes and cleavage. J Neurochem *72*, 327-337.

van den Bogaart, G., Holt, M.G., Bunt, G., Riedel, D., Wouters, F.S., and Jahn, R. (2010). One SNARE complex is sufficient for membrane fusion. Nat Struct Mol Biol *17*, 358-364.

Varoqueaux, F., Sigler, A., Rhee, J.S., Brose, N., Enk, C., Reim, K., and Rosenmund, C. (2002). Total arrest of spontaneous and evoked synaptic transmission but normal synaptogenesis in the absence of Munc13-mediated vesicle priming. Proc Natl Acad Sci U S A *99*, 9037-9042.

Vilinsky, I., Stewart, B.A., Drummond, J., Robinson, I., and Deitcher, D.L. (2002). A Drosophila SNAP-25 null mutant reveals context-dependent redundancy with SNAP-24 in neurotransmission. Genetics *162*, 259-271.

Washbourne, P., Thompson, P.M., Carta, M., Costa, E.T., Mathews, J.R., Lopez-Bendito, G., Molnar, Z., Becher, M.W., Valenzuela, C.F., Partridge, L.D*., et al.* (2002). Genetic ablation of the t-SNARE SNAP-25 distinguishes mechanisms of neuroexocytosis. Nat Neurosci *5*, 19-26.

Weber, H.S., and Cyran, S.E. (1998). Transvenous "snare-assisted" coil occlusion of patent ductus arteriosus. Am J Cardiol *82*, 248-251.

Weber, T., Zemelman, B.V., McNew, J.A., Westermann, B., Gmachl, M., Parlati, F., Sollner, T.H., and Rothman, J.E. (1998). SNAREpins: minimal machinery for membrane fusion. Cell *92*, 759-772.

Wei, S., Xu, T., Ashery, U., Kollewe, A., Matti, U., Antonin, W., Rettig, J., and Neher, E. (2000). Exocytotic mechanism studied by truncated and zero layer mutants of the C-terminus of SNAP-25. EMBO J *19*, 1279-1289.

White, K.E., Humphrey, D.M., and Hirth, F. (2010). The dopaminergic system in the aging brain of Drosophila. Front Neurosci *4*, 205.

Wiederhold, K., and Fasshauer, D. (2009). Is assembly of the SNARE complex enough to fuel membrane fusion? J Biol Chem *284*, 13143-13152.

Winkler, H., and Westhead, E. (1980). The molecular organization of adrenal chromaffin granules. Neuroscience *5*, 1803-1823.

Wu, C.F., and Haugland, F.N. (1985). Voltage clamp analysis of membrane currents in larval muscle fibers of Drosophila: alteration of potassium currents in Shaker mutants. J Neurosci *5*, 2626-2640.

Wucherpfennig, T., Wilsch-Brauninger, M., and Gonzalez-Gaitan, M. (2003). Role of Drosophila Rab5 during endosomal trafficking at the synapse and evoked neurotransmitter release. J Cell Biol *161*, 609-624.

Yamaoka, K., and Ikeda, K. (1988). Electrogenic responses elicited by transmembrane depolarizing current in aerated body wall muscles of Drosophila melanogaster larvae. J Comp Physiol A *163*, 705-714.

Yersin, A., Hirling, H., Steiner, P., Magnin, S., Regazzi, R., Huni, B., Huguenot, P., De los Rios, P., Dietler, G., Catsicas, S.*, et al.* (2003). Interactions between synaptic vesicle fusion proteins explored by atomic force microscopy. Proc Natl Acad Sci U S A *100*, 8736-8741.

Yoshihara, M., and Littleton, J.T. (2002). Synaptotagmin I functions as a calcium sensor to synchronize neurotransmitter release. Neuron *36*, 897-908.

Young, B., Lowe, J.S., Stevens, A., and Heath J.W. (2006). Wheater's Functional Histology: A Text and Colour Atalas, 5th Edition. Churchill Livingstone Elsevier.

Young, W.F., Jr., and Abboud, A.L. (2006). Editorial: paraganglioma--all in the family. J Clin Endocrinol Metab *91*, 790-792.

Zhang, B., Freeman, M.R., and Wadde, S. (2010). Drosophila Neurobiology: A Laboratory Manual. Cold Spring Harbor Laboratory Press, Plainview, NY.

Zhang, B., Koh, Y.H., Beckstead, R.B., Budnik, V., Ganetzky, B., and Bellen, H.J. (1998). Synaptic vesicle size and number are regulated by a clathrin adaptor protein required for endocytosis. Neuron *21*, 1465-1475.

Zhang, X., Kim-Miller, M.J., Fukuda, M., Kowalchyk, J.A., and Martin, T.F. (2002). Ca2+-dependent synaptotagmin binding to SNAP-25 is essential for Ca2+-triggered exocytosis. Neuron *34*, 599-611.

Zhong, H., Yokoyama, C.T., Scheuer, T., and Catterall, W.A. (1999). Reciprocal regulation of P/Q-type Ca2+ channels by SNAP-25, syntaxin and synaptotagmin. Nat Neurosci *2*, 939-941.

Zucker, R.S., and Regehr, W.G. (2002). Short-term synaptic plasticity. Annu Rev Physiol *64*, 355-405.

Acknowledgments

In the first place, I want to thanks Prof. Zordan, my supervisor, for giving me the possibility to work in his lab and for the critical reading of my thesis.

Thanks to Prof. Megighian for introducing me in the field of electrophysiology and for the teaching in the field and to Prof. Costa, Prof. Montecucco and Prof. Rossetto and also their collaborators for their suggestions and technical help.

Special thanks to Mike, not only a labmate but also a friend.

My sincere thanks to everyone who have either contributed time and resources, or been kind enough to support my studies: Caterina, Clara, Diego, Elena, Francesca, Jessica, Luca, Pamela, Paola C, Paola dP, Paola Q, Stefano M and Stefano V.

Finally I would like to arknowledge Fondazione CaRiPaRo (Cassa di Risparmio di Padova e Rovigo) for providing me with founding to carry out my research.